Master's Thesis

Multivalent Polyaspartamide-based Hydrogels with Controllable Physical and Biological Properties

Jinhyeong Jang

Department of Chemistry

Graduate School of UNIST

2018

Multivalent Polyaspartamide-based Hydrogels with Controllable Physical and Biological Properties

Jinhyeong Jang

Department of Chemistry

Graduate School of UNIST

Multivalent Polyaspartamide-based Hydrogels with Controllable Physical and Biological Properties

A thesis/dissertation
submitted to the Graduate School of UNIST
in partial fulfillment of the
requirements for the degree of
Master of Science

Jinhyeong Jang

12/27/2017 of submission

Approved by

Advisor
Prof. Chaenyung Cha

Multivalent Polyaspartamide-based Hydrogels with Controllable Physical and Biological Properties

Jinhyeong Jang

This certifies that the thesis/dissertation of Jinhyeong Jang is approved.

12/27/2017 of submission

signature

Advisor: Prof. Chaenyung Cha

signature

Prof. Ja-Hyoung Ryu

signature

Prof. Min Sang Kwon

Abstract

Hydrogels provide suitable microenvironment for various fields of bioengineering, as they can be engineered to mimic the structure and properties of natural extracellular matrix (ECM); a network of hydrophilic and biocompatible polymers possessing elasticity and high water content ideal for supporting biological molecules and species. Due to these attractive properties, hydrogels are widely used in such biomedical applications as tissue engineering and drug delivery. Their structure can be designed and altered at a molecular level with various functional groups of constituting polymers, which results in the changes in various physically properties (e.g. rigidity, toughness, and permeability). However, controlling those physical properties via chemical modifications are usually difficult, requiring several time-consuming steps. Herein, highly versatile polyaspartamide, which allows for the efficient control of the type and number of functional groups, was developed in order to engineer hydrogels with tunable properties for biomedical applications.

In Chapter 1, a brief introduction to hydrogels as biomaterials and the importance of controlling their mechanical properties are described. Also, a history of polysuccinimide and its derivatization to various forms of polyaspartamide is introduced to highlight the importance of this subject in the field of biomedical engineering. Chapter 2 presents the development of various polyaspartamides, presenting thiol, hydrazide, and amine functional groups, and their applications into fabricating hydrogels with controllable physical properties. In addition, the biomedical application of polyaspartamide-based hydrogels is demonstrated through controlled drug release and in vitro cell culture. Finally in Chapter 3, the multifunctional nature of polyaspartamide is further introduced with the polyaspartamide presenting isopropyl groups for thermoresponsiveness.

Table of Contents

List of Figure

to control the mechanical properties.

Figure 2.15. (a) Stress-strain curves of OAlg-PHHZA hydrogels, obtained by uniaxial compression. Only the first 10 % of the strain is shown. The concentrations of OAlg and PHHZA were controlled while only varying the DS of PHHZA. (b) The hydrogels with lower DS (from DS 1 to DS 3) were magnified.

Figure 2.16. (a) Elastic moduli (kPa) and (b) degree of swelling (%) data for hydrogels made by PHHZA (DS x, y %) and OAlg (DS 40, 5%). All data was acquired after 1-day swelling in PBS at room temperature.

Figure 2.17. SEM images for hydrogels made by PHHZA (DS x, y %) and OAlg (DS 40, 5%). (a, b), (c, d), (e, f), and (g, h) represent the following PHHZA conditions, respectively; (DS 4, 10 %), (DS 4, 7.5 %), (DS 2, 10 %), and (DS 2, 7.5 %).

Figure 2.18. Stress-strain curves of PEGDA-PHEDA hydrogels obtained by uniaxial compression. The concentration and DS of PHEDA were controlled while keeping the PEGDA concentration at 10 %. The plots in (a) show the stress-strain curves in all strain range, and those at the first 10 % strain are magnified and presented in (b).

Figure 2.19. (a) Elastic moduli (kPa) and (b) degree of swelling (%) PEGDA-PHEDA hydrogels.

Figure 2.20. (a) Elastic modulus (kPa) and (b) Swelling ratio (%) data for hydrogels made by PHEDA (DS x, y %) and PEGDA (Mn 700, 20%). All data was acquired after 1-day swelling in PBS buffer at room temperature with four samples.

Figure 2.21. Hydrogel fabrication of PHHZA and PHEDA via (a) Schiff base formation, and (b) Michael addition.

Figure 2.22. Degradation of (a,b) alginate-PHHZA and (c,d) PEG-PHEDA hydrogels were determined by measuring the change in moduli (E/E_0) over time and calculating degradation rate constants (k_d). The moduli (E) measured at various time points were normalized with the initial value (E_0). k_d were calculated by fitting with Eq.(1).

Figure 2.23. Standard curve for FITC-BSA (Gain: 50). [Intensity = 72159 * FITC-BSA + 126.06] is calculated by linear fitting to raw data.

Figure 2.24. Drug release studies of (a-c) alginate-PHHZA and (d-f) PEG-PHEDA hydrogels. The release profiles (cumulative release over time) in (a) and (d) were fitted with Eq.(2) and Eq.(3), respectively. From the release profiles of alginate-PHHZA hydrogels in (a), (b) kinetic rate constants (k_1) and (c) exponents (n) were obtained. From the release profiles of PEG-PHEDA hydrogels in (d), (e) kinetic rate constants (k_2) and (f) lag time constants (T) were obtained.

Figure 2.25. Mass analysis for GRGDS peptide using MALDI-TOF-MS. α-cyano-4-hydroxycinnamic acid (HCCA) and ethanol/acetonitrile (60 : 40) were used as matrix and solvent, respectively. Spectrum (a) is for the mixture with GRGDS peptide, which shows the expected peak at the m/z value of 449.14 (the theoretical value for $[GRGDS+H]^+$ is 491.221). Spectrum (b) is for the matrix only, which does not have the characteristic peak.

Figure 2.26. ^{13}C-NMR spectrum of (a) GRGDS-PHHZA (DS 4'), (b) PHHZA (DS 4), (c) GRGDS-PHEDA (DS 4'), and (d) PHEDA (DS 4). (a) and (c) show the conjugated-GRGDS peak at 129 ppm and 125 ppm.

Figure 2.27. The 3T3 fibroblasts cultured on alginate hydrogels coated with PHHZA, visualized with a fluorescent labeling of live (green) and dead (red) cells at Day 1 and 3. (a, b) RGD-PHHZA (DS 4), (c, d) PHHZA (DS 4), (e, f) RGD-PHHZA (DS 3'), (g, h) PHHZA (DS 3), (i, j) no coating.

Figure 2.28. The 3T3 fibroblasts cultured on alginate hydrogels coated with PHEDA, visualized with a fluorescent labeling of live (green) and dead (red) cells at Day 1 and 3. (a, b) RGD-PHEDA (DS 4), (c, d) PHEDA (DS 4), (e, f) RGD-PHEDA (DS 3'), (g, h) PHEDZA (DS 3), (i, j) no coating.

Figure 3.1. FT-IR spectra of PHIPA (DS = 20, 40, 60, 80) measured by ATR method. The peaks in blue region are increasing with DS. The peaks in red region are decreasing with DS. The spectra in (a) are the full measured spectra, while those from 1000 cm^{-1} to 1900 cm^{-1} are magnified and presented in (b).

Figure 3.2. ^{13}C-NMR spectra of PHIPA. (a) DS 20, (b) DS 40, (c) DS 60, and (d) DS 80.

Figure 3.3. UV-Vis absorption spectra of PHIPA (10 % in DI water). (a) DS 0, (b) DS 20, (c) DS 40, (d) DS 60, (e) DS 80. Black, red, blue, and pink spectra represent the absorbance intensity difference between 30 ^{o}C and 24 ^{o}C, 36 ^{o}C and 24 ^{o}C, 40 ^{o}C and 24 ^{o}C, and 44 ^{o}C and 24 ^{o}C, respectively.

Figure 3.4. Absorbance at (a, b) 382 nm and (c, d) 500 nm of PHIPA (10 %, DS 0, 20, 40, 60, 80) with temperature from 24 ^{o}C to 45 ^{o}C. (a) and (c) represent the average intensity, and (b) and (d) represent the normalized intensity.

List of Table

List of Scheme

Scheme 3.1. Synthesis of poly(2-hydroxyethyl-co-isopropyl) (PHIPA).

List of Abbreviation

AAD	Adipic acid dihydrazide
ATR	Attenuated total reflectance
BCA	Bicinchoninic acid
BSA	Bovine serum albumin
D	Fmoc-Asp(OtBu)-OH
DCC	N,N'-Dicyclohexylcarbodiimide
DCM	Dichloromethane
DETA	Diethylenetriamine
DI	Deionized
DIC	1,3-Diisopropylcarbodiimide
DMAP	4-Dimethylaminopyridine
DMF	Dimethylformamide
DMSO	Dimethyl sulfoxide
DS	The degree of substitution
DTDP	3,3`-Dithiodipropionic acid
DTNB	5,5′-Dithiobis(2-nitrobenzoic acid)
ECM	Extracellular matrix
FITC	Fluorescein isothiocyanate
FT-IR	Fourier-transform infrared
FT-NMR	Fourier-transform nuclear magnetic resonance
G	Fmoc-Gly-OH
GAGs	Glycosaminoglycans
GRGDS	Gly-Arg-Gly-Asp-Ser

HOBt	1-Hydroxybenzotriazole
LCST	Lower critical solution temperature
MALDI-TOF-MS	Matrix assisted laser desorption ionization (MALDI) -time of flight (TOF) mass spectrometry (MS)
Mn	Number-average molecular weight
NOE	Nuclear Overhauser effect
OAlg	Oxidized alginate
PBS	Phosphate buffered saline
PEGDA	Polyethylene glycol diacrylate
PHEA	Poly(2-hydroxyethyl aspartamide)
PHEDA	Poly(2-hydroxyethyl-co-ethylenediaminoethyl aspartamide)
PHHZA	Poly(2-hydroxyethyl-co-hydrazidoadipoyl aspartamide)
PHIPA	Poly(2-hydroxyethyl-co-isopropyl aspartamide)
PHMCA	Poly(2-hydroxyethyl-co-2-mercaptoethyl aspartamide)
PSI	Polysuccinimide
R	Fmoc-Arg(Tos)-OH
RGD	Arg-Gly-Asp
S	Fmoc-Ser(tBu)-OH
SEM	Scanning electron microscopy
TEA	Triethylamine
TFA	Trifluoroacetic acid
TIPS	Triisopropylsilane
TNBS	Trinitrobenzene sulfonic acid
Tris	Tris(hydroxymethyl)-aminomethane
UCST	Upper critical solution temperature
UTM	Universal testing machine

Chapter 1. Introduction to Polymer Hydrogel

1.1. Hydrogels mimicking extracellular matrix (ECM)

A cell is a basic component of all tissues within an organism. The cells that make up a tissue are not simply put together by direct cell-to-cell interactions nor assembled in a random fashion. They reside within an intricately designed framework that provides suitable mechanical and nutritional microenvironment for their optimal functions as well as guide the cells to assemble into a well-defined overall architecture, called extracellular matrix (ECM).

ECM is composed of glycosaminoglycans (GAGs) and randomly oriented fibrous proteins, such as collagen, elastin, fibronectin and laminin, via chemical and physical crosslinking (Figure 1.1). [1] Collagen is the main component of ECM and mainly acts to support the cell-bonded structure, and elastin imparts elasticity to the ECM from an external force, so the structure can sustain and easily recover to original state from an external and internally-applied forces, while providing protection to the residing cells. [2, 3] These biomolucules mainly control the mechanical properties of ECM. The other fibrous proteins, fibronectin and laminin, allow the cells to bind to the ECM by providing ligands for intergrins, a group of transmembrane receptor proteins which activate signal transduction pathways for important cellular functions by binding with the ligands. [4, 5] Also, ECM is abundantly hydrated, which allows for the exchange of oxygen and nutrients, as well as other soluble biomolecular factors (e.g. cytokines, growth factors, and hormones) involved with important cellular functions. [6] The adhesion of cells to the ECM via integrin binding itself is important in guiding various important functions such as proliferation, differentiation, morphological control by altering gene expression (Figure 1.2). [7].

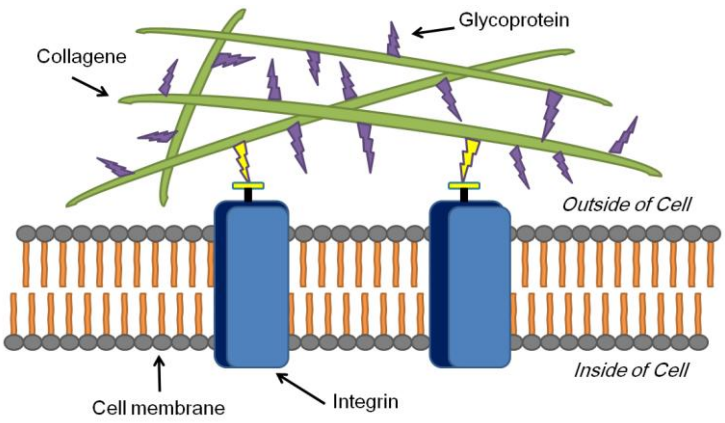

Figure 1.1. Schematic of extracellular matrix (ECM).

One of the main purposes to develop hydrogels as biomaterials is to mimic natural ECM for tissue engineering applications. [7] If hydrogels can be designed and engineered to accommodate specific cell types and induce tissue formation in vitro, they have a great potential in developing artificial patient-specific tissues and organs for revolutionary regenerative medicine (Figure 1.3) [8] In particular, the cells derived from patient's own tissue could minimize immune response compared to those from allogeneic and xenogeneic sources, as well as circumvent ethical issues associated with embryonic stem cells. Therefore, hydrogels from biocompatible natural and synthetic polymers have been developed. For example, natural polymers, such as collagen, gelatin, hyaluronate, fibronectin, alginate, agarose, and chitosan, are used to fabricate hydrogels with varying mechanical and biological properties, though controlling mechanical properties is often limited due to limited available chemical modifications. However, synthetic polymers, such as poly(ethylene oxide), poly(vinyl alcohol), and poly(acrylic acid) allow more robust control of mechanical properties of hydrogels by controlling the molecular weight, concentration and the number and type of functional groups. Since synthetic polymers generally do not have cell-recognition moieties, ECM proteins (e.g. collagen, fibronectin) or cell-responsive peptides (e.g. RGD peptides) are incorporated to the polymeric network. [18, 19]

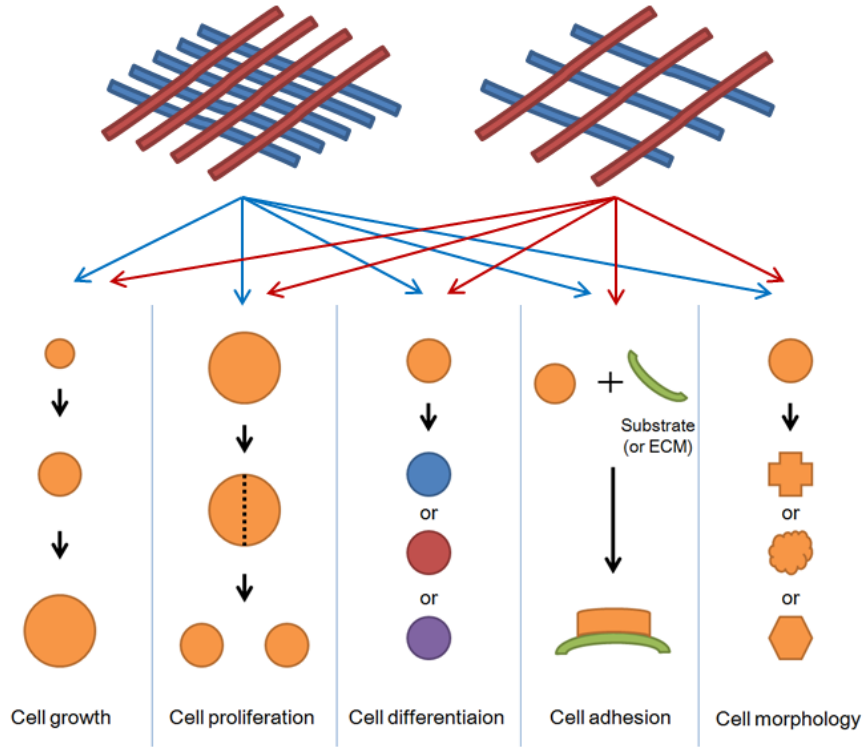

Figure 1.2. Schematic of hydrogels mimicking ECM controlling various cellular functions (e.g. cell growth, proliferation, differentiation, adhesion, and morphology), which are influenced by physical properties of hydrogels.

Although these methods have been widely used to engineer hydrogels with varying degrees of properties, it is still desirable to attain the controllability of multiple hydrogel properties by utilizing a multifunctional and tunable component. This is usually accomplished by the assembly of various modalities serving different purposes to fabricate hydrogels. For example, the rigidity of a hydrogel is controlled by the amount of crosslinking molecules used for the fabrications. [10-12] This method is also commonly used to control the hydrogel porosity for drug delivery applications, as the crosslinking density influences both factors inversely. [9, 13, 14] Also, increasing fracture toughness and structural durability as well as imparting novel functionalities of a hydrogel is often accomplished by creating interpenetrating networks or composite formation using various nanomaterials as fillers. [15-17]

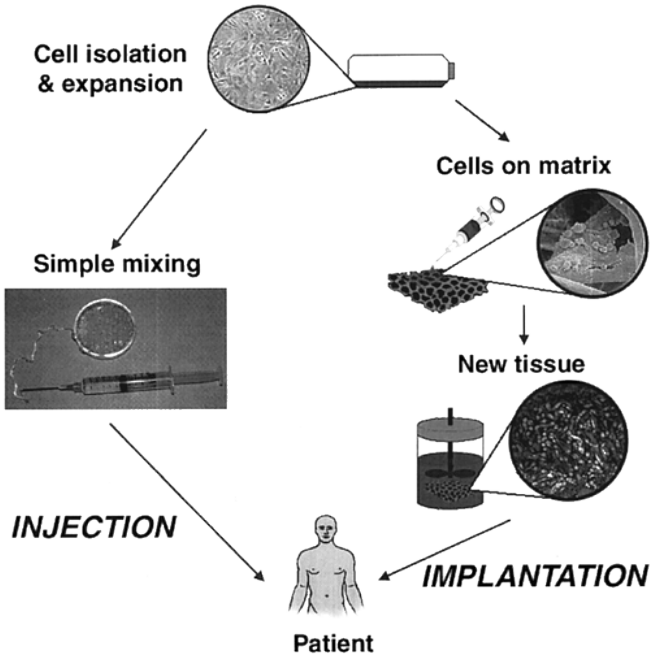

Figure 1.3. Schematic of a tissue engineering strategy. [8] [*Permission has been obtained from publisher.]

1.2. Mechanical properties of hydrogels

Hydrogels demonstrate different ranges of mechanical properties, depending on the physical parameters of polymers (e.g. molecular weight, degree of functional group substitution, concentration) and crosslinking density. Hydrogels can be classified into physical hydrogels or chemical hydrogels based on the mode of crosslinking. Physical hydrogels often display reversible gelation behavior, due to the reversibility of the physical force involved with the crosslinking. For example, the degree of molecular entanglement, environmental temperature with hydrophilicity change related to an upper critical solution temperature (UCST) and lower critical solution temperature (LCST), pH change with the degree of hydrogen bonding, and ionic interaction between polycation and polyanion or between polyelectrolyte and multivalent ion have all shown to drive the reversibility. [8] Their mechanical properties can be controlled by polymer chain length and its topology, temperature-sensitive or pH-sensitive segments in a polymer chain, and concentration of polyelectrolyte or ions. On the other hand, many of the chemical hydrogels are formed irreversibly as many chemical reactions used for crosslinking are irreversible in nature. Copolymerization between monomers, between monomer and macromers, or between macromers are used to fabricate hydrogels with various chemical reactions, such as radical polymerization, Michael reaction, and Schiff base formation. [8] Their mechanical properties can be controlled by monomer/macromer concentration or amount of the reactive functional groups, which are directly related to crosslinking density.

Bulk mechanical properties of hydrogels, such as elastic modulus and ultimate strength, are commonly characterized by applying compressive or tensile force on the hydrogels and measuring the accompanying deformation, mostly using a universal testing machine (UTM) (e.g. Instron® , MTS®) (Figure 1.4). This stress-strain relationship of a hydrogel is obtained at a constant compression or elongation rate. Elastic modulus (or Young's modulus) is calculated as the slope of stress-strain curve at the initial linear "elastic" region, which represents the stiffness of the sample. Beyond this region, the deformation is not reversible ("plastic deformation") and the curve deviates from the linearity. For most hydrogels, the elastic region lies within the first 10 % strain region. Also, toughness of a hydrogel can also be evaluated by the area under the same stress-strain curve, which represents the amount of absorbed energy to reach the point of fracture. Ultimate strength is defined as the highest stress point during the entirety of the curve, which also represents the toughness.

Rheology also provides valuable mechanical characterization of the hydrogels. A rheometer allows the measurement of elastic component, storage modulus (G'), and viscous component, loss modulus (G") of the hydrogel by applying cyclic shear stress. Various parameters of rheological measurements, such as amplitude and frequency of the stress, as well as the mode of experiment, such as frequency sweep and time sweep, can be controlled for more refined measurement of the viscoelasticity. [20] The rheology is especially useful for measuring the gelation kinetics, by

monitoring the change in G' and G'' during crosslinking reaction. The gelation time is defined as the time for the G' curve to cross over the G'' curve, which represents the dramatic rise in the elastic component.

Another hallmark of a hydrogel is the molecular diffusion through the polymeric network imbibing large quantity of water. The swelling behavior of a hydrogel when placed in an aqueous environment is governed by two mechanisms; osmotic pressure between the inner network and the surrounding fluid, and the chain relaxation of the polymeric network. Since mechanical properties of a hydrogel is mostly controlled by the crosslinking density, the swelling properties are inversely correlated with the mechanical properties; the higher the crosslinking density, the smaller the porosity and swelling. The degree of swelling is easily calculated as the mass ratio of the swollen hydrogel to the dried polymeric mesh. Scanning electron microscopy (SEM) is often employed to measure the porosity of the hydrogels. The diffusional properties is important for drug delivery applications, as it controls the drug release rate and overall release kinetics of drugs within the hydrogels. [9, 13, 14]

Mechanical properties of a hydrogel in tissue engineering are important not only for maintaining the structural integrity during the culture and eventual implantation, but also many different cell types are heavily influenced by the mechanical environment provided by the ECM. It has been shown that ECMs in different tissues have different stiffness. [21] For example, the ECM of a neural tissue is very soft, with the modulus ranging from 0.1 to 1 kPa, whereas that of a bone tissue is ~10^3 times stronger (Figure 1.5). [22, 23] Many studies reported that native or artificial ECM's mechanical properties directly affects cell functions, such as adhesion, proliferation, differentiation, gene expression, and even apoptosis. [24-26] The ability to form hydrogel by spontaneous ("in situ") reaction between polymeric components is also desired in the case of developing injectable hydrogel systems for not only tissue engineering scaffolds, but also as surgical sealants and hemostatic agents. This type of hydrogels utilizes chemical reaction such as Michael addition and Schiff base formation which occur in aqueous physiological conditions, and are mild enough to cause minimal inflammatory and immune response. [27] For this purpose, it is imperative to control of gelation kinetics and viscoelasticity of the hydrogels. The control of degradation rate of hydrogel is also important, as it is desired to allow native ECM to take over the tissue while the hydrogel is slowly removed from the site by degradation (this also avoids an invasive surgical procedure to remove the hydrogel). The degradation of a hydrogel is induced by presenting hydrolysable functional groups, such as esters and anhydrides.

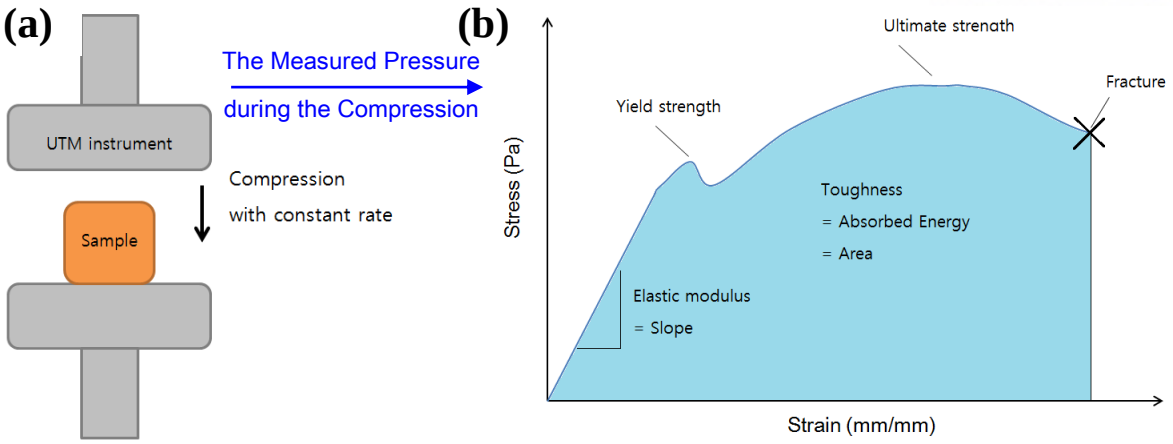

Figure 1.4. (a) Schematic of a compression test performed by UTM. (b) A typical stress-strain curve obtained from the compression test. Mechanical properties such as elastic modulus, ultimate strength, and yield strength are obtained.

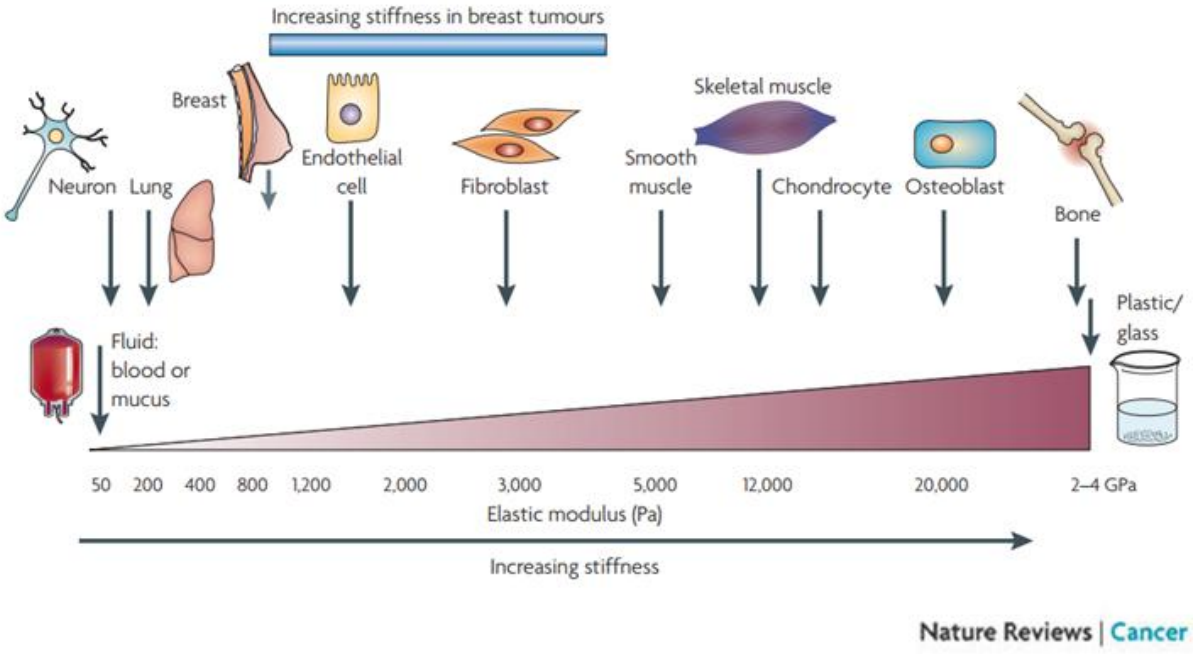

Figure 1.5. Variations in tissue stiffness. [23] [*Permission has been obtained from publisher.]

1.3. Brief history of polysuccinimide and polyaspartamide derivatives

The research presented in this thesis is focused on utilizing polysuccinimide (PSI) and its polyaspartamide derivatives for engineering hydrogels mimicking ECM. These polymers have several advantages for this purpose. First, the PSI is synthesized by acid-catalyzed polycondensation of aspartic acid, thus it is facile and capable of mass production. The molecular weight of PSI also can be easily controlled by the reaction condition (i.e. solvent composition). The polyaspartamide is conveniently derived from PSI by amine-mediated ring-opening nucleophilic addition; various functional groups involved with physical and chemical interactions, such as radical crosslinking, pi-pi stacking, pH- or thermosensitivity, for use as biocompatible materials can be conjugated to the backbone (Scheme 1.1). In addition, the polyaspartamide, a β-polypeptide, possesses biodegradability as well as biocompatibility.

The recent history of synthesizing polypeptide via organic synthesis goes back to mid-20th century, when several research groups had succeeded in synthesizing amino acids, which was in turn used to make polypeptide through thermal polycondensation reaction as an artificial protein motif and to elucidate origin of protein at the middle of 20th century. [28-30] For example, poly(glutamic acid) was first developed as a plasma expander for medical treatment, but its toxicity derived from the highly charged polymer chain in physiological pH was a critical issue. [31] Polysuccinimide synthesized from thermal condensation of L-aspartic acid was expected to solve this issue for the controllable charge density. Various polyaspartamide derivatives from PSI were developed, but most of the products were lost during dialysis step because of their low molecular mass and very fast hydrolysis properties. [30] Soon after in 1973, Gazze et al. had succeeded synthesizing PSI having molecular weight ranging from 10,000 to 90,000 g/mol, by using varying amounts of phosphoric acid (40 to 200 %) as catalyst. [32] Their report provided a synthetic route for high molecular weight PSI, but too much acid in the final product was hard to remove completely, restricting their use in biomedical applications. In the late 1990s, Kakuchi et al. reported the synthesis of PSI having controllable molecular weight, from 20,000 to 70,000 g/mol using mesitylene/sulfolane two-solvent system and a catalytic amount of phosphoric acid. [33, 34] This acid-removable and convenient one-step synthesis of PSI opened the door for more expansive applications of PSI and polyaspartamide derivatives in various industrial and scientific fields.

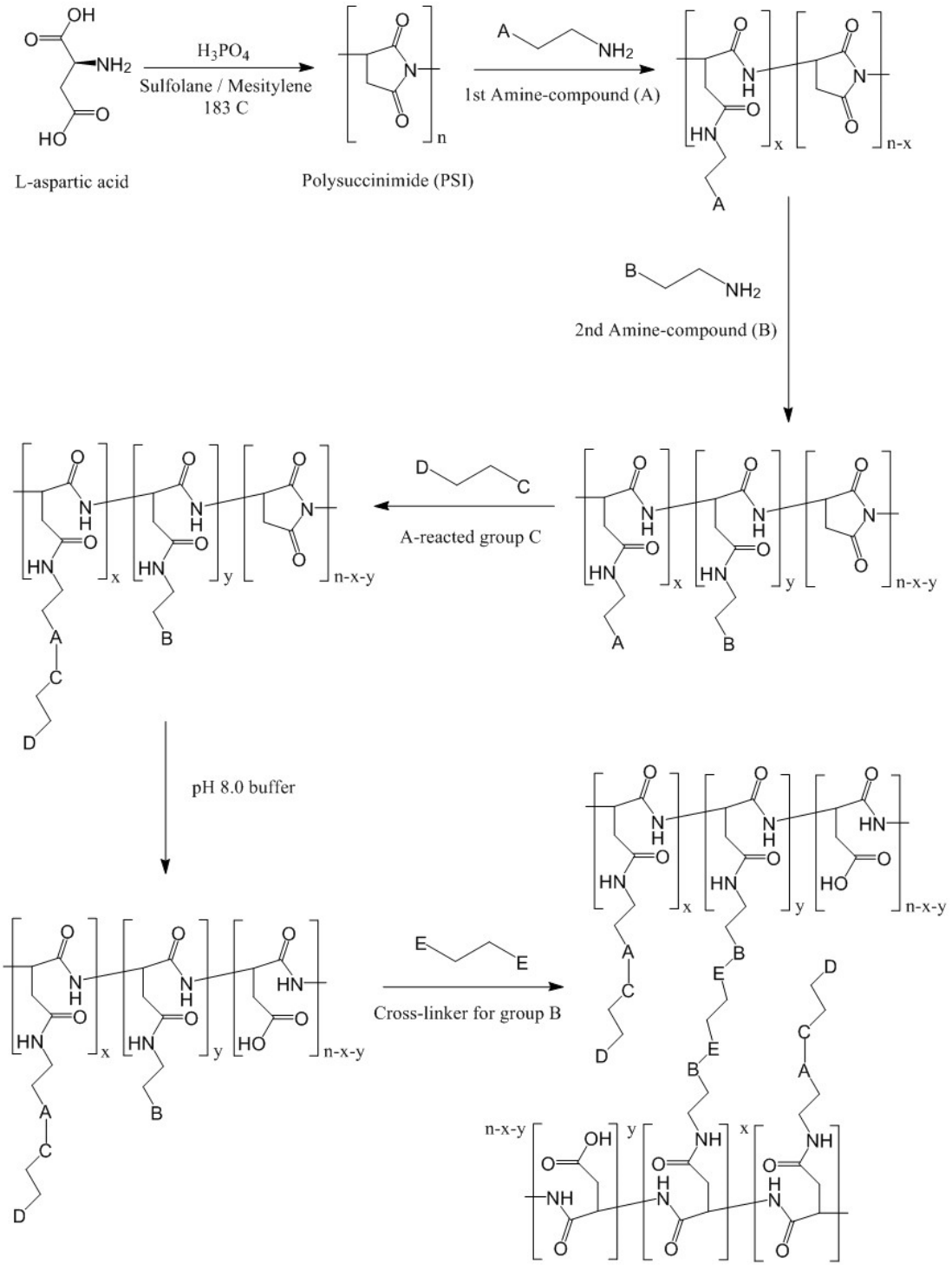

Scheme 1.1. Reactions for Polysuccinimide and its derivatives.

Subsequent studies on polyaspartamide derivatives have been largely focused on industrial applications utilizing their degradability and non-toxicity, such as dispersant, surfactant, absorbent resin with metal chelating and complexing agent, and even fertilizer. [35] For example, Yixin et al. reported polyaspartamide enhanced the yield of maize as green fertilizer based on its biodegradability and biocompatibility. [36] Wu et al. reported the chelating effect of polyaspartamide to calcium ion and calcite ($CaCO_3$). [37] Nakato et al. reported dodecylamine-modified polyaspartamide with its high magnesium oxide (MnO_2) disparity. [38] Furthermore, the use of polyaspartamide in biomedical engineering has been demonstrated, such as alkyl chain-linked polyaspartamide derivatives used to fabricate self-assembled nanoparticles for drug delivery applications. [39] These reports highlighted the broad applicability of polyaspartamide.

In the last decade, the biomedical application of polyaspartamide derivatives has increased significantly, to tissue engineering and biosensing. For example, in 2011 Cha et al. demonstrated polyaspartamide linked to microgels and bio-MEMS devices allowed the attachment of various cell-responsive proteins, as the proteins naturally containing amine groups for conjugation to the polyaspartamide having functional groups reactive towards a particular material. [40] Yan et al. develpoed a magnetic resonance imaging (MRI) contrast agents by conjugating gadolinium and porphyrin structure to polyaspartamide. [41] Self-assembled nanoparticles based on polyaspartamide derivatives for drug delivery and diagnostic applications have also been extensively investigated. Jeong et al. demonstrated the fabrication of self-assembled polymersomes using alkyl chain-grafted amphiphilic polyaspartamide laden with platinum for theranostic applications. [42, 43] Others have similarly reported the delivery of anti-tumor drugs, growth factors and genes using polyaspartamide-based carriers. [44-47]

With the tunable physicochemical and biological properties as well as facile synthetic routes of polyaspartamide derivatives as highlighted above, the research presented here was aimed at developing polyaspartamide-based hydrogels with varying mechanical and biological properties as well as biodegradation behavior for drug delivery and tissue engineering applications, which will be covered in detail in the next two chapters.

1.4. Summary

Extracellular matrix (ECM) is an essential component of tissue, controlling cellular activities; proliferation, differentiation, cell morphology by altering gene expression induced by signal transduction through ECM-integrin interactions. This natural scaffold dynamically interacts with cells and environment, so it is extremely difficult to recreate the exact ECM structures using artificial polymers. However, recent development in hydrogels have made it possible to mimic essential features of ECM for desired cell culture outcomes, and have become a powerful platform for tissue engineering and drug delivery applications. [8-10]

Needless to say, imparting biological functionality to hydrogels is necessary for its use as cell culture platform. However, it is also important to control the mechanical properties of hydrogels. It has been well established in the field of mechanobiology that cellular activities are directly affected by these properties. Also, drug delivery is commonly affected by hydrogel rigidity and porosity, as crosslinking density influences both factors. [9, 13, 14]

Polysuccinimide is a unique polymer which undergoes nucleophilic substitution with amine-based molecules, resulting in the conjugation of desired functional groups. [33-40] Polyaspartamide derivatives have been utilized in various biomedical applications in biomedical applications. It is expected that the versatility of this polymer can further give rise to a new collection of polyaspartamide derivatives with diverse functionalities for tailor-made biomaterials.

1.5. Reference

[1] Alberts, B; Johnson, A; Lewis, J. *Molecular Biology of the Cell*, 4th ed,; Garland Science, **2002**.

[2] Lee, C.H.; Singla, A.; Lee, Y. Biomedical applications of collagen. *Int. J. Pharm.* **2001**, 221, 1–22.

[3] Debelle, L.; Tamburro, A. M. Elastin: molecular description and function. *Int. J. Biochem. Cell.* Biol. **1999**, 31, 261-272.

[4] Hynes, R. O. Integrins: A family of cell surface receptors. *Cell* **1987**, 48 (4), 549-554.

[5] Ruoslahti, E.; Pierschbacher, M. D. New perspectives in cell adhesion: RGD and integrins. *Science* **1987**, 238 (4826), 491-497.

[6] Daley, W. P.; Peters, S. B.; Larsen, M. Extracellular matrix dynamics in development and regenerative medicine. *J. Cell Sci.* **2008**, 121 (3), 255–264.

[7] Tibbitt, M. W.; Anseth K. S. Hydrogels as Extracellular Matrix Mimics for 3D Cell Culture. *Biotechnol Bioeng.* **2009**, 103 (4), 655–663.

[8] Hoffman A. S. Hydrogels for biomedical applications. *Adv. Drug Deliv. Rev.* **2012**, 64, 18-23.

[9] Hoare, T. R.; Kohane, D.S. Hydrogels in drug delivery: progress and challenges. *Polymer.* **2008**, 49, 1993-2007.

[10] Drury, J. L.; Mooney, D. J. Hydrogels for tissue engineering: scaffold design variables and applications. *Biomaterials.* **2003**, 24, 4337-4351.

[11] Lee, K. Y.; Rowley, J. A.; Eiselt, P.; Moy, E.M.; Bouhadir, K. H.; Mooney, D. J. Controlling mechanical and swelling properties of alginate hydrogels independently by cross-linker type and cross-linking density. *Macromolecules.* **2000**, 33, 4291-4294.

[12] Cha, C.; Kohman, R. H.; Kong, H. Biodegradable polymer crosslinker: independent control of stiffness, toughness, and hydrogel degradation rate. *Adv Funct Mater.* **2009**, 19, 3056-3062.

[13] Weber, L. M.; Lopez, C.G.; Anseth, K. S. Effects of PEG hydrogel crosslinking density on protein diffusion and encapsulated islet survival and function. *J Biomed Mater Res A.* **2009**, 90A, 720-729.

[14] Satish, C. S.; Satish, K.P.; Shivakumar, H. G. Hydrogels as controlled drug delivery systems: Synthesis, crosslinking, water and drug transport mechanism. *Indian J Pharm Sci.* **2006**, 68, 133-140.

[15] Dragan, E. S. Design and applications of interpenetrating polymer network hydrogels. A review. *Chem Eng J.* **2014**, 243, 572-590.

[16] Schexnailder, P.; Schmidt, G. Nanocomposite polymer hydrogels. *Colloid Polym Sci.* **2009**, 287, 1-11.

[17] Ju, H. K.; Kim, S. Y.; Kim, S. J.; Lee, Y. M. pH/temperature-responsive semi-IPN hydrogels composed of alginate and poly(N-isopropylacrylamide). *J Appl Polym Sci.* **2002**, 83, 1128-1139.

[18] Hern, D. L.; Hubbell, J. A. Incorporation of adhesion peptides into nonadhesive hydrogels useful for tissue resurfacing. *J Biomed Mater Res.* **1998**, 39, 266-276.

[19] Fittkau, M. H.; Zilla, P.; Bezuidenhout, D.; Lutolf, M. P.; Human, P.; Hubbell, J. A.; Davies, N. The selective modulation of endothelial cell mobility on RGD peptide containing surfaces by YIGSR peptides. *Biomaterials.* **2005**, 26, 167-174.

[20] Zuidema, J. M.; Rivet, C. J.; Gilbert, R. J.; Morrison, F. A. A protocol for rheological characterization of hydrogels for tissue engineering strategies. *J. Biomed. Mater. Res. B. Appl. Biomater.* **2014**, 102 (5), 1063-1073.

[21] Black, L. D.; Allen, P. G.; Morris, S. M.; Stone, P. J.; Suki, B. Mechanical and Failure Properties of Extracellular Matrix Sheets as a Function of Structural Protein Composition. *Biophys. J.* **2008**, 94 (5), 1916–1929.

[22] Cox, T .R.; Erler J. T. Remodeling and homeostasis of the extracellular matrix: implications for fibrotic diseases and cancer. *Dis. Model. Mech.* **2011**, 4(2), 165-78

[23] Butcher, D. T.; Alliston, T.; Weaver, V. M. A tense situation: forcing tumour progression. *Nat. Rev. Cancer* **2009**, 9, 108-122.

[24] Du, J.; Zu, Y.; Li, J.; Du, S.; Xu, Y.; Zhang, L.; Jiang, L.; Wang, Z.; Chien, S.; Yang, C. Extracellular matrix stiffness dictates Wnt expression through integrin pathway. *Sci Rep.* **2016**, 6, 20395.

[25] Khatiwala, C. B.; Peyton, S. R.; Putnam, A. J. Intrinsic mechanical properties of the extracellular matrix affect the behavior of pre-osteoblastic MC3T3-E1 cells, *Am. J. Physiol.* **2006**, 290 (6), 1640-1650.

[26] Hadjipanayi, E.; Mudera, V.; Brown, R.A. Close dependence of fibroblast proliferation on collagen scaffold matrix stiffness. *J. Tissue Eng. Regen. Med.*, **2009**, 3, 77-84.

[27] Yu, L.; Ding, Injectable hydrogels as unique biomedical materials. *J.Chem. Soc. Rev.*, **2008**, 37, 1473-1481.

[28] Wolff, J. Ueber Asparaginsäure aus Aepfelsäure, *Justus Liebigs Annalen der Chemie*. **1850**, 75, 294.

[29] Fox, S. W. ; Johnson, J. E.; Middlebrook, M. Pyrosynthesis of Aspartic Acid and Alanine from Citric Acid Cycle Intermediates1 *J. Am. Chem. Soc.*, **1955**, 77, 1048.

[30] Harada, K., Polycondensation of Thermal Precursors of Aspartic Acid1, *J. Org. Chem.* **1959**, 24, 1662.

[31] Loebl, W. Y.; Ullmann, T. D.; Yaron, A.; Sela, M.; Berger, A.; Katchalski E. Evaluation of Multichain Polyglutamic Acid as a Possible Plasma Expander. *Proc. Soc. Exp. Biol. Med.* **1961**, 108, 661-663.

[32] Neri, P.; Antoni, G.; Benvenuti, F.; Cocoda, F.; Gazze, G. J. Synthesis of a,b-Poly [(2-hydroxyethyl)-D L-aspartamide] , a New Plasma Expander. *Med. Chem.* **1973**, 16, 893.

[33] Tomida, M.; Nakato, T.; Kuramochi, M.; Shibata, M.; Matsunami, S.; Kakuchi, T. Novel method of synthesizing poly(succinimide) and its copolymeric derivatives by acid-catalysed polycondensation of l-aspartic acid. *Polymer* **1996**, 37, 4435.

[34] Tomida, M.; Nakato, T.; Matsunami, S.; Kakuchi, T. Convenient synthesis of high molecular weight poly(succinimide) by acid-catalyses polycondensation of L-aspartic acid. *Polymer* **1997**, 38, 4733–4736.

[35] Thombre, S. M.; Sarwade, B. D. Synthesis and Biodegradability of Polyaspartic Acid: A Critical Review. *J. Macromol. Sci., Phys., Part A.* **2005**, 42, 1299–1315.

[36] Yixin, L.; Xinsheng, R.; Peihua, H. Study of the yield increasing of maize by using polyaspartic acid. *Journal of Maize Sciences* **2005**, 13 (3), 100-102.

[37] Wu, Y.; Grant, C. Effect of Chelation Chemistry of Sodium Polyaspartate on the Dissolution of Calcite. *Langmuir* **2002**, 18, 6813-6820.

[38] Nakato, T.; Tomida, M.; Suwa M.; Morishima, Y.; Kusuno A.; Kakuchi, T. Preparation and characterization of dodecylamine-modified poly(aspartic acid) as a biodegradable water-soluble polymeric material. *Polym. Bull.* **2000**, 44 (4), 385–391.

[39] Kang, H.S.; Shin, M.S.; Kim, J.D.; Yang, J.W. Self-aggregates of poly(aspartic acid) grafted with long alkyl chains. *Polym. Bull.* **2000**, 45 (1), 39–43.

[40] Cha, C.; Jeong, JH; Tang, X; Zill, AT; Prakash, YS; Zimmerman, SC. Top-down synthesis of versatile polyaspartamide linkers for single-step protein conjugation to materials. *Bioconjugate Chem.* **2011**, 22, 2377-2382.

[41] Yan, G.; Li, Z.; Xu, W.; Zhou, C.; Yang, L.; Zhang, Q.; Li, L.; Liu F.; Han, L.; Ge, Y.; Guo, J. Porphyrin-containing polyaspartamide gadolinium complexes as potential magnetic resonance imaging contrast agents. Int. J. Pharm. **2011**, 407, 119–125.

[42] Jeong, JH.; Cha. C; Kaczmarowski, A; Haan, J; Oh. S; Kong. H. Polyaspartamide vesicle induced by metallic nanoparticles. *Soft Matter.* **2012**, 8, 2237-2242.

[43] Lai, M-H; Jeong, JH; DeVolder, RJ; Brockman, C; Schroeder, C; Kong, H.; Ellipsoidal polyaspartamide polymersomes with enhanced cell-targeting ability. *Adv Funct Mater.* **2012**, 22, 3239-3246.

[44] Moon, J. R.; Kim, M. W.; Kim, D.; Jeong, J. H.; Kim, J. Synthesis and self-assembly behavior of novel polyaspartamide derivatives for anti-tumor drug delivery. *Colloid. Polym. Sci.* **2011**, 289, 63–71.

[45] Kim, Y.; Singh, B.; Jiang, H.; Park, T.; Jiang, T.; Park, I,; Cho, M.; Kang, S.; Choi, Y.; Cho, S. N-acetylglucosamine-conjugated block copolymer consisting of poly(ethylene oxide) and cationic polyaspartamide as a gene carrier for targeting vimentin-expressing cells. *Eur. J. Pharm. Sci.* **2014**, 51, 165–172.

[46] Hill, M. R.; MacKrell, E. J.; Forsthoefel,C. P.; Jensen, S. P.; Chen, M.; Moore, G. A.; He, Z. L.; Sumerlin, B. S. Biodegradable and pH-Responsive Nanoparticles Designed for SiteSpecific Delivery in Agriculture. *Biomacromolecules*, **2015**, 16, 1276–1282.

[47] Matricardi, P.; Pitarresi, G.; Salvatore, F.; Meo, P. D.; Albanese, A.; Coviello, T.; Cencetti, C.; Fiorica, C.; Giammona, G. Mechanical characterization of polysaccharide/polyaminoacid hydrogels as potential scaffolds for tissue regeneration. *Macromol. Res.* **2011**, 19, 1264–1271.

[48] Pitarresi, G.; Fiorica, C.; Palumbo, F. S.; Rigogliuso, S.; Ghersi, G.; Giammona, G. Heparin functionalized polyaspartamide/polyester scaffold for potential blood vessel regeneration. *Biomed. Mater. Res. Part A*, **2014**, 102, 1334–1341.

Chapter 2. Polyaspartamide Hydrogels with Controllable Physical Properties

2.1. Abstract

Hydrogels are widely used in various biotechnology applications. To tailor to specific needs, various modification strategies are employed to tune their properties. Herein, a multifunctional polymeric crosslinker based on polyaspartamide is developed, which allows for the facile adjustment of the type and number of reactive functional groups to fit different reaction schemes and control the mechanical properties of the hydrogels. The amine-based nucleophiles containing desired functional groups are reacted with polysuccinimide to synthesize polyaspartamide crosslinkers. The crosslinking density and the concurrent change in mechanical and properties of the resulting hydrogels are controlled in a wide range only with the degree of substitution. The multivalency of the polyaspartamide linkers also allowed for the degradation of hydrogels by the unreacted functional groups involved in the chain lysis. Furthermore, the polyaspartamide crosslinker conjugated with cell-recognition molecules via the same conjugation mechanism (i.e. nucleophilic substitution) render the hydrogels cell responsive without having to additional processing steps. This polyaspartamide-based crosslinker is expected to provide an efficient and versatile route to engineer hydrogels with controllable properties for biomedical applications.

2.2. Experimental section

2.2.1. Synthesis of polysuccinimide (PSI)

Polysuccinimide (PSI) was synthesized by polycondensation of aspartic acid under acidic condition, following a procedure described in a previously published report. [1-3] Briefly, aspartic acid (50 g, 375.6 mmol, Kanto Chemical Co.) and ortho-phosphoric acid (23.4 mmol, Sigma Aldrich) were mixed in sulfolane (130 mL, Junsei Chemical Co.), and refluxed at 183 ℃ with mechanical stirring for 7 hours under dry N_2. Water being formed during the reaction was continuously removed with a Dean-Stark trap. After the reaction, the product was precipitated in methanol. This crude product was filtered and washed several times with deionized (DI) water to remove the remained sulfolane and phosphoric acid, and lyophilized to obtain the final product. The number-average (Mn) molecular weight of PSI is expected 22000 g mol^{-1}.

2.2.2. Synthesis of PHMCA; thiol linked polyaspartamide

Poly(2-hydroxyethyl-co-2-mercaptoethyl aspartamide) (PHMCA), a polyaspartamide presenting thiol groups, was synthesized by derivatizing PSI with a varying amount of nucleophile containing both amine and thiol via ring opening nucleophilic reaction, following a previously published procedure with modifications. [3, 4] Briefly, PSI (0.8 g, 8.247 mmol) was dissolved in dimethylformamide (5 mL, DMF, Samchun Chemical Co.). Ethanolamine (Sigma Aldrich) was first added and stirred overnight at 73 ^{o}C under dry N2 to first develop polyaspartamide with hydroxyl groups (i.e. poly(2-hydroxyethyl aspartamide), PHEA). Cysteamine-hydrochloride (2 eq. to the remaining unopened succinimidyl rings, Sigma Aldrich) and triethylamine (TEA, 3eq. to unopened ring, Sigma Aldrich,) were mixed in 20-mL glass vial with DMF (5 mL) and stirred 30 min at room temperature to separate cysteamine from the complex. The entire mixture including the generated TEA-hydrochloride salt was added to PHEA solution, with 2-mercaptoethanol (4 eq. to unopened ring, Kanto Chemical Co.) to prevent disulfide bond formation, and stirred 73 ^{o}C under dry N_2 during 2-days. Scheme 2.2 and Table 2.1 represents the chemical reactions and amount of the used chemicals, respectively. The solution was filtered to remove the remained salt, and extensively purified by 1-day dialysis (dialysis tubing with MWCO of 14,000, Sigma Aldrich). After lyophilization step, the final

product, poly(2-hydroxyethyl-co-2-mercaptoethyl aspartamide) (PHMCA), was obtained. The degree of substitution (DS) of thiol groups on PHMCA was confirmed by comparing the peak integration ratios from ^{13}C-NMR spectra, identifying characteristic peaks in FT-IR spectra, and verifying through a colorimetric 5,5′-Dithiobis(2-nitrobenzoic acid) (DTNB) assay. [5]

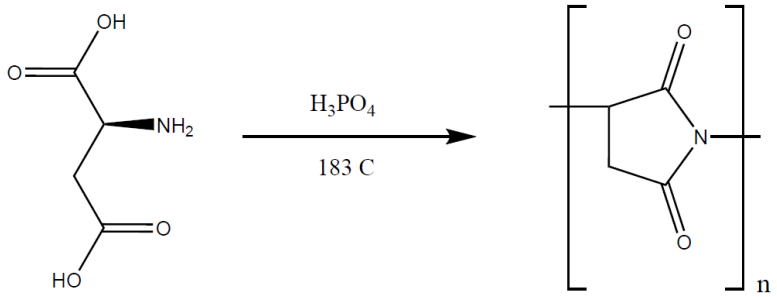

L-aspartic acid Polysuccinimide (PSI)

Scheme 2.1. Synthesis of polysuccinimide (PSI).

Polysuccinimide (PSI)	0.8 g			
Desired Thiol DS	20 %	40 %	60 %	80 %
Desired Hydroxyl DS	80 %	60 %	40 %	20 %
Ethanolamine (1 eq.)	398.2 uL	298.7 uL	199.1 uL	99.6 uL
Cysteamine-HCl (2 eq.)	0.375 g	0.750 g	1.124 g	1.499 g
Triethylamine (3 eq.)	0.690 mL	1.379 mL	2.069 mL	2.759 mL
2- Mercaptoethanol (4 eq.)	0.464 mL	0.929 mL	1.393 mL	1.858 mL

Table 2.1. Amount of the chemicals used to synthesize poly(2-hydroxyethyl-co-2-mercaptoethyl aspartamide) (PHMCA).

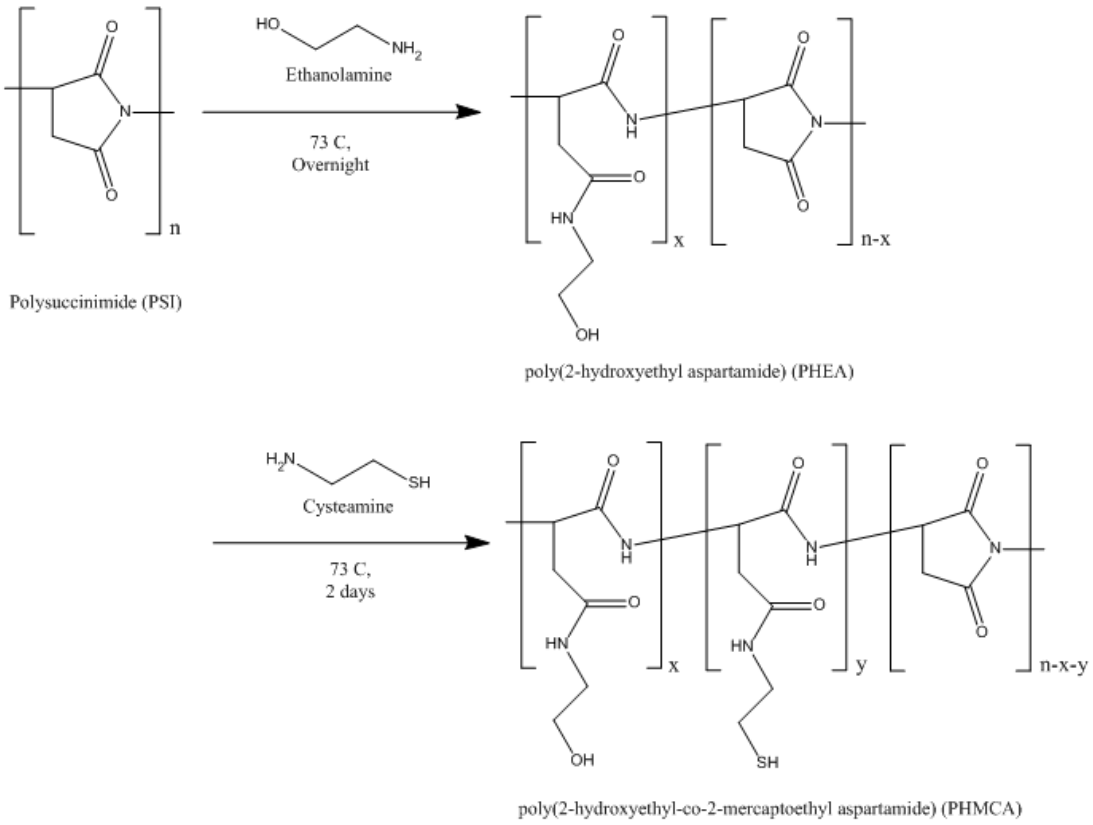

Scheme 2.2. Synthesis of poly(2-hydroxyethyl-co-2-mercaptoethyl aspartamide) (PHMCA).

2.2.3. Synthesis of PHHZA; hydrazide linked polyaspartamide

Polyaspartamide with hydrazide groups, termed poly(2-hydroxyethyl-co-hydrazidoadipoyl aspartamide) (PHHZA), is also synthesized by a similar procedure for PHMCA. PSI (0.8 g, 8.247 mmol) was dissolved in DMF (5 mL), and reacted with a desired amount of ethanolamine at 73 ^{o}C under dry N_2 during overnight. After then, adipic acid dihydrazide (AAD) (2 eq. to the unopened succinimidyl rings, Sigma Aldrich) was added to the solution with additional DMF (5 mL), and reacted at 73 ^{o}C under dry N_2 for 48 hours. The mixture was filtered to remove the remained AAD, and dialyzed extensively against DI water. The product was obtained by lyophilization. The DS of hydrazide groups on PHHZA was confirmed by comparing the peak integration ratios from ^{13}C-NMR spectra, identifying characteristic peaks in FT-IR spectra, and verifying through a colorimetric trinitrobenzene sulfonic acid (TNBS) assay. [6 ,7] Scheme 2.3 and Table 2.2 represent the chemical reactions and amount of used chemicals respectively.

Polysuccinimide (PSI)	0.8 g			
Desired Hydrazide DS	20 %	30 %	40 %	50 %
Desired Hydroxyl DS	80 %	70 %	60 %	50 %
Ethanolamine (1 eq.)	398.2 uL	348.4 uL	298.7 uL	248.9 uL
Adipic acid dihydrazide (2eq.)	0.575 g	0.862 g	1.149 g	1.437 g

Table 2.2. Amount of the used chemicals to synthesize poly(2-hydroxyethyl-co-hydrazidoadipoyl aspartamide) (PHHZA).

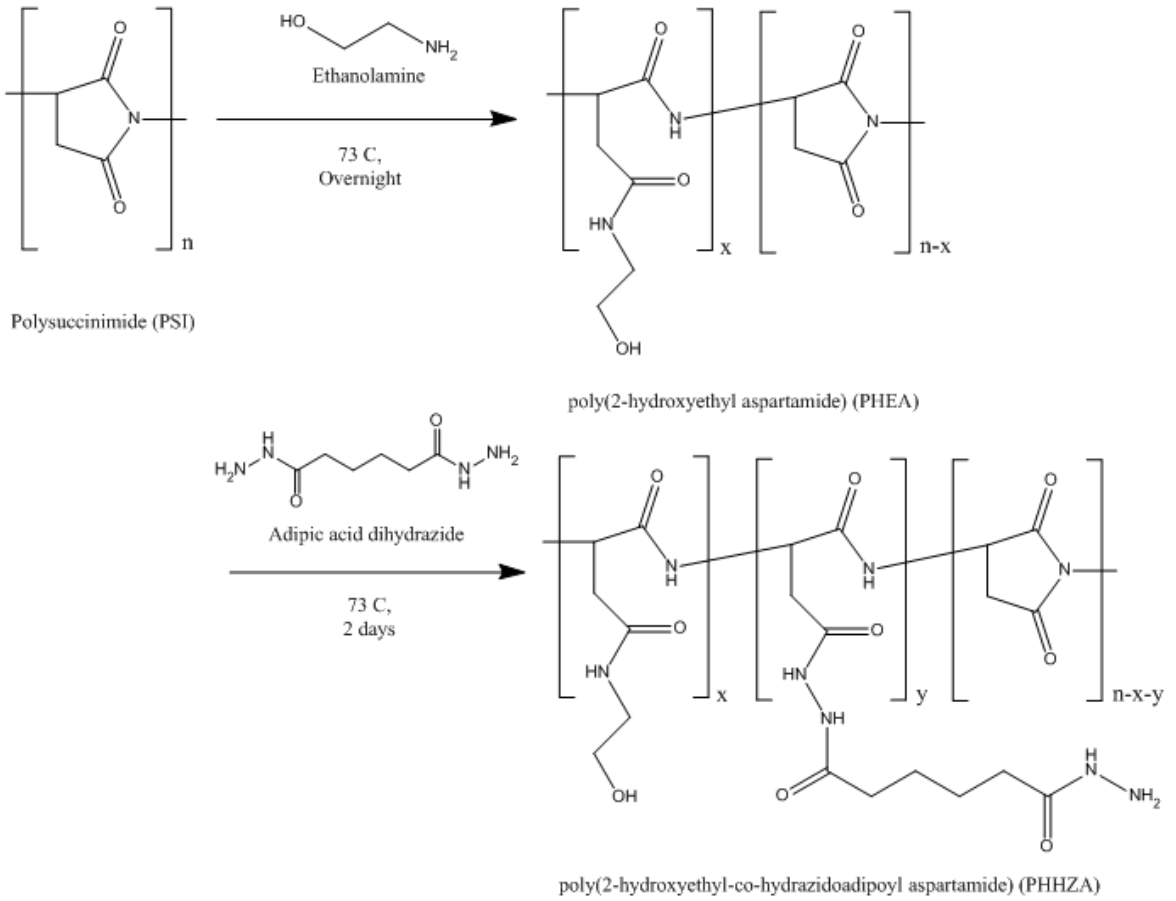

Scheme 2.3. Synthesis of poly(2-hydroxyethyl-co-hydrazidoadipoyl aspartamide) (PHHZA).

2.2.4. Synthesis of PHEDA; amine linked polyaspartamide

Polyaspartamide with amine groups, termed poly(2-hydroxyethyl-co-ethylenediaminoethyl aspartamide) (PHEDA), is also synthesized by the similar procedure for PHMCA and PHHZA. Because of high polarizability of the synthesized polymer, DMF solvent could not be used since the polymer showed self-aggregation phenomena. Therefore, dimethyl sulfoxide (DMSO, Samchun Chemical Co.), which has higher polarizability than DMF, was instead used. First, PSI (1.6 g) was completely dissolved in DMSO (10 mL). A desired amount of ethanolamine (1 eq. to the design) was added to the solution and stirred at 73 ^{o}C under dry N_2 overnight. Additional DMSO (10 mL) and desired amount of diethylenetriamine (2eq. to the unopened succinimidyl ring., Sigma Aldrich) were added to the solution and stirred at 73 ^{o}C under dry N_2 during 2-days. The solution was precipitated with excess diethyl ether (400 mL, Samchun Chemical Co.) and stirred during 30 min to remove DMSO solvent. This step was repeated once again. The precipitated polymer was dissolved in 30-mL DI water with stirring during 1 hour without cap to remove the remained solvent. After then, fifthly, the polymer solution was purified by 1-day dialysis against DI water. After lyophilization step, the DS of amine groups was confirmed by comparing the peak integration ratios from ^{13}C-NMR spectra, identifying characteristic peaks in FT-IR spectra, and verifying through TNBS assay. [6, 7] Scheme 2.4 and Table 2.3 represent the chemical reactions and amount of used chemicals respectively.

Polysuccinimide (PSI)	1.6 g			
Desired Amine DS	20 %	30 %	40 %	50 %
Desired Hydroxyl DS	80 %	70 %	60 %	50 %
Ethanolamine (1 eq.)	796.4 uL	696.8 uL	597.3 uL	497.8 uL
Diethylenetriamine (2eq.)	0.713 mL	1.069 mL	1.426 mL	1.782 mL

Table 2.3. Amount of the used chemicals to synthesize poly(2-hydroxyethyl-co-ethylenediaminoethyl aspartamide) (PHEDA).

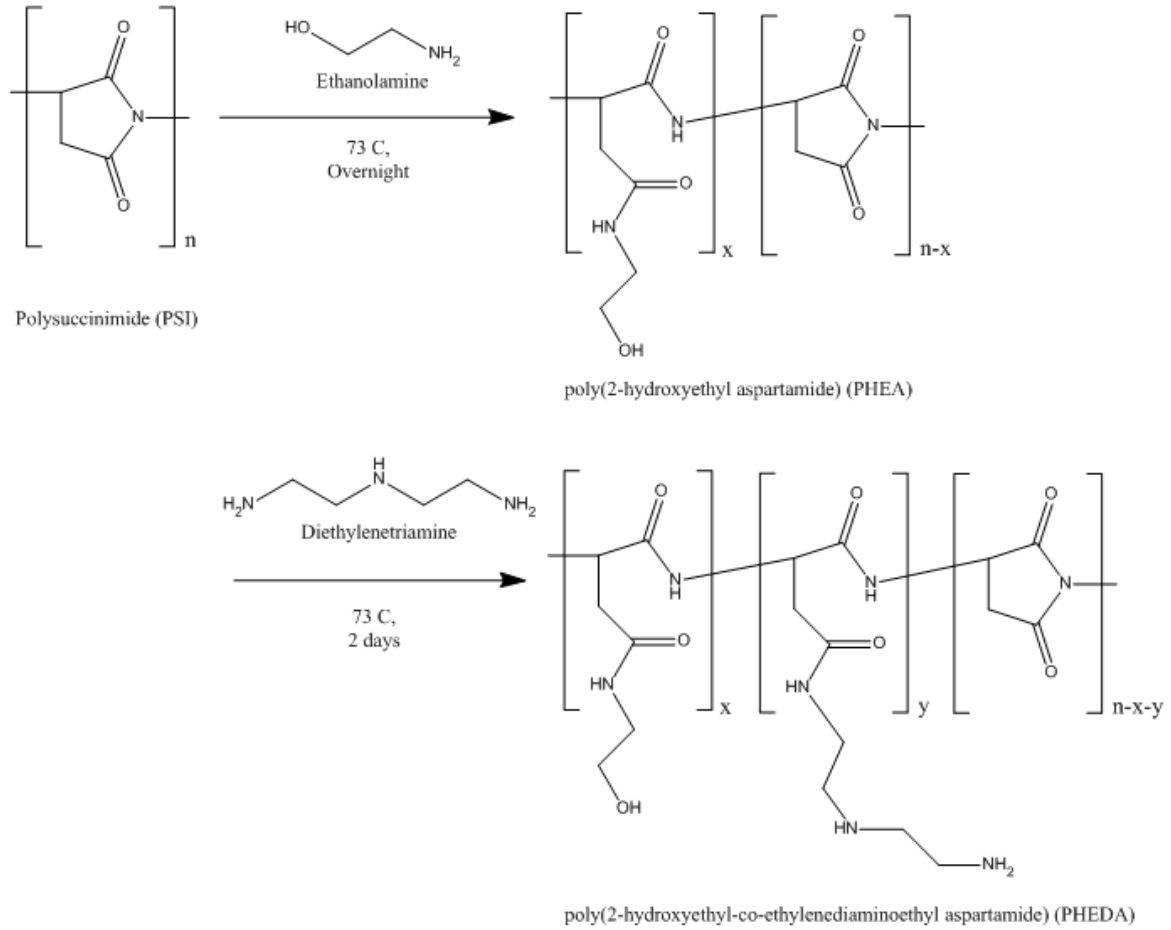

Scheme 2.4. Synthesis of poly(2-hydroxyethyl-co-ethylenediaminoethyl aspartamide) (PHEDA).

2.2.5. FT-IR measurement

FT-IR spectrometer (Model 670, Varian) was used to further characterize the polyaspartamide. All samples were measured by the attenuated total reflectance (ATR) mode with the wavenumber range from 650 to 4000 cm^{-1}.

2.2.6. FT-NMR measurement

400 MHz FT-NMR (Model AVANCE III HD, Bruker) was used to measure both ^{13}C-NMR and ^{1}H-NMR with deuterium oxide (Sigma Aldrich) as a solvent. In this experiment, all ^{13}C-NMR data was measured with C13IG mode that has decoupling but no Nuclear Overhauser Effect (NOE). This mode supports the nearly exact peak integration of ^{13}C-NMR spectrum, and uses to confirm the amount of carbon-attached functional groups in polyaspartamide derivatives.

2.2.7. DTNB assay

A colorimetric 5,5′-dithiobis(2-nitrobenzoic acid) (DTNB) assay, which is also called Ellman's test, was used to measure the amount of thiol groups in PHMCA [5] A DTNB stock solution was made by mixing 2 mM 5,5'-dithiobis(2-nitrobenzoic acid) (DTNB, Sigma Aldrich) and 50 mM sodium acetate (Sigma Aldrich), dissolved in DI water. For each test, 50 uL of DTNB stock solution, 100 uL of Tris buffer (1M, pH 8.0), 840 uL of DI water, and 10 uL of a sample were mixed. After 5 min incubation at room temperature, the 1,000 uL solution was moved in 96-well plate with 200 uL x 4, and measured the sample absorbance at 412 nm using UV/Vis spectrophotometer (Multiskan GO, Thermo Fisher). The standard curve was made by 2-mercaptoethanol (Kanto Chemical Co.). DS of thiol was determined by subtracting the absorbance of PHEA (hydroxyl group DS = 100 %) as a negative control from absorbance of PHMCA.

2.2.8. TNBS assay

Trinitrobenzene sulfonic acid (TNBS) assay measures the amount of amine and related functional groups. [6, 7] A TNBS stock solution was made by 0.01% picrylsulfonic acid (2,4,6-Trinitrobenzenesulfonic acid, TNBS, Tokyo Chemical Industry Co.) and 4% sodium bicarbonate (Junsei Chemical Co.) in DI water with final pH 8.5. For each test, 300 μL of the stock solution and 300 μL of a sample solution were mixed, and incubated 37 ^{o}C for 2 hours. After the addition of 300 μL of 1 M HCl addition to the working solution with de-gassing step, the mixture was moved to 96-well plate with 200 μL x 4 and measured the absorbance at 335nm using UV/Vis spectrophotometer (Multiskan GO, Thermo Fisher). The standard curve was made by ethanolamine. DS of hydrazide and amine was determined to subtract absorbance of PHEA (hydroxyl group DS = 100 %) from absorbance of PHHZA and PHEDA, respectively.

2.2.9. Hydrogel fabrication

The hydrogel was fabricated in between two glass slides with 1-mm thick spacer ("Sandwitch model", Figure 2.1). Due to the amphiphilic nature of polyaspartamide and the weakness of some of the hydrogel conditions, one of the glass slides were hydrophobic-coated using Sigmacoat® (Sigma Aldrich) to prevent the hydrogel from sticking to the surface. Sigmacoat was spread across the glass surface, and let it stand for 10 min to completely react the glass surface, and washed several times using water. 800 μL of precursor solution using a micropipette to the Sandwich model and incubated to fabricate the hydrogel. The 1-mm thickness polymer hydrogel was easily separated from glass without any damage.

To make hydrogel structure using polyaspartamide crosslinker, 0.1 M sodium phosphate buffer (Sigma Aldrich, pH 8.05) was used as default solvent. PSI was reported that its ring structure is opened by hydroxyl ion attack and becomes to polyaspartic acid. [2] pH 8.0 buffer is very mild base, but polysuccinimide can be converted to polyaspartic acid. Even though three polyaspartamide derivatives were synthesized with excess amine-compound (2 eq. to unopened ring), it is possible that some unopened-succinimide parts exist in the derivatives because of the steric hindrance for the nucleophilic addition. So the pH 8.0 buffer was used to finish the ring-opening reaction. In experiment, we observed that this buffer was really reduced kinetics for hydrogelation. The controllable gelation time was achieved by this buffer, compared to DI water, especially to PHHZA.

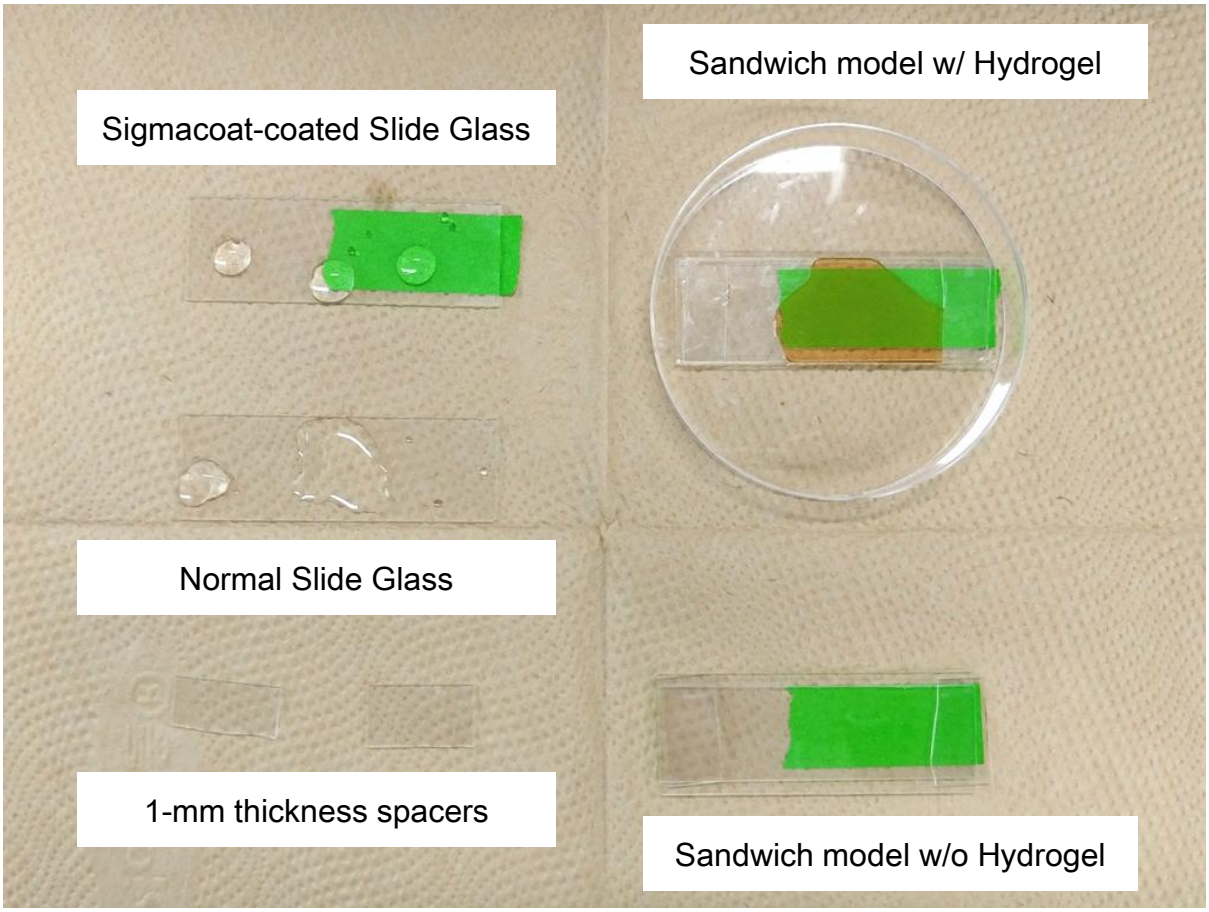

Figure 2.1. Sandwich model to fabricate hydrogel structure. The hydrophobic-coated glass slide was used to prevent the hydrogel from sticking to the surface.

2.2.10. Hydrogel made by PHHZA with natural polymer

To make hydrogel using PHHZA as crosslinker, we selected oxidized alginate (DS of aldehyde group = 40%) as a gel-forming macromer. The two solutions were mixed and incubated at 37 ^{o}C for 2 hours to form hydrogel by Schiff base formation between hydrazide group in PHHZA and aldehyde group in oxidized alginate (Scheme 2.5).

To make oxidized alginate with 40% of aldehyde group, firstly, 2 g sodium alginate (Junsei Chemical Co., S2245) was completely dissolved in 200 mL DI water at room temperature. 0.836 g sodium periodate (0.40 eq., Junsei Chemical Co.) was added to the solution, and stirred at 40 ^{o}C under dry N_2 for 1 day (Scheme 2.6). [3, 8, 9] After 3-days dialysis and lyophilization, the oxidized alginate was prepared.

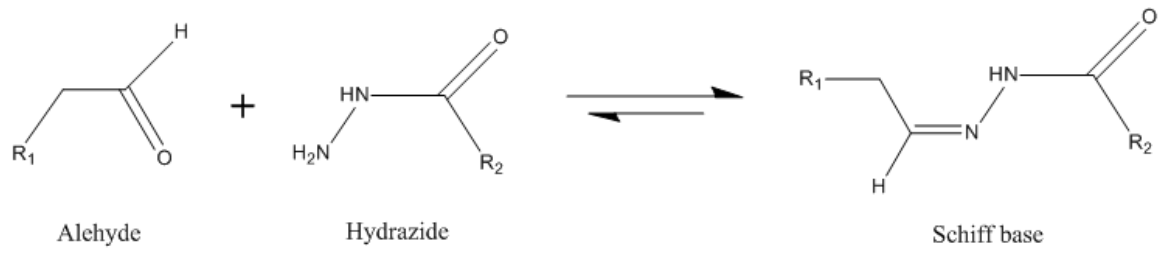

Scheme 2.5. Schiff base formation from aldehyde and hydrazide group.

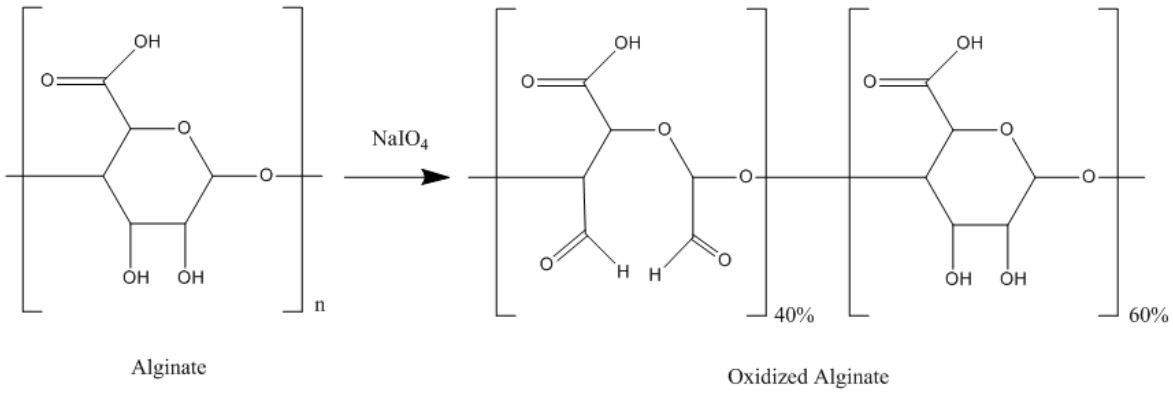

Scheme 2.6. Synthesis of oxidized alginate with aldehyde DS = 40%.

2.2.11. Hydrogel made by PHEDA with synthetic polymer

To make hydrogel using PHEDA as crosslinker, we selected poly(ethylene glycol) diacrlyate (PEGDA, Mn~700, Sigma Aldrich) as a gel-forming macromer (Scheme 2.7). The two solutions were mixed and incubated at 37 ^{o}C for 2 hours to form hydrogel through Michael addition reaction between amine group in PHHZA and acrylate group in PEGDA (Scheme 2.8)

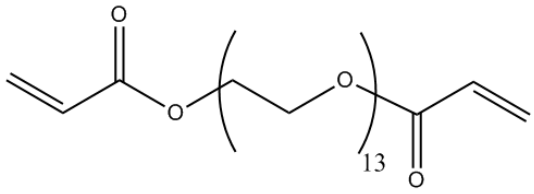

.

Scheme 2.7. Structure of PEGDA (Mn 700).

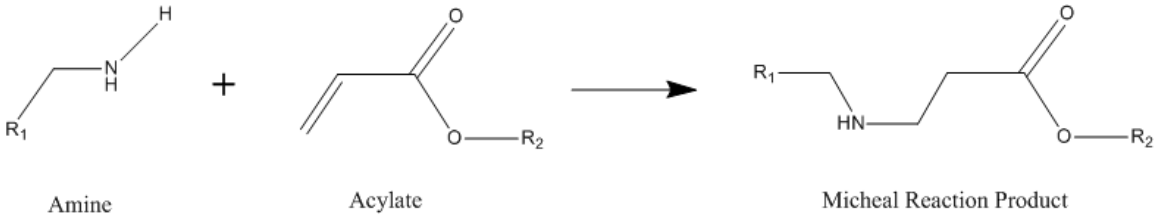

Scheme 2.8. Michael addition between amine and acrylate group.

2.2.12. Elastic modulus measurement

Mechanical properties of hydrogels were evaluated by calculating elastic moduli from stress-strain relationship obtained from uniaxial compression experiments. [10, 11] Briefly, the hydrogel disk was cut 5-mm diameter and subjected to uniaxial compressed at 1 mm min^{-1} (Model 3343, Instron®), and a stress-strain curve was obtained from converting force-compression curve. The elastic moduli were then calculated as the slope of the stress-strain curve at the first 10 % strain where the curve remained linear (the elastic region).

Three different conditions were used to measure the elastic modulus of hydrogels, which are summarized in Table 2.4. First, the hydrogel disks (5 mm diameter) were incubated in phosphate buffered saline (PBS) buffer at room temperature for 1 day prior to measuring the elastic moduli. This step led to equilibrium with the surrounding fluid and removed the unreacted molecules through diffusion.

Hydrogel degradation was monitored by measuring the change in elastic moduli over time. [12, 13] The hydrogel disks were swollen in PBS at 37 ^{o}C, and at various time points the moduli of the hydrogels were measured by uniaxial compression as described above. The degradation rate (k_d) of a hydrogel was determined by fitting the fractional change in moduli vs. time profile with the following an exponential decay model,

$$\frac{E_t}{E_0} = e^{-k_d \cdot t} \quad \text{..... (1)}$$

where E_t was the modulus measured at time, t, and E_0 was the initial modulus. [12] The elastic moduli of the hydrogels were measured without the incubation in PBS and used as a control.

	Incubation Temp	Incubation Time	Swelling Temp	Swelling Time
Method 1	37 ^{o}C	2 hours	Room Temp.	24 hours
Method 2	37 ^{o}C	2 hours	37 ^{o}C	Variable
Method 3	37 ^{o}C	Variable	-	-

Table 2.4. Three conditions for elastic modulus measurement.

2.2.13. Swelling ratio measurement

The swelling ratio of a hydrogel was calculated as the mass ratio of a swollen hydrogel (W_S) to its dried polymeric mesh (W_D) which was obtained by lyophilization. W_S was measured after incubating the hydrogel disk in PBS for 24 hours at room temperature, and W_D was measured after drying the disk by lyophilization.

$$\text{Swelling Ratio } (\%) = \frac{W_S - W_D}{W_D} \text{x} 100 \quad \ldots\ldots\ldots\ldots \ (2)$$

2.2.14. Scanning electron microscopy (SEM)

Scanning electron microscopy (SEM, S-4800, Hitachi) was used to image the difference of hydrogel structures depends on functional groups, degree of substitution, and concentration of polyaspartamide derivatives.

First the hydrogel samples were incubated in PBS buffer at room temperature for 1 day. Then the samples were frozen by soaking in liquid nitrogen to prevent the crystallization of water molecules in the gel, and quickly broken by tweezers to expose their cross-section. After lyophilization step, the samples were sputter-coated with platinum (E-1045, Hitachi), and visualized their inner structure.

2.2.15. Drug release measurement

Drug release profiles from various hydrogels were measured to evaluate their permeability. Fluorescein isothiocyanate conjugated bovine serum albumin (FITC-BSA) was used as a model protein drug in this study. Polyaspartamide hydrogel disks (8 mm diameter) were made with 5 mg/mL FITC-BSA with pH 8.0 buffer. Each hydrogel disk was placed in a well of a 24-well plate with 1 mL PBS buffer, and incubated at 37 ^{o}C. At each designated time point, the surrounding buffer was collected and analyzed for the amount of FITC-BSA released to the buffer. 100 μL of the acquired solution and 900 μL of PBS buffer were mixed and moved to 96-well plate (200 μL for each well). The fluorescence intensity was measured by multi-mode microplate reader (Synergy HTX, BioTek Instruements. Inc). All data was acquired by excitation at 485 nm and absorbance at 528 nm with gain value of 50. The cumulative drug release profile was fitted to the following two models,

$$\frac{M_t}{M_\infty} = k_1 \cdot t^n \quad \text{..... (3)}$$

$$\frac{M_t}{M_\infty} = 1 - e^{-k_2(t-T)^b} \quad \text{..... (4)}$$

where M_t is the amount of drug released at a time, t, M_∞ is the total amount of drug in the hydrogel, k_1 and k_2 are the kinetic rate constants, T is the lag time constant, n and b are the exponents related to the release mechanism. [14-16] The Ritger-Peppas model (Eq.(3)) was used for the power-law time dependence, while Weibull model (Eq.(4)) was used for the sigmoidal time dependence.

The BCA protein assay could not be used for the detection of unmodified BSA encapsulated in polyaspartamide-linked hydrogels. Since the polyaspartamide, a beta-polypeptide, is also capable of reaction with BCA, the degraded polyaspartamide released to the buffered solutions was also detected by the BCA assay, interfering with the accurate BSA analysis.

2.2.16. Solid state synthesis of GRGDS peptide

RGD motif peptide is well-known ligand for integrin and induced cell adhesion. [17] Here, GRGDS peptide (Scheme 2.7) was synthesized by a solid state synthesis (Scheme 2.8). Following chemicals were used; Wang resin, Fmoc-Arg(Tos)-OH (R), Fmoc-Asp(OtBu)-OH (D) , Fmoc-Gly-OH (G), Fmoc-Ser(tBu)-OH (S) (all purchased from BIOxAPE), 1,3-diisopropylcarbodiimide (DIC), 1-hydroxybenzotriazole (HOBt), triisopropylsilane (TIPS), ninhydrin, potassium cyanide (all purchased from Sigma Aldrich), phenol, piperidine, (all purchased from Junsei Chemical Co.), dichloromethane (DCM), 4-dimethylaminopyridine (DMAP), trifluoroacetic acid (TFA), and pyridine (all purchased from Samchun Chemical Co.)

First, we prepared three nynhydrin test solutions; Solution A (0.5 g ninhydrin with 10 mL ethanol), Solution B (8 g phenol in 2 mL ethanol), and Solution C (0.2 mL KCN (1 mM) in 9.8 mL pyridine). For each ninhydrin test to detect amine groups, a small amount of resin was moved to a 5-mL vial, washed by ethanol, and added 100 uL of each of the three solutions to the vial. After then a heat gun was applied to vial less than 1 min. The amine-protected resin showed yellow color, and amine-deprotected showed blue color.

To make peptide sequence using solid state synthesis, serine (S), the C-terminus amino acid in GRGDS, was linked to the Wang resin. The resin was swelled in DMF at room temperature for 1 hour in a 100-mL beaker. Fmoc-Ser(tBu)-OH (2 eq. relative to maximum capacity to resin) and DIC (2 eq.) are dissolved separately in DCM (10 mL) in a 25-mL round-bottom flask and stirred for 1 hour. DCM solvent is removed by rotary evaporation, and re-dissolved in DMF (20 mL). The solution is moved to resin-contained beaker with DMAP (0.1 eq.), and allowed resin-conjugation reaction for 2 h using a shaker. The procedure was repeated once more.

The resin was rinsed with 15 mL DMF for 10 minutes. Nynhydrin test was performed to confirm amino acid coupling (yellow). 15 mL of 20% piperidine in DMF was added to the resin and agitated for 10 min. This procedure was repeated three times. The resin was rinsed with 15 mL DMF for 10 min in two times. Nynhydrin test was performed to confirm deprotection (blue).

The next amino acid (2.5 eq.), Asp(OtBu)-OH (D), was dissolved in 100-mL beaker with DMF (20 mL). HOBt (2.5 eq.) and DIC (3 eq.) were also added to the beaker and stirred for 30 min. This solution is added to the deprotected resin and agitated for 3 hours. The resin was washed with DMF (3 × 20 mL), and checked the yellow color in nynhydrin test. This (1) resin deprotection, (2) amino acid activation, and (3) resin-amino acid coupling steps were processed in same way for subsequent amino acid conjugation. Table 2.5 presents the amounts of chemicals used.

After the last amino acid conjugation, the resin was rinsed with ethanol (20mL) three times and dried overnight in a desiccator. The resin was transferred to a 100-mL beaker and 20 mL of TFA/TIPS/H_2O (95: 2.5: 2.5) was added, and sealed it using parafilim. After 2 hours shaking at room

temperature, the solution was collected from the resin and moved to 250-mL round-bottom flask. TFA was removed by rotary evaporation. The residue solution was precipitated by 200 mL of diethyl ether and washed for 1 hour, and the precipitated white powder, peptide, was collected by a centrifuge machine with 8000 rpm for 5 min. The collection was re-dissolved in diethyl ether to remove TFA completely for two times more. The washed product was dried overnight in a desiccator.

The synthesized peptide was further analyzed by a matrix assisted laser desorption ionization-time of flight mass spectrometry (MALDI-TOF-MS, Model Ultraflex III, Brucker) based on m/z of GRGDS using α-cyano-4-hydroxycinnamic acid (HCCA, Sigma Aldrich) as a matrix. The solvent to both matrix and peptide was ethanol and acetonitrile (60 : 40). Expected m/z value of $[GRGDS+H]^+$ was 491.221.

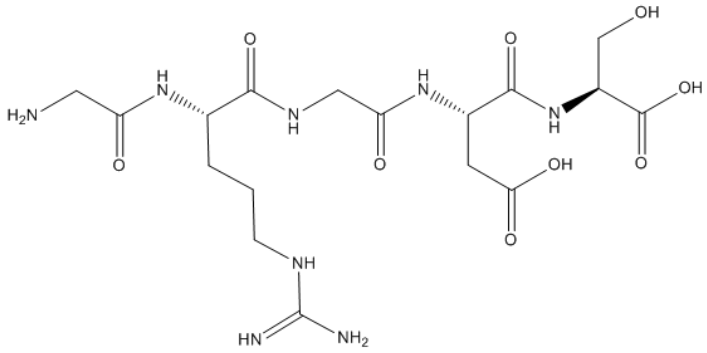

GRGDS peptide

Scheme 2.9. Structure of GRGDS peptide.

Wang resin		1.0 g
Resin's Maximum peptide capacity		1.2 mmol
Fmoc-Ser(tBu)-OH (S)	2.0 eq.	0.9203 g
DIC	2.0 eq.	371.6 uL
DMAP	0.1 eq.	0.0147 g
Fmoc-Asp(OtBu)-OH (D)	2.5 eq.	1.2344 g
Fmoc-Gly-OH (G)		0.8919 g
Fmoc-Arg(Tos)-OH (R)		1.6519 g
DIC	3.0 eq.	557.4 uL
HtOB	2.5 eq.	0.4053 g

Table 2.5. Amount of chemicals used to synthesize GRGDS peptide.

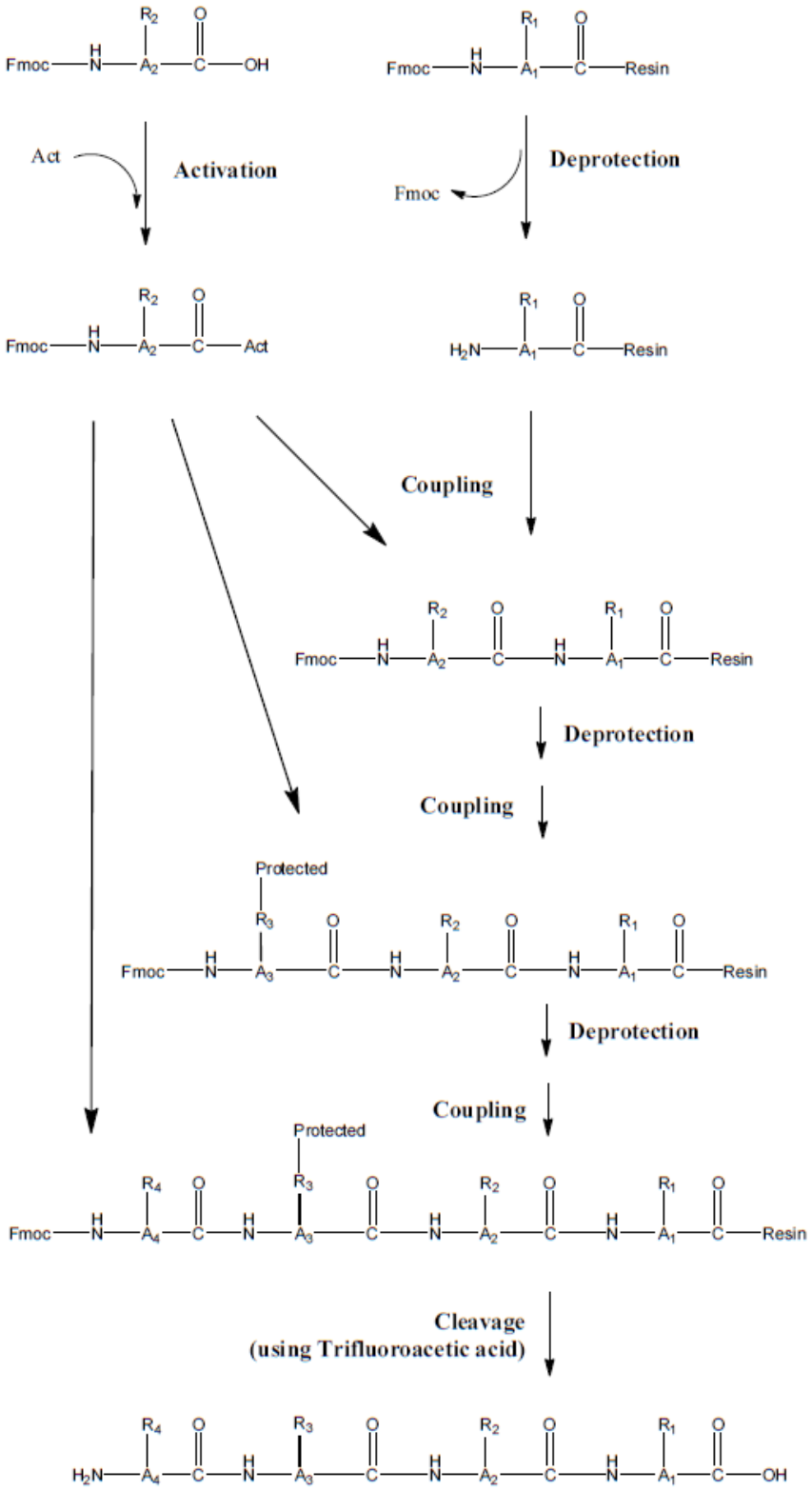

Scheme 2.10. Schematic of a solid state peptide synthesis.

2.2.17. GRGDS-peptide-conjugated polyaspartamide derivatives

The DS of GRGDS peptide to the polyaspartamide was set at 3% . The starting material, PSI, was completely dissolved in solvent at 73 ^{o}C under dry N_2, and GRGDS peptide was added and stirred for 7 hours. The amount of the ethanolamine to be used was reduced by the amount of GRGRDS peptide, and stirred for overnight (Table 2.6). After then, the amine-contained molecule was added in same methods with Section 2.2.3 and 2.2.4.

Polysuccinimide (PSI)	0.8 g			
Desired Functional DS	20 %	30 %	40 %	50 %
Desired GRGDS peptide DS	3%			
Desired Hydroxyl DS	77 %	67 %	57 %	47 %
GRGDS peptide	0.1212 g			
Ethanolamine (1 eq.)	383.3 uL	333.5 uL	283.8 uL	234.0 uL

Table 2.6. Amount of chemicals used to synthesize GRGDS-conjugated polyaspartamide derivatives.

2.2.18. Cell viability test

NIH/3T3 fibroblasts (ATCC) were used in this study, with the cell culture medium consisting of Dulbecco's Modified Eagle Medium (DMEM) supplemented with 10 % fetal bovine serum and 1 % penicillin/streptymycin (all purchased from Thermo Fisher). Culture condition was 37 ^{o}C with 5 % atmospheric CO_2.

To visualize the cells and evaluate their viability, the cells were treated with calcein-AM and ethidium homodimer-1 to label live (green fluorescence) and dead (red fluorescence) cells, respectively (LIVE/DEAD® Viability/Cytotoxicity Kit, Thermo Fisher). A fluorescence microscope was then used to visualize the cells (XDS-3FL, Optika). We measured the cell viability for Day 1 and Day 3.

Four methods were used to test the biocompatibility of the hydrogels. First, 3D encapsulation method was applied to the hydrogel system (Figure 2.2.a). Both polymer solutions were dissolved in DMEM (pH 8.0) to conserve cell viability during 2 hours of incubation for hydrogel fabrication. The cells were gently dispersed in the gel-forming macromer solution, either oxidized alginate or PEGDA, with the cell density of 2.0×10^6 cells/mL. The polyaspartamide solution was added and gently mixed using micropipette without vortexing in equal volumes, so the final cell density in the hydrogel became 1.0×10^6 cells/mL. The hydrogel was formed after incubation at 37 ^{o}C with 5% CO_2 environment for 2 hours. The hydrogel disks (8 mm diameter) were cut out as previously stated, and immersed in the cell culture media at 37 ^{o}C with 5% CO_2.

The cell encapsulation into the hydrogel was also accomplished by soaking the dried gel mesh with the cell solution (i.e. lyophilization-encapsulation method) (Figure 2.2.b). Briefly, polyaspartamide hydrogel was fabricated without the cells, and incubated in PBS for 1 day. Hydrogels were frozen quickly using liquid nitrogen and lyophilized to obtain the dried gel mesh having large pore size. The gel mesh was then soaked in a cell-containing culture medium in order to allow the cells to enter the mesh structure, resulting in a pseudo 3D microenvironment.

The cells were also cultured on the hydrogel surface (2D) (Figure 2.2.c). In this method, the cell solution (30,000 cells/mL) was placed into the well of a 12-well plate having hydrogel disks at the bottom on the surface to induce cell culture on the hydrogel surface.

To assess the ability of RGD-conjugated polyaspartamide to induce cell adhesion onto the hydrogel surface, the hydrogel disks linked with RGD-polyaspartamide was fabricated and used for 2D cell culture (Figure 2.2.d). In this method, the hydrogel was fabricated by oxidized alginate (aldehyde DS = 40%) crosslinked with adipic acid dihydrazide (AAD). Both 10% polymer solutions were mixed with same amounts and placed into the Sandwich model as described in section 2.2.9. Here, one glass slide without the hydrophobic coating was coated with 3 % polyaspartamide solution with or without RGD, by air drying the solution placed on the slide. Thus, the top of hydrogel was

chemically bonded via Schiff base formation between aldehyde in oxidized alginate and hydrazide/amine group in polyaspartamide derivatives. After overnight incubation at 37 ^{o}C to fabricate the hydrogel, the hydrogel disks were prepared and placed in 24-well plate. The hydrogel disks were treated with 0.5 M sodium borohydride (dissolved in PBS buffer, final pH 7.4, Samchun Chemical Co.) for 24 hours at room temperature to completely and irreversibly reduce the imine bond into secondary amine to prevent premature hydrogel degradation by reverse hydrolysis of Schiff base (Scheme 2.7), and washed the gel in several times by PBS buffer to remove the unreacted reagent. The cells were cultured on the hydrogels as stated above.

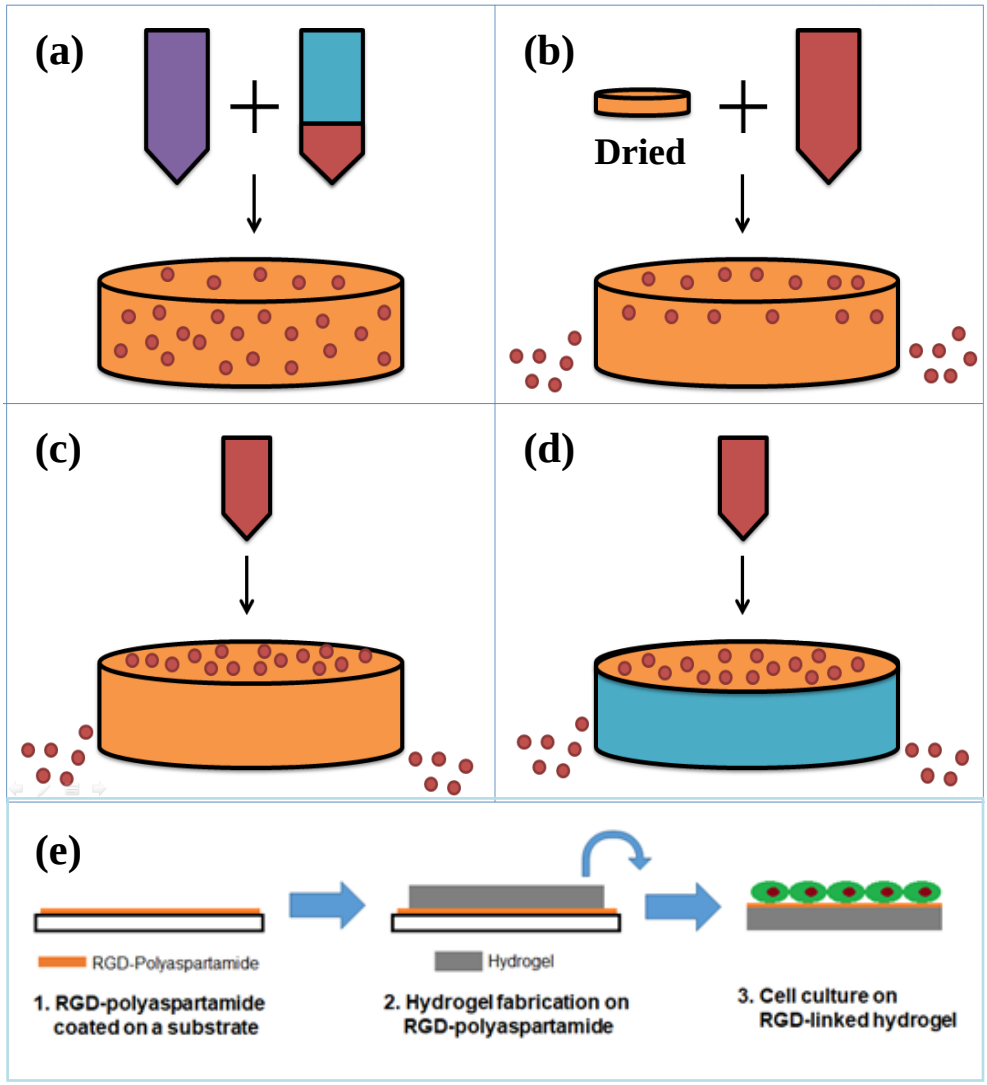

Figure 2.2. Cell viability test methods for evaluating the biocompatibility of hydrogels. (a) 3D cell encapsulation method. Cells (red) are dispersed in a gel-forming macromer solution (blue). The solution is mixed gently with polyaspartamide derivatives solution (purple) to fabricate the cell-encapsulated hydrogel (orange). (b) Lyophilization-encapsulation method. The fabricated hydrogel was lyophilized to prepare a dried gel mesh which was then re-swollen by cell-containing media to guide the cells into the hydrogel structure. (c) 2D cell culture method. Cell-contained solution is dropped to a hydrogel surface and incubated to allow cell adhesion onto the hydrogel surface. (d) The 2D cell culture method is applied to the hydrogel coated with polyaspartamide containing cell-responsive moieties (e.g. RGD) (blue). (e) Hydrogel fabrication with surface coating is depicted.

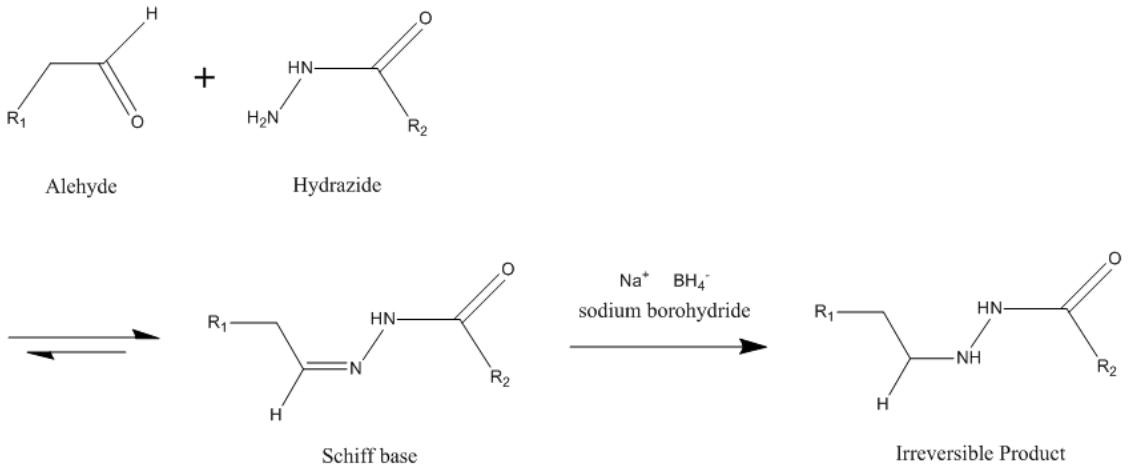

Scheme 2.11. Reduction of Schiff base (imine) by sodium borohydride to irreversibly generate secondary amine, and prevent the premature hydrogel degradation by the reverse hydrolysis of Schiff base.

2.3. Result and discussion

2.3.1. Characterization of PHEA

PSI consists of succinimidyl ring structures that could undergo nucleophilic substitution reaction with amine-based molecules, resulting in polyaspartamide formation. Therefore, the polyaspartamide backbone conjugated with the amine-based nucleophiles containing functional groups that can react with a particular gel-forming monomer or macromer could be utilized as the polymeric crosslinker to engineer hydrogels. Furthermore, the number of reactive functional groups on polyaspartamide could be controlled simply by adjusting the molar feed ratio of the nucleophile to the PSI. With this adjustable multivalency of a polyaspartamide crosslinker, it would be possible to control the crosslinking density of a polymeric network without having to change the concentration.

In this study, DMF and DMSO were used as solvents to make various polyaspartamide derivatives; PHMCA, PHHZA, and PHEDA. Many studies to functionalize PSI have been reported using DMF as a solvent, but the use of DMSO has not been reported. [1-4] In this study, DMSO was used as a solvent to synthesize PHEDA because its self-aggregation phenomena in DMF solvent occurred immediately after addition of DETA due to the strong hydrophilicity of the amine-rich polymer. Therefore, the solvent effect for DMF and DMSO solvent on the synthesis of PHEA, a polyaspartamide derivative with hydroxyl group and unopened succinimide rings, was first explored,.

FT-IR spectrum were measured for four PHEA samples, which are the designed hydroxyl group DS = 60% and 80% and made by DMF and DMSO solvent (Figure 2.3). The data showed that there was minimal difference in PHEA made by DMF and DMSO solvents. Also, ^{13}C-NMR spectra in Figure 2.4 and Table 2.7 showed the larger hydroxyl DS than anticipated, by approximately 5 %, likely due to the unexpected ring opening reaction during dialysis step. However, it was determined that the difference in hydroxyl DS was not significant enough to warrant further investigation.

Next, FT-IR spectra of DS-controlled PHEA samples made by DMF were also measured and presented in Figure 2.5 (a) and (b). The peaks in blue region are increasing because of the attached hydroxyl group; C-O stretching in the hydroxyl region (1060 cm^{-1}), N-H stretching (1535 cm^{-1}) and C=O stretching in the secondary amide (1650 cm^{-1}), C-H stretching (2940 cm^{-1}) and O-H stretching in the attached chain (3300 cm^{-1}). The red region, on the other hand, is decreasing because of the decreasing succinimide ring; fingerprint region of PSI (1150 – 1400 cm^{-1}), C=O stretching in the cyclic amide (1715 cm^{-1}). ^{13}C-NMR spectra in Figure 2.5 further demonstrated that the DS of hydroxyl group and unopened succinimidyl rings in polyaspartamide derivatives could be controlled in a wide range.

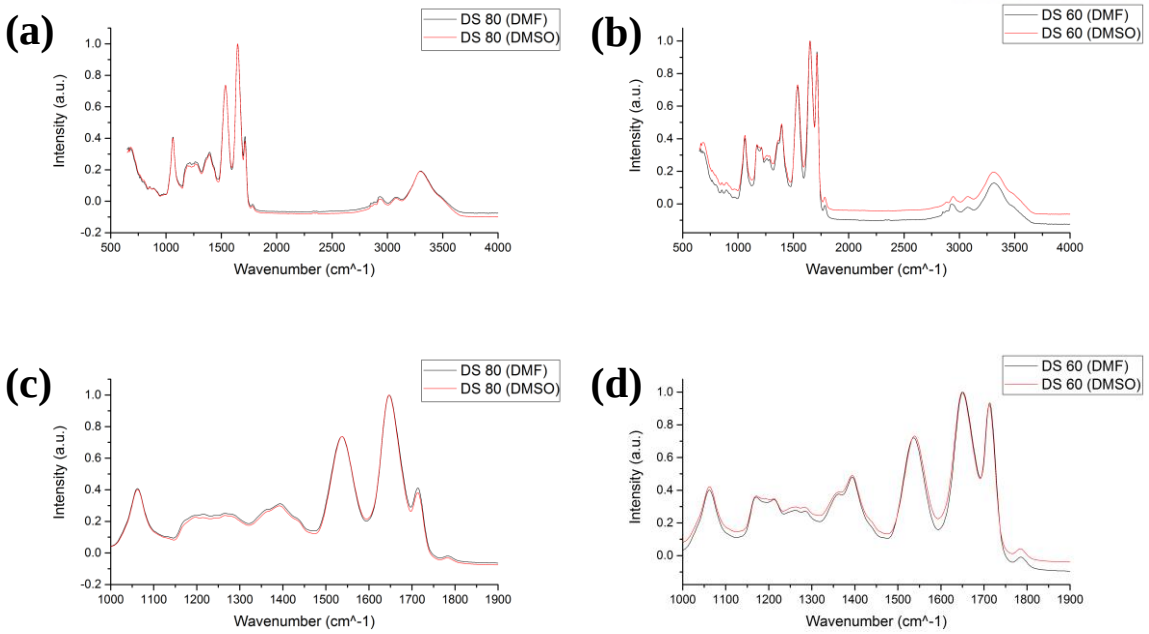

Figure 2.3. FT-IR spectrum of PHEA having (a) DS 80 and (b) DS 60 made with DMF and DMSO. The region between 1000 and 1900 cm^{-1} in (a) and (b) are magnified and presented in (c) and (d), respectively. All spectrums have been normalized.

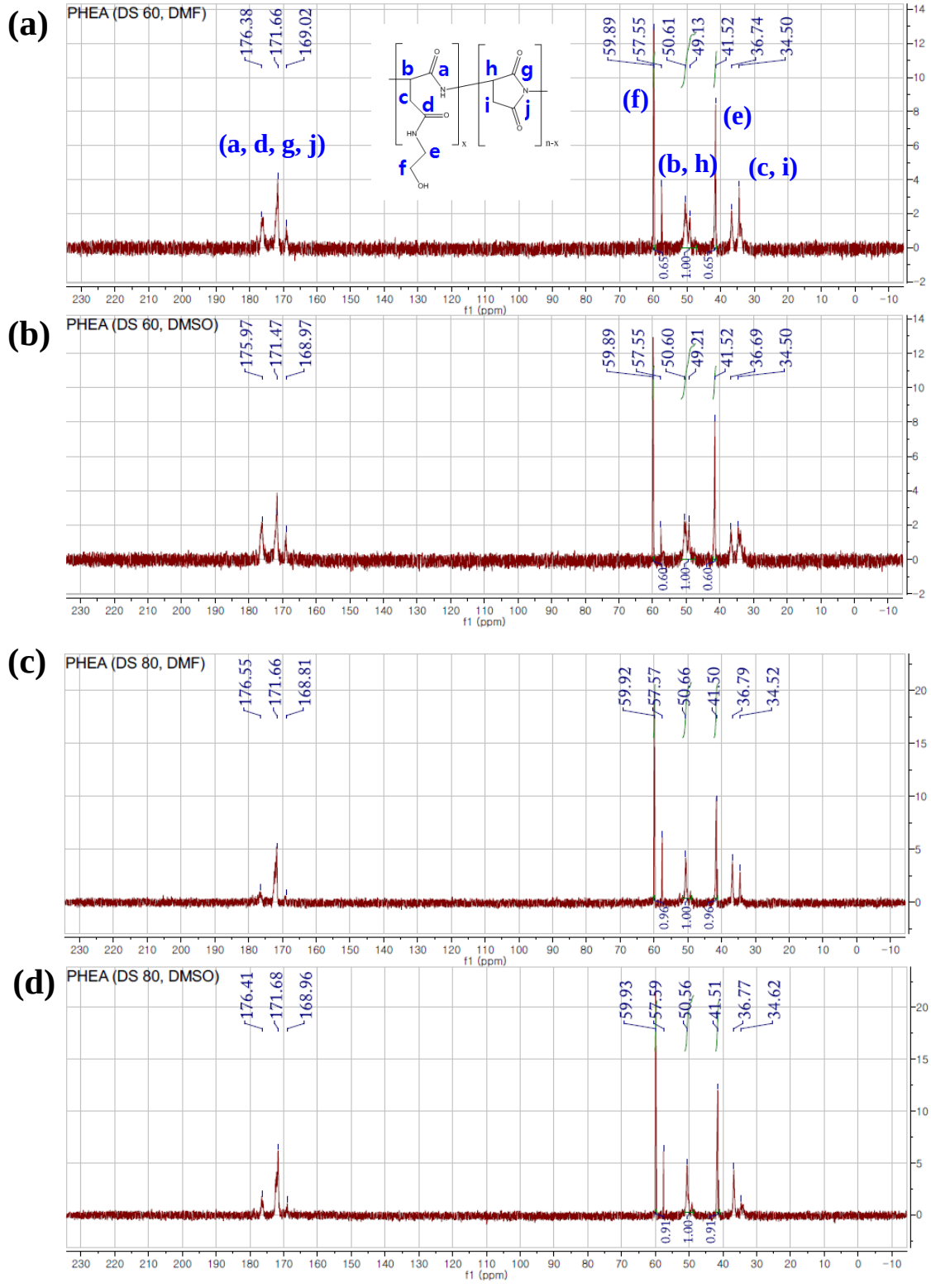

Figure 2.4. ^{13}C-NMR spectrum of PHEA. The theoretical DS of (a) 60 % and (b) 80 % made with DMF. The theoretical DS (c) 60 % and (d) 80 % made with DMSO.

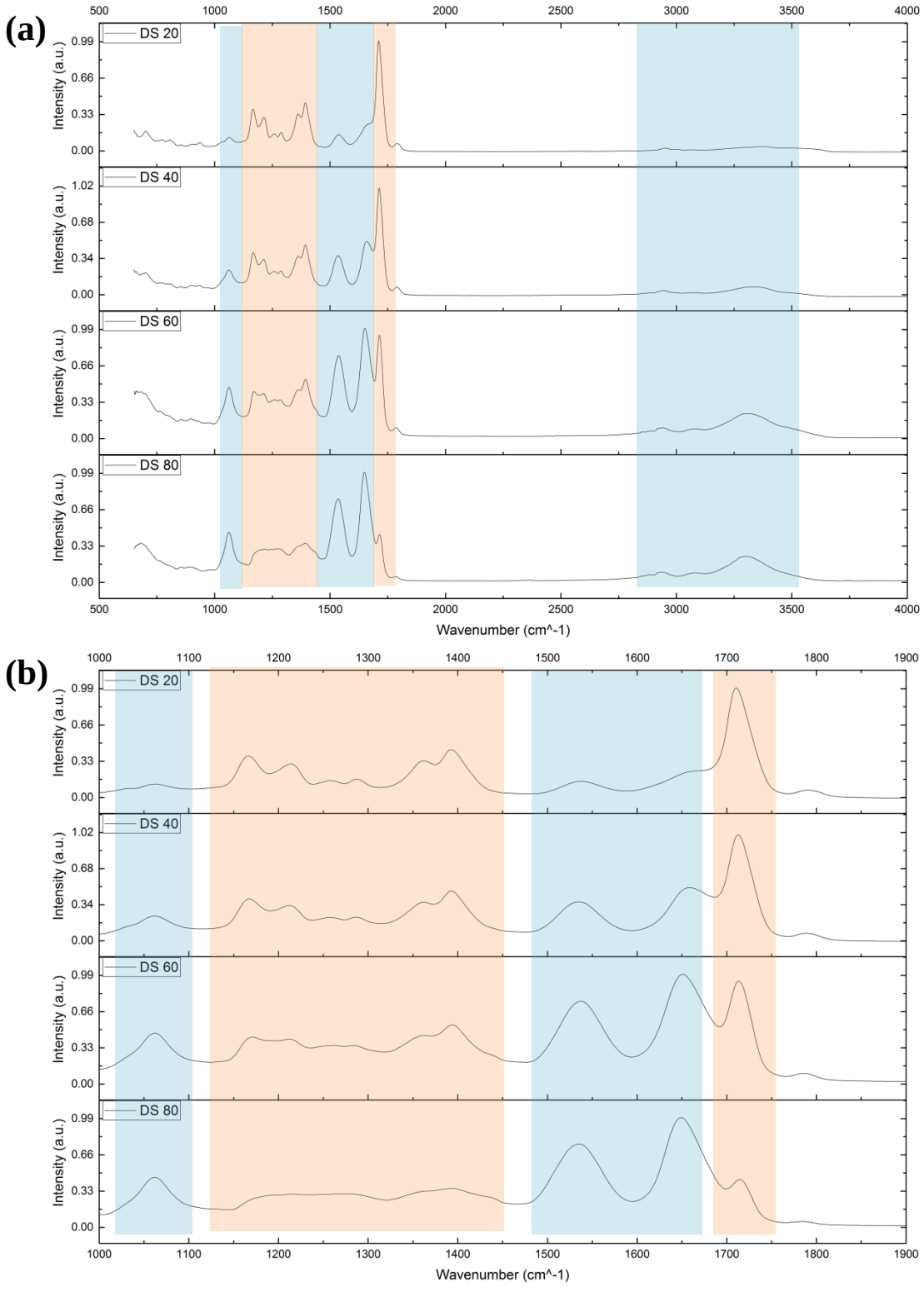

Figure 2.5. FT-IR spectrum of PHEA (DS = 50, 60, 70, 80) made with DMF, measured with ATR mode. Peaks in blue region are increasing with increasing DS. Peaks in red region are decreasing with increasing DS. (a) shows the full spectrum, and (b) shows the magnified region between 1000 cm^{-1} and 1900 cm^{-1}.

PHEA	DS of hydroxyl group	
Designed DS	60 %	80 %
DMF solvent	65 %	96 %
DMSO solvent	60 %	91 %
DS (DMF) – DS (DMSO)	5 %	

Table 2.7. DS of hydroxyl group in PHEA (DS = 60 and 80) made by DMF and DMSO, calculated by the integration ratio in ^{13}C-NMR spectrum in Figure 2.4.

2.3.2. Characterizations of PHMCA

First, we aimed to synthesize thiol-conjugated polyaspartamide for reaction with other polymers via thiol-ene reaction and disulfide bond formation. Thiol-ene reactions have several advantages, such as rapid reaction in mild condition, well-characterized mechanism, and relatively simple modifications from other functional groups to thiol/alkene. [18] Hydrogels made using this chemistry have been applied to tissue engineering and bio-sensor applications. [3] Disulfide bond has interesting aspects that can be explored in hydrogel synthesis. It is easily generated between thiol groups under oxidizing environment and even in air (e.g. disulfide bonds are common in proteins). It can be reversed back to thiols under reducing environment. [19] Therefore, this can be utilized to engineer dynamic reversible hydrogels for stimuli-responsive drug delivery systems.

The synthesized thiol group-linked polyaspartamide, poly(2-hydroxyethyl-co-2-mercaptoethyl aspartamide) (PHMCA), was analyzed via FT-IR, ^{13}C-NMR, and DTNB assay. FT-IR spectra for PHMCA showed the existence of very few unopened succinimide rings with small peak in 1715 cm^{-1} (C=O stretching in the cyclic amide), but any thiol peak (2400 – 2600 cm^{-1}) could not be observed (Figure 2.6). One of the possibilities was thiol-deactivation by disulfide bond formation (500 cm-1), but it was out of FT-IR instrument range and could not be observed. However, ^{13}C-NMR data showed very few amount of disulfide bond and thiol group, but a completely unknown peak at 8.3 ppm was also observed with strong intensity (Figure 2.7). For example, amount of pendent group in DS 1 is 80 % of –C-OH, 0 % -C-SH, 14 % of –C-S-S-C-, and 20% of unknown carbon peak to polyaspartamide backbone carbons. Also, amount of pendent group in DS 4 is 50 % of –C-OH, 5 % of –C-SH, 10 % of –C-S-S-C-, and 53 % of unknown carbon peak. This result implied that there was an unknown reaction to deactivate thiol groups during synthesis, which could not be verified. However, the amount of thiol determined by DTNB assay did demonstrate the control of DS of thiol from DS 1 to DS 6 (Figure 2.8, Table 2.8). It should be noted that the actual DS measured by the assay was much lower than the theoretical value.

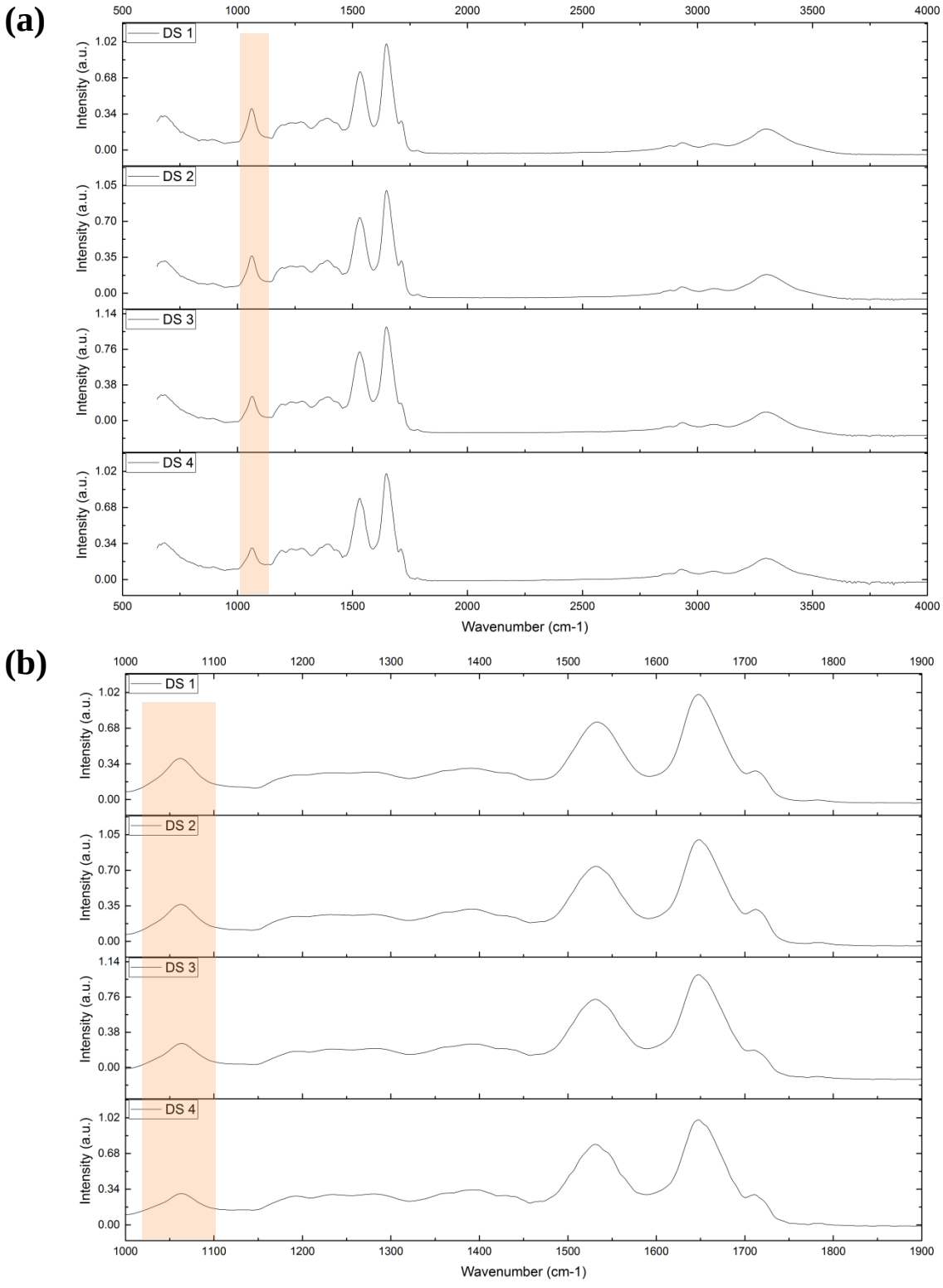

Figure 2.6. FT-IR spectrum of PHMCA (DS = 1, 2, 3, 4) measured by ATR method. Peaks in blue part are increasing with increasing DS. Peaks in red part are decreasing with increasing DS. Figure (a) is the measured full spectrum. Figure (b) is same with (a) but magnification from wavenumber 1000 cm^{-1} to 1900 cm^{-1}.

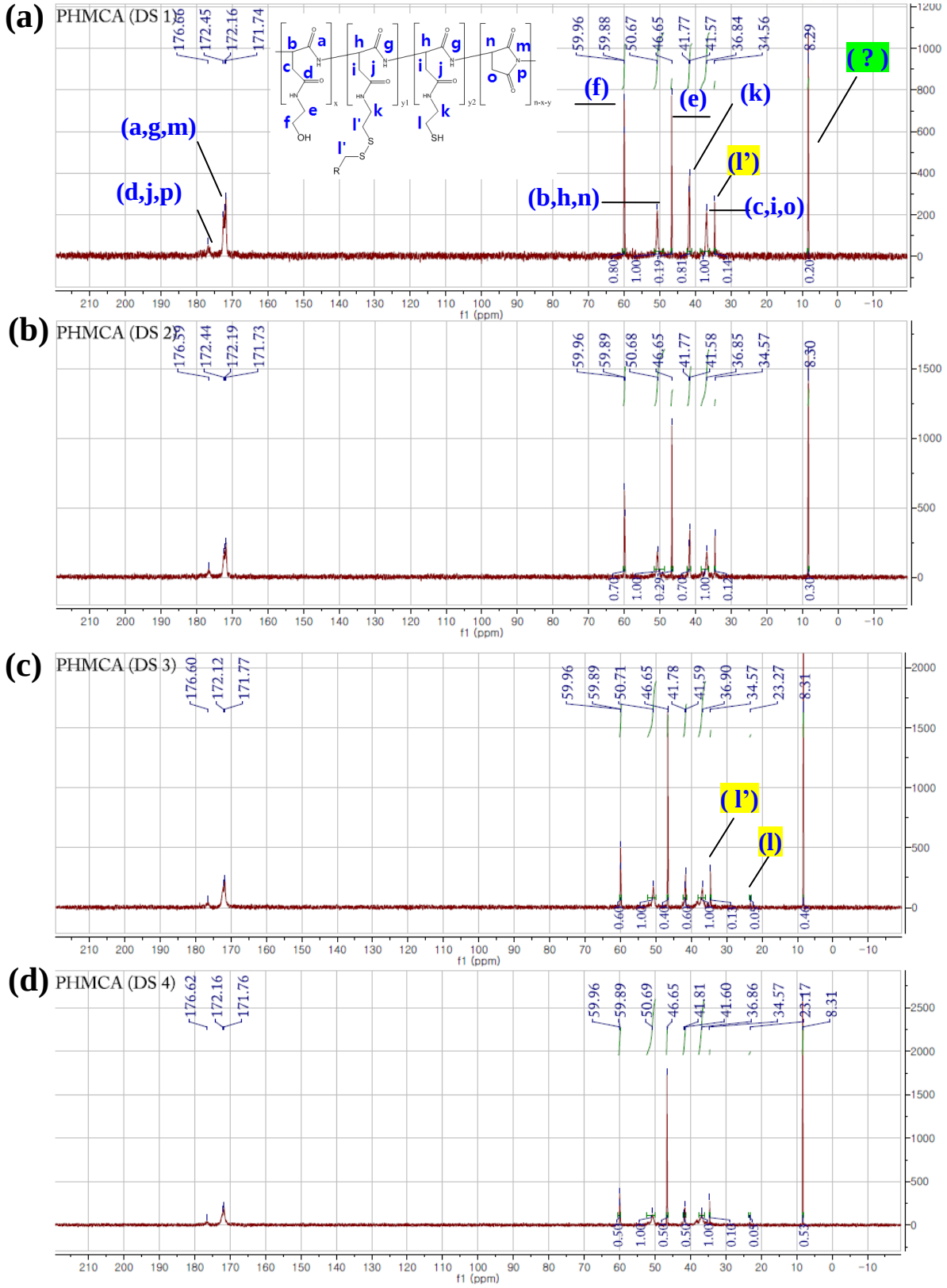

Figure 2.7. ^{13}C-NMR spectrum of PHMCA. (a) DS 1, (b) DS 2, (c) DS 3, and (d) DS 4.

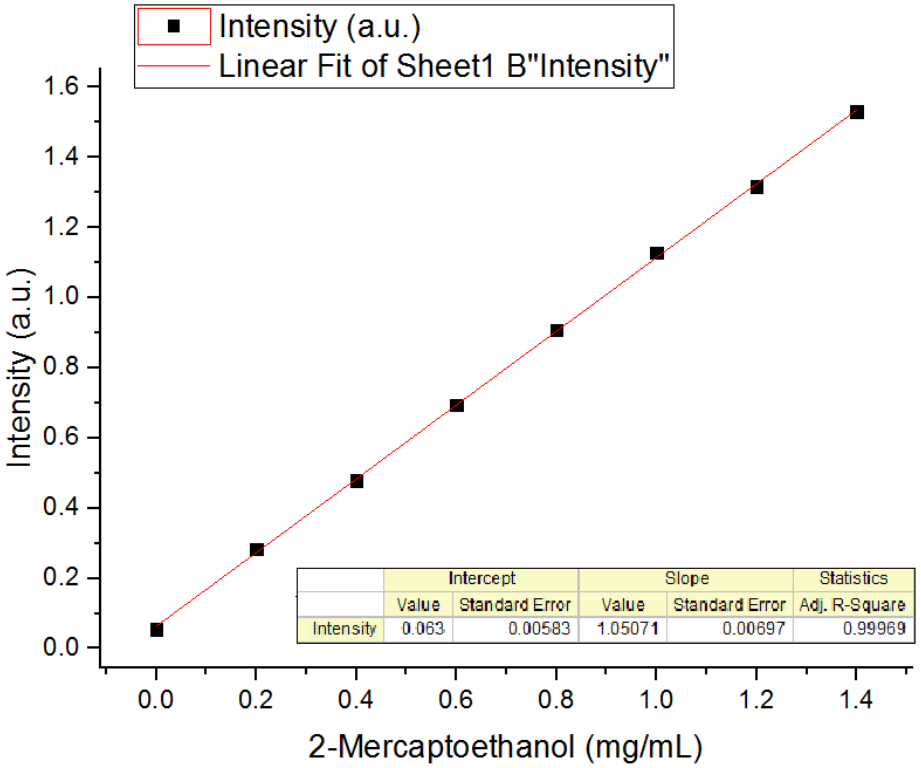

,

Figure 2.8. Standard Curve for DTNB assay. [Intensity = 1.05701 * 2-Mercaptoethanol (mg/mL) + 0.063] is calculated by linear fitting to raw data.

Thiol group	DS 1	DS 2	DS 3	DS 4	DS 5	DS 6	DS 7
Designed DS	20 %	30 %	40 %	50 %	60 %	70 %	80 %
^{13}C-NMR	No peak	No peak	5 %	5 %	X	X	X
DTNB assay	1.15 %	1.53 %	3.07 %	4.20 %	7.90 %	14.95 %	22.40 %
Disulfide bond DS	7 %	6 %	6.5 %	5 %	X	X	X

Table 2.8. DS of hydrazide group for PHHZA determined by ^{13}C-NMR and TNBS assay. DS of disulfide bond is also detected from ^{13}C-NMR. DS 60 to DS 80 couldn't measured by ^{13}C-NMR because of their solubility.

2.3.3. Characterizations of PHHZA

Hydrazide-conjugated polyaspartamide derivative was also produced using ethanolamine and adipic acid dihydrazide, termed poly(2-hydroxyethyl-co-hydrazidoadipoyl aspartamide) (PHHZA). Hydrazide react with aldehyde to form Schiff base, which has been successfully utilized to fabricate hydrogels. [7] For example, poly(aldehyde guluronate) crosslinked with adipic acid dihydrazide to form mechanically-controlled cell-adhesive hydrogel, and aldehyde/hydrazide alginate with hydrazide/aldehyde hyaluronic acid fabricated myocardial tissue generating hydrogel. [7, 20]

The DS of hydrazide on PHHZA was controlled by the amount of reactant, adipic acid dihydrazide, and characterized with FT-IR, FT-NMR, and TNBS assay. First, FT-IR spectra showed that all conditions had peaks corresponding to the unopened succinimide ring, and it increased with hydrazide DS (e.g. PSI fingerprint region (1150 – 1400 cm^{-1}) and C=O stretching in cyclic amide (1715 cm^{-1})) (Figure 2.9). This result suggested that the conjugation efficiency of adipic acid dihydrazide diminished with increasing DS. Therefore, in order to open all succinimide rings of PHHZA, if needed, the PHHZA was dissolved in slightly basic buffer (pH 8.0) to induce hydrolysis.

^{13}C-NMR spectra was used to calculate the DS of hydrazide on PHHZA using peak integration ratios (Figure 2.10). The peaks corresponding to central two carbons (**m**, **n**) and their next two carbons (**l**, **o**) of the hydrazide molecule are shown at 24.28 ppm and 34.55 ppm, respectively. These peaks were integrated and compared to the peak corresponding to the polyaspartamide backbone at 50.63 ppm (**b**, **h**, **r**). The calculated DS was varied from 5.5 % to 14.5 %.

In addition, a colorimetric TNBS assay was performed to detect the attached hydrazide group. This method is based on the absorption intensity for primary amine concentration. The standard curve was made by ethanolamine and compared with the values obtained with the PHHZA samples (Figure 2.11). The measured DS of PHHZA was varied from 5.02 % to 11.03 %.

The DS obtained from ^{13}C-NMR was slightly larger than those from TNBS assay (Table 2.9)., Two possible reasons can be inferred to interpret this phenomenon. First, some adipic acid dihydrazide were conjugated to polyaspartamide backbone using hydrazide group in both side as a crosslinker, since NMR targeted carbon and TNBS targeted amine group in hydrazide. Secondl, TNBS assay was developed for the detection of amine group, not for hydrazide. So it is possible that not all hydrazide on PHHZA were able to react with TNBS. In any case, both methods did provide evidence that DS of hydrazide could be controlled with the amount of reactant.

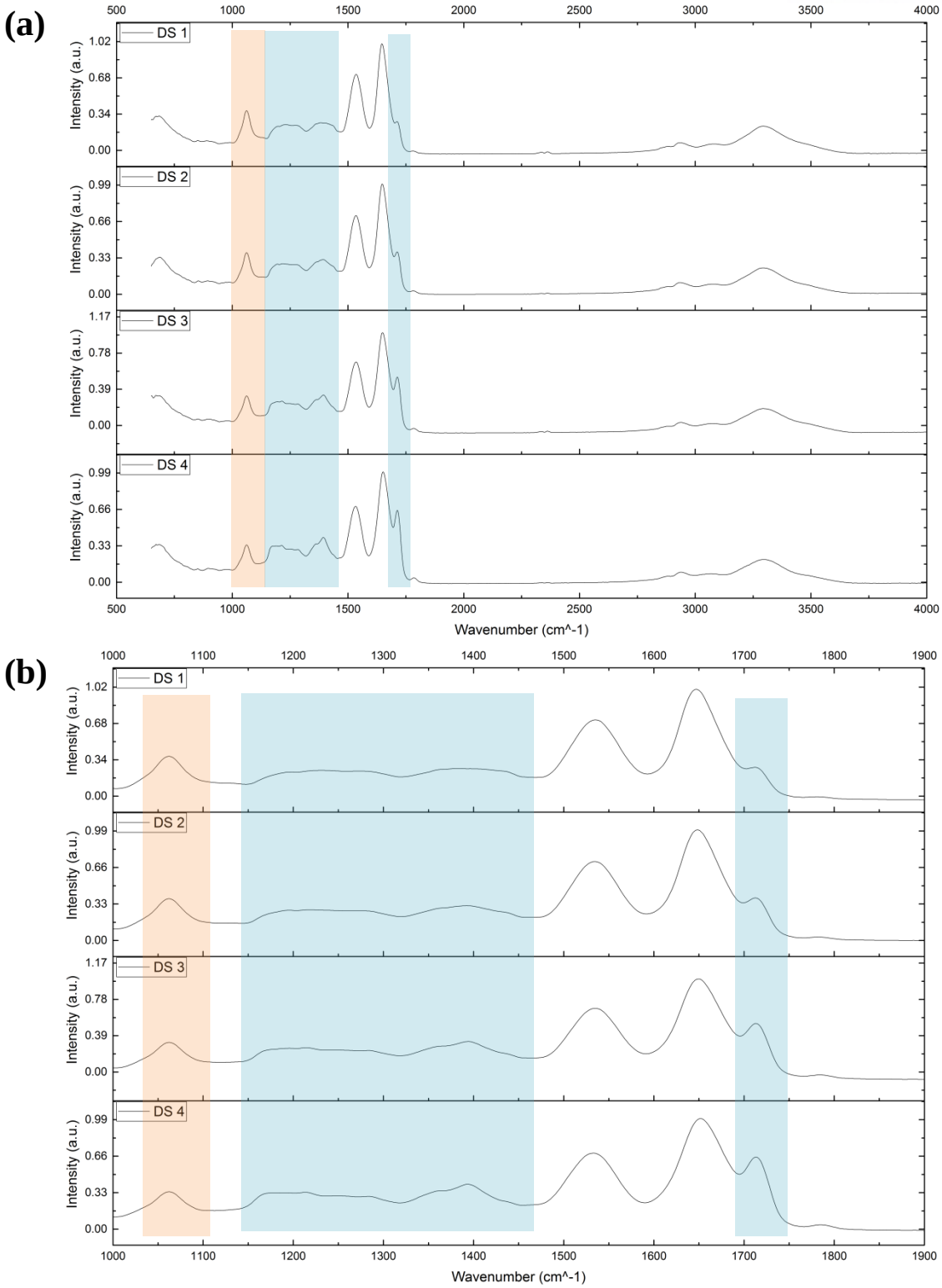

Figure 2.9. FT-IR spectra of PHHZA (DS = 1, 2, 3, 4) measured by ATR method. The peaks in blue region are increasing with increasing DS. The peaks in red region are decreasing with increasing DS. The spectra in (a) represent the entire measured spectra, while those in (b) show the magnified region from 1000 cm^{-1} to 1900 cm^{-1}.

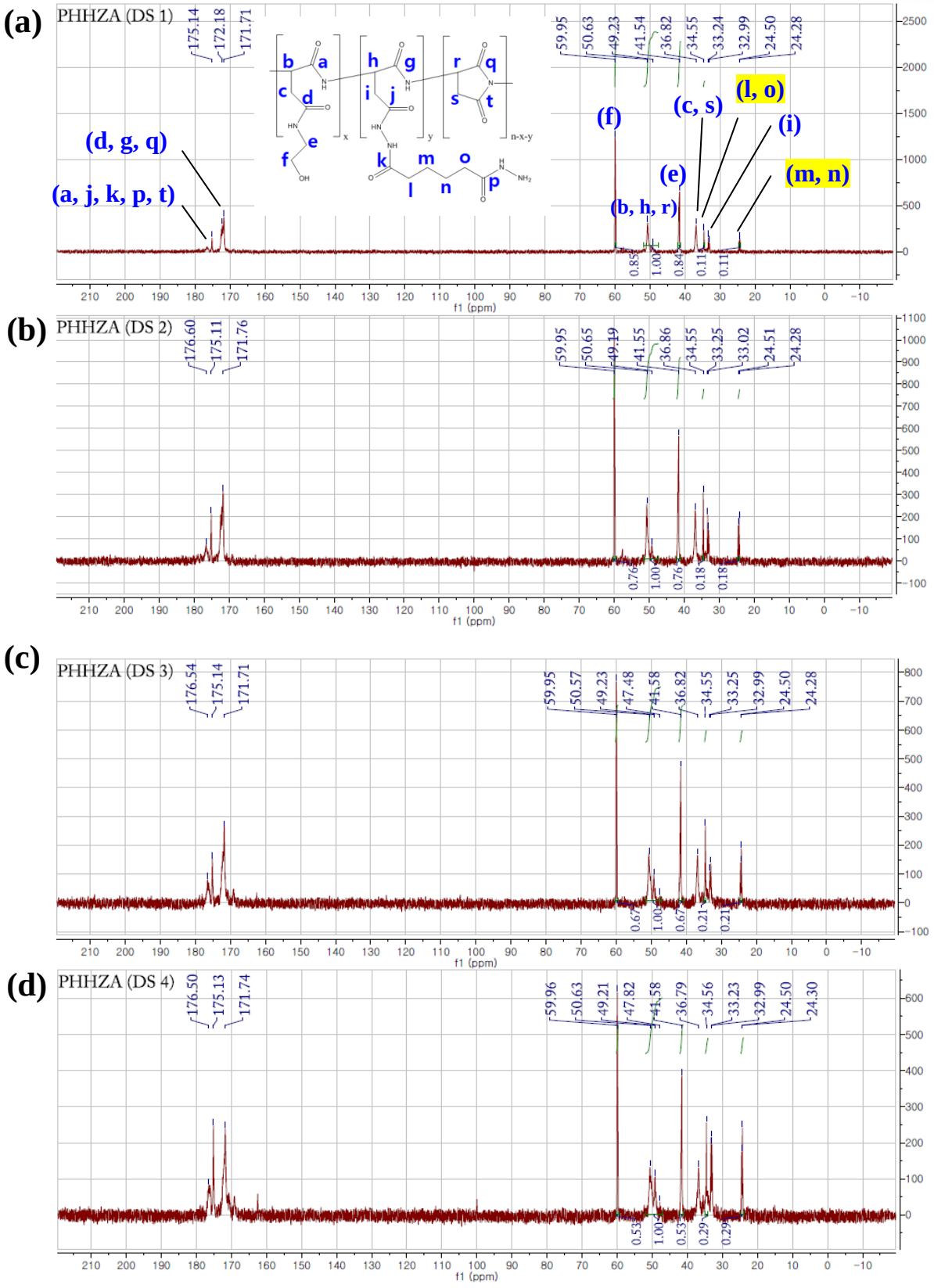

Figure 2.10. ^{13}C-NMR spectrum of PHHZA. (a) DS 1, (b) DS 2, (c) DS 3, and (d) DS 4.

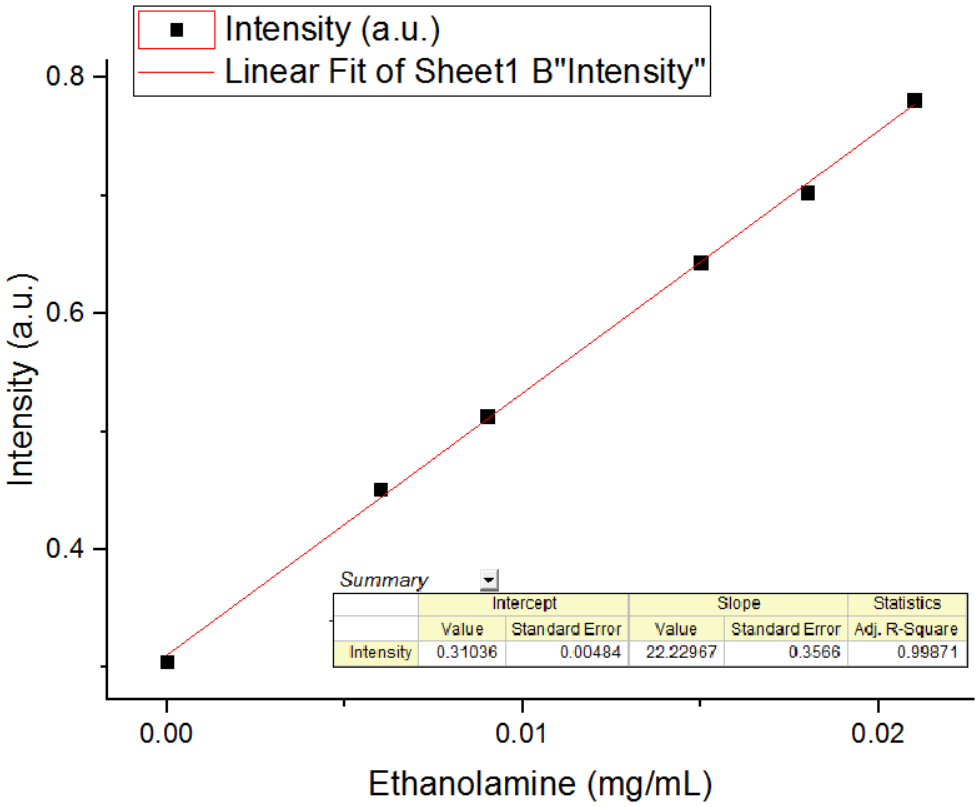

Figure 2.11. Standard curve for TNBS assay. [Intensity = 22.23 * Ethanolamine (mg/mL) + 0.31] is calculated by linear fitting to raw data.

Hydrazide group	DS 1	DS 2	DS 3	DS 4
Designed DS	20 %	30 %	40 %	50 %
^{13}C-NMR	5.5 %	9.0 %	10.5 %	14.5 %
TNBS assay	5.02 %	5.68 %	6.80 %	11.03 %

Table 2.9. DS of hydrazide group of PHHZA, obtained from ^{13}C-NMR and TNBS assay.

2.3.4. Characterizations of PHEDA

Lastly, we synthesized polyaspartamide with amine groups, poly(2-hydroxyethyl-co-ethylenediaminoethyl aspartamide (PHEDA). Amine has more advantage than hydrazide group since it is generally more reactive, and therefore accommodate various chemical reactions. For example, amine group in fibronectin and collagen can make Michael addition with acrylate or methacrylate group in synthetic polymers to fabricate hydrogels with varying mechanical properties and controlled cell adhesion. [3] EDC coupling between amine and carboxyl group has been also used to engineer hydrogels. [21] Furthermore, amine can make reaction with phosphorous oxychloride. [22]

PHEDA with varying DS of amine groups were synthesized by reacting with diethylenetriamine (DETA) and characterized using the same methods as described in the previous section. FT-IR spectra of PHEDA did not show any peak for the unopened succinimide ring, which was observed for PHHZA (Figure 2.12). The intersection (1595 cm^{-1}) of two main peaks from the primary amide increased with DS. Similarly, the peak for C-N stretching (1125 cm^{-1}) also increased with DS. This result indicated the increasing amount of conjugation of DETA to polyaspartamide backbone.

^{13}C-NMR spectra was also used to analyze the DS of PHEDA (Figure 2.13). The peaks corresponding to the two carbons next to the nitrogen of DETA (**l**, **m**) at 47.00 ppm and the peak corresponding to one carbon between the nitrogen atoms (**k**) at 40.22 ppm were used to calculate the amount of conjugated DETA. The reduction in amine peaks indicated that they reacted PSI and became conjugated to the polyaspartamide backbone. For example, the theoretical DS of DS 1 was 20 %, but only 7 % free amine occurred after synthesis. The DS measured from the ^{13}C-NMR was controlled from 7 % to 18 % (Table 2.10).

Furthermore, TNBS assay was also performed to measure the DS of amine as similarly done with the PHHZA in the previous section. The DS was controlled from 9.24 % to 19.85 %. Even though the two methods showed the similar trend, the DS of PHEDA was generally larger in ^{13}C-NMR than TNBS assay. This was opposite to the result shown for PHHZA. This may have been due to the secondary amine groups in DETA also participated in the reaction with TNBS assay, leading to increased values.

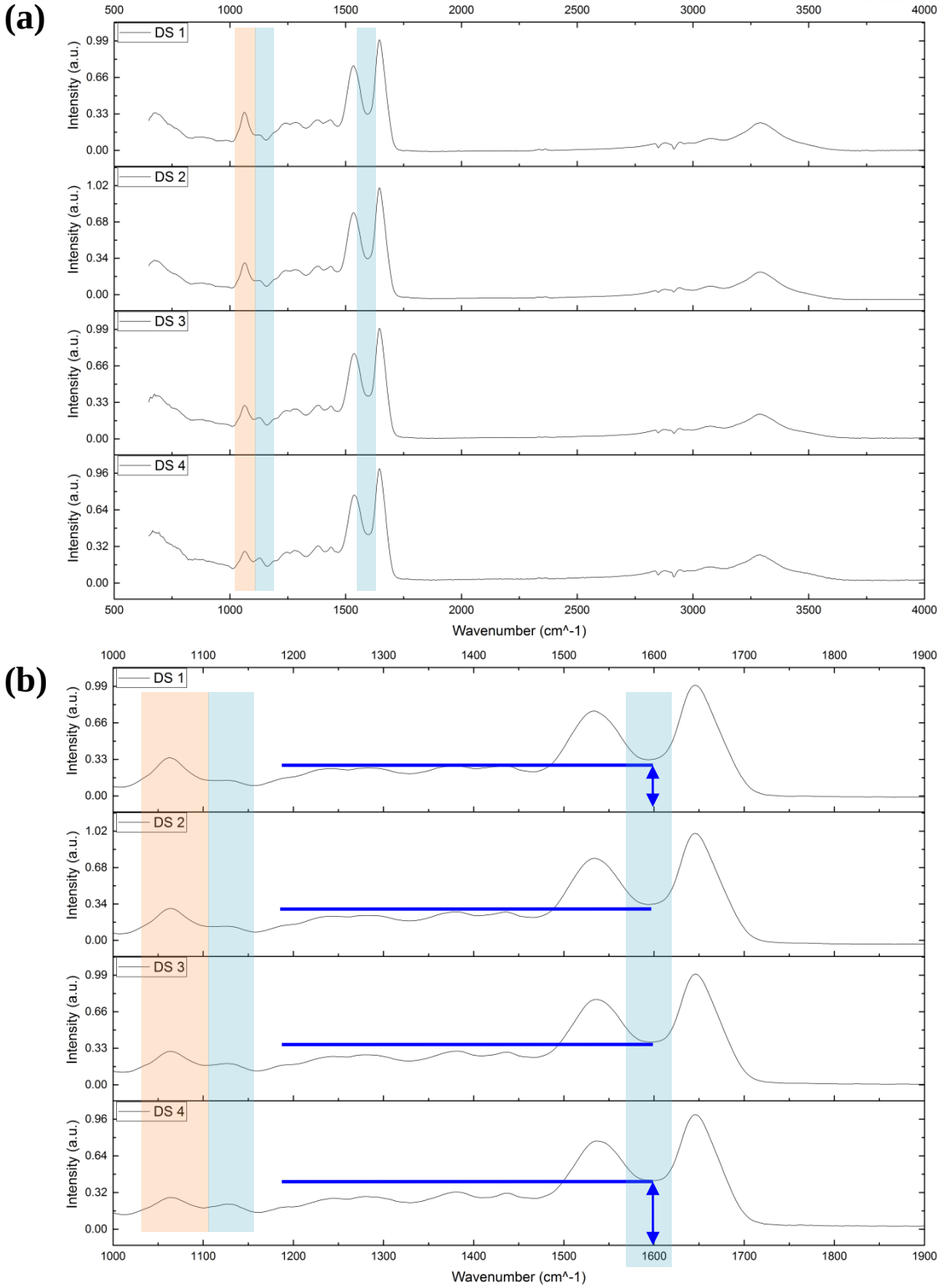

Figure 2.12. FT-IR spectra of PHEDA (DS = 1, 2, 3, 4) measured by ATR method. The peaks in blue region are increasing with increasing DS. The peaks in red region are decreasing with increasing DS. The spectra in (a) represent the entire measured spectra, while those in (b) show the magnified region from 1000 cm^{-1} to 1900 cm^{-1}.

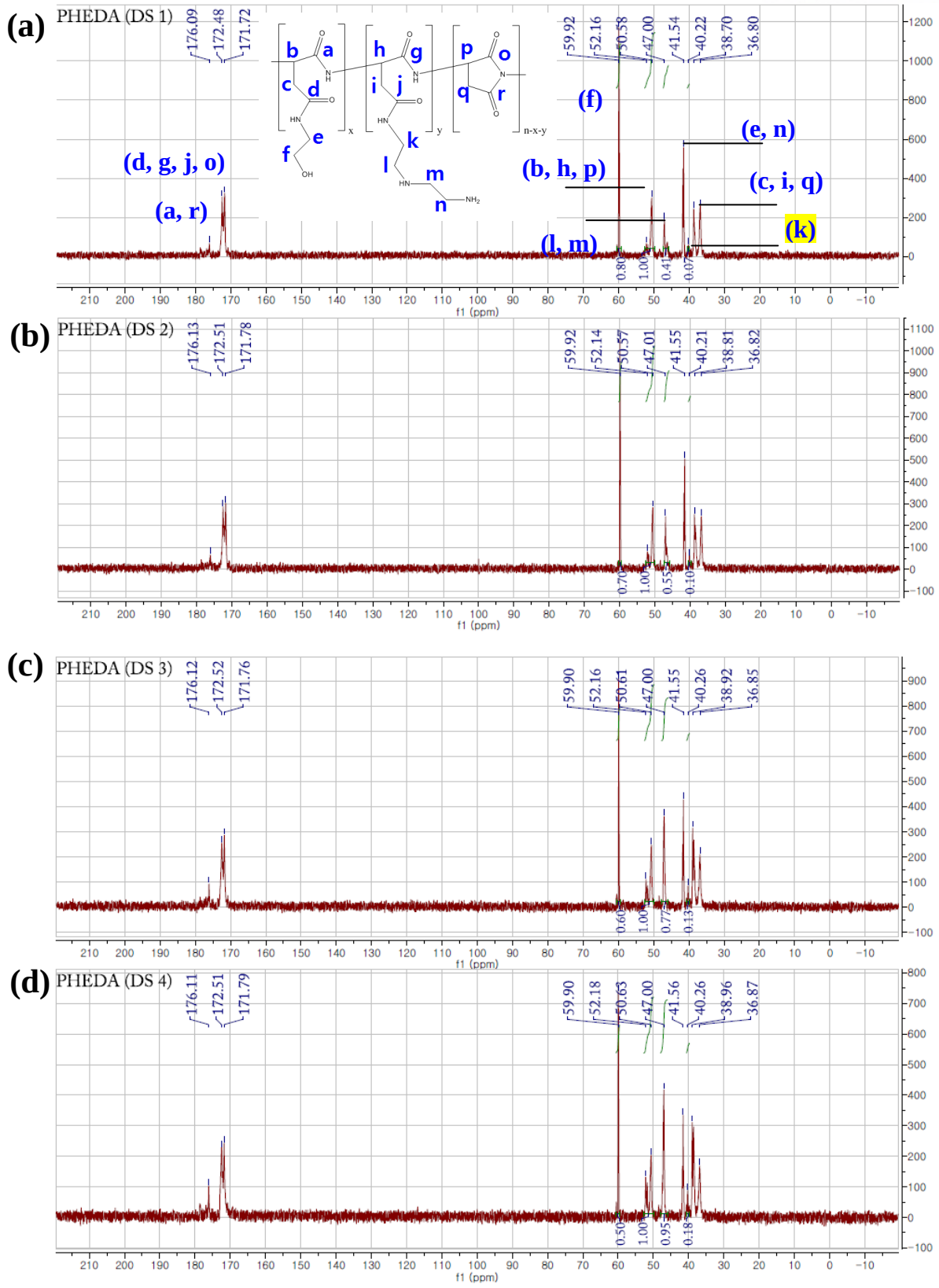

Figure 2.13. ^{13}C-NMR spectra of PHEDA. (a) DS 1, (b) DS 2, (c) DS 3, and (d) DS 4.

Amine group	DS 1	DS 2	DS 3	DS 4
Designed DS	20 %	30 %	40 %	50 %
^{13}C-NMR	7 %	10 %	13 %	18 %
TNBS assay	9.24 %	13.54 %	16.31 %	19.85 %

Table 2.10. DS of amine group of PHEDA by ^{13}C-NMR and TNBS assay.

2.3.5. Mechanical properties of PHHZA hydrogel

Alginate has been extensively investigated as a biomaterial for biocompatibility and the ability to form hydrogel by interaction with multivalent cations. [23]. Since alginate only has two functional groups, carboxylate and hydroxyl, it is desirable to introduce other functionalities to further diversify the biomaterial fabrication. [8, 9, 17, 20] In order to demonstrate the hydrogel fabrication via Schiff base formation with PHHZA or PHEDA, oxidized alginate was used as a gel-forming macromer. The oxidized alginate was synthesized by partial oxidation of uronic acid residues to present aldehyde functional groups.

PHHZA and oxidized alginate (OAlg) was first used as the macromer system for hydrogel fabrication via Schiff base formation. [7] The concentration of oxidized alginate in hydrogel was kept constant at 5 % (w/v), and the concentration of PHHZA was varied from 2.5 to 10 % to fabricate the hydrogels. The gelation occurred approximately 5 minutes after the mixing of two stock solutions, demonstrating the extent of Schiff base formation in the given concentration range was sufficient for hydrogel fabrication.

When the DS of hydrazide group on PHHZA increased at the same OAlg and PHHZA concentration, the crosslinking density is expected to increase and as a result make more rigid hydrogels (Figure 2.14). Thus, OAlg was reacted with PHHZA with varying DS to form hydrogels, and their mechanical properties were measured by obtaining stress-strain curves from uniaxial compression (Figure 2.15). The conditions which resulted in hydrogel degradation after 1 day of incubation in PBS, such as (DS 2, 5.0 %) and (DS 1, 7.5 %), were not included. The moduli of the alginate-PHHZA hydrogels increased with DS of PHHZA, and the range of moduli became greater with PHHZA concentration, as expected; 0.5-72 kPa for 10% PHHZA, 0.3-24 kPa for 7.5 % PHHZA, and 2-12 kPa for 5 % PHHZA (Figure 2.16.a). On the other hand, the degree of swelling expectedly followed the opposite trend to the moduli, decreasing with DS and concentration of PHHZA; increasing crosslinking density limits the permeability of the hydrogels as outlined by the rubber-elasticity theory (Figure 2.16.b). This result clearly demonstrated the increased number of reactive functional groups on PHHZA were able to sufficiently participate in the crosslinking of oxidized alginate, leading to enhanced hydrogel rigidity. Also, the lowest DS of PHHZA for hydrogel became higher with decreasing PHHZA concentration (e.g. DS1 for 10 % PHHZA, DS2 for 7.5 % PHHZA, DS3 for 5 % PHHZA), highlighting the critical number of reactive functional groups needed for sufficient crosslinking reaction.

Additionally, SEM images in Figure 2.17 support this phenomenon. Figure 2.17 (a) and (c) represent DS 4 and DS 2 with same concentration, which showed DS 4 has larger pore density, supporting much harder hydrogel. Also, Figure 2.17 (b) and (d) represent 10 % and 7.5 % with the same DS, which showed that the larger concentrations have denser structure. These results proved that

the chemical crosslinking density controlled by DS of PHHZA allowed the control of mechanical properties of the resulting hydrogels, even without changing the concentration.

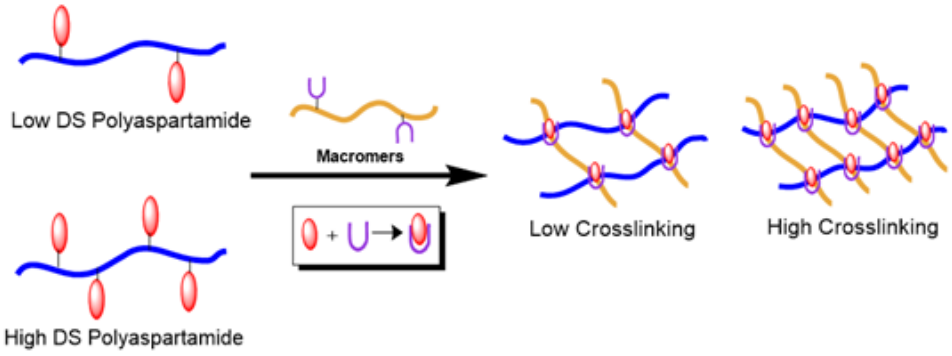

Figure 2.14. Fabrication of polyaspartamide-linked hydrogels with varying DS of functional groups to control the mechanical properties.

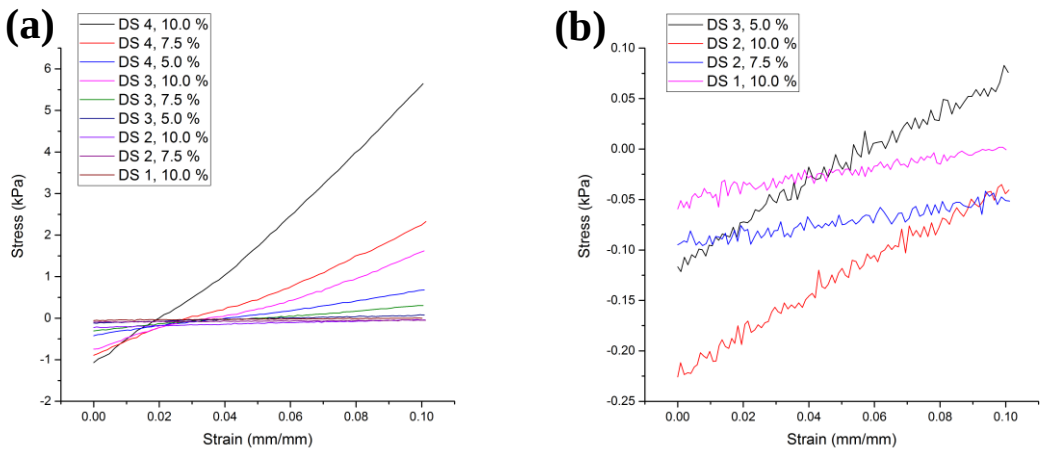

Figure 2.15. (a) Stress-strain curves of OAlg-PHHZA hydrogels, obtained by uniaxial compression. Only the first 10 % of the strain is shown. The concentrations of OAlg and PHHZA were controlled while only varying the DS of PHHZA. (b) The hydrogels with lower DS (from DS 1 to DS 3) were magnified.

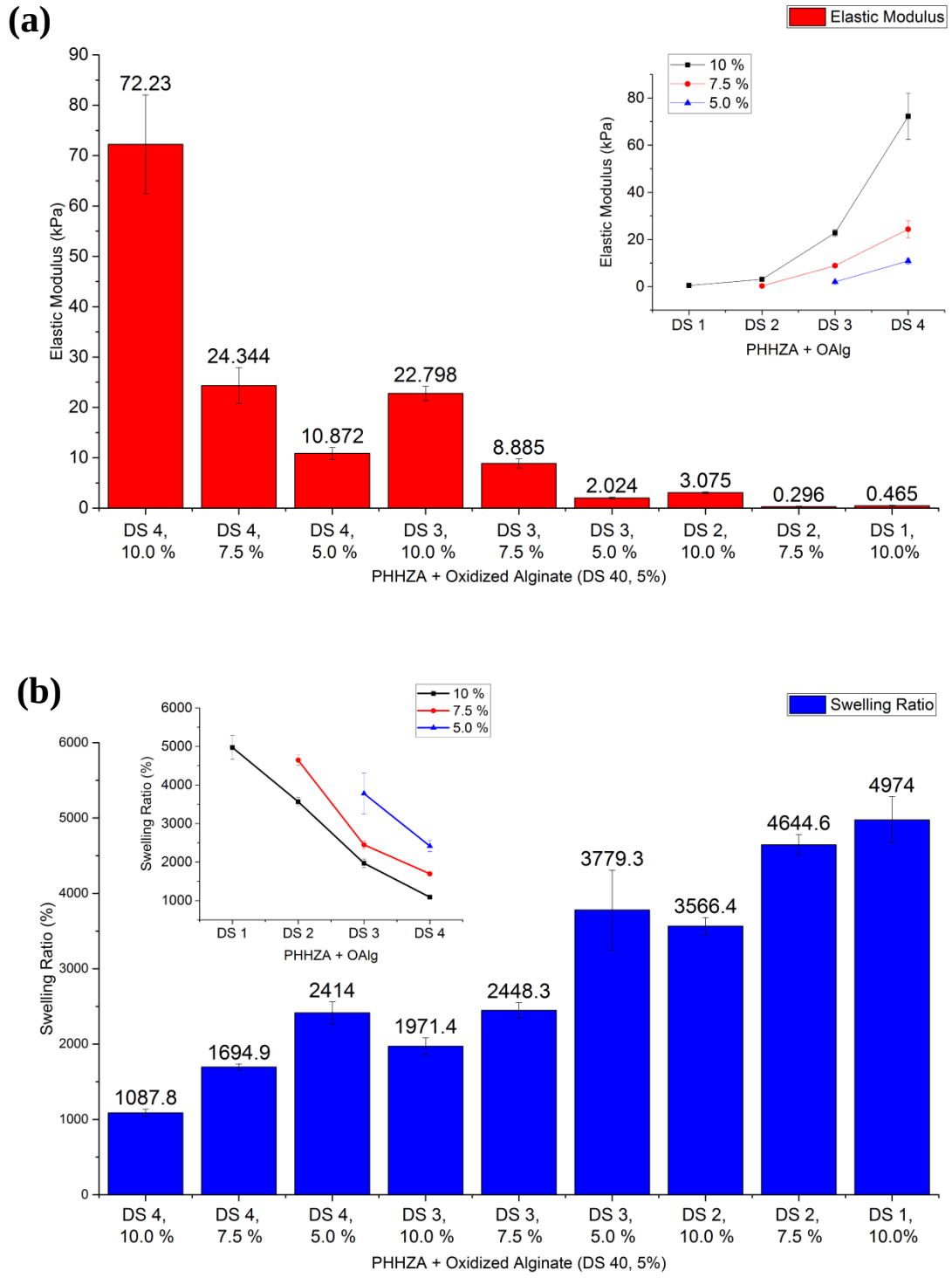

Figure 2.16. (a) Elastic moduli (kPa) and (b) degree of swelling (%) data for hydrogels made by PHHZA (DS x, y %) and OAlg (DS 40, 5%). All data was acquired after 1-day swelling in PBS at room temperature.

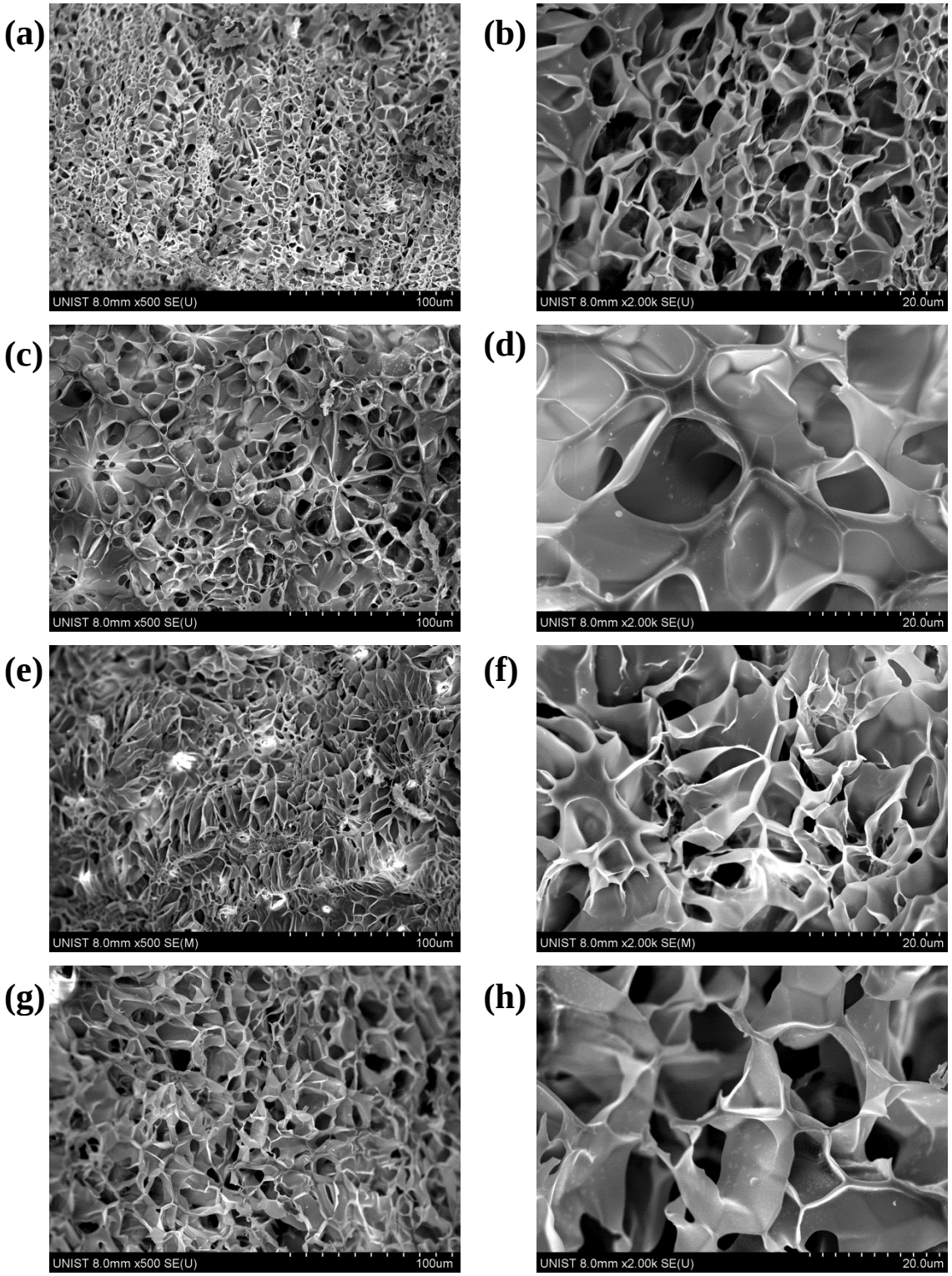

Figure 2.17. SEM images for hydrogels made by PHHZA (DS x, y %) and OAlg (DS 40, 5%). (a, b), (c, d), (e, f), and (g, h) represent the following PHHZA conditions, respectively; (DS 4, 10 %), (DS 4, 7.5 %), (DS 2, 10 %), and (DS 2, 7.5 %).

2.3.6. Mechanical properties of PHEDA hydrogel

In this section, the versatility of polyaspartamide as a crosslinker was demonstrated by crosslinking a synthetic polymer via a different chemical reaction. Here, PHEDA was used to crosslink poly(ethylene glycol) diacrylate (PEGDA) through Michael addition to form hydrogels. Poly(ethylene glycol) (PEG) is one of the most widely used synthetic polymers for biomedical applications due to its anti-fouling property as well as hydrophilicity and biocompatibility. The end functional groups of PEG is commonly modified to impart different functionalities. Physical properties of the PEG, such as molecular weight and topology (e.g. linear, branched, dendrimer), are also modified. [24] PEGDA, a linear PEG chain with acrylate at both ends capable of different reaction schemes, was used as a gel-forming polymer.

The hydrogels were fabricated by reacting varying concentrations and DS of PHEDA with PEGDA (Mn 700). The elastic moduli and the degrees of swelling were measured as previously done (Figure 2.18, Figure 2.19). Generally, increasing the concentration and DS of PHEDA increased the elastic moduli of the hydrogels, as expected, and the degree of swelling followed the opposite trend, due to the increased crosslinking density. However, PHEDA (DS 4, 10 %) had less elastic modulus than both PHEDA (DS 4, 7.5 %) and PHEDA (DS 3, 10%), even though the concentration and DS were higher. This result may have been due to the presence of unreacted amine groups in PHEDA, as all the acrylate groups in PEGDA under the given concentration were completely reacted, induce large osmotic pressure during swelling, causing deterioration of the hydrogel structure.

The mechanical properties of PEGDA-PHEDA hydrogels were further explored by increasing the PEGDA concentration from 10 % to 20 (Figure 2.20). In this case, increasing the concentration and DS of PHEDA also resulted increased the elastic moduli of the hydrogels, as expected. The range of moduli were greater than that shown for 10 % PEGDA. Two conditions, PHEDA (DS 4, 5.0 %) and PHEDA (DS 1, 10 %), which induced the hydrogel formation at 10 % PEGDA could not induce hydrogel formation at 20 %, possibly due to insufficient number of amine groups to react with the increased number of acrylate in PEGDA. Taken together, the mechanical properties of PEGDA-PHEDA hydrogel can be controlled in a wide range by varying the DS of amine groups in PHEDA as a crosslinker, as well as the concentration.

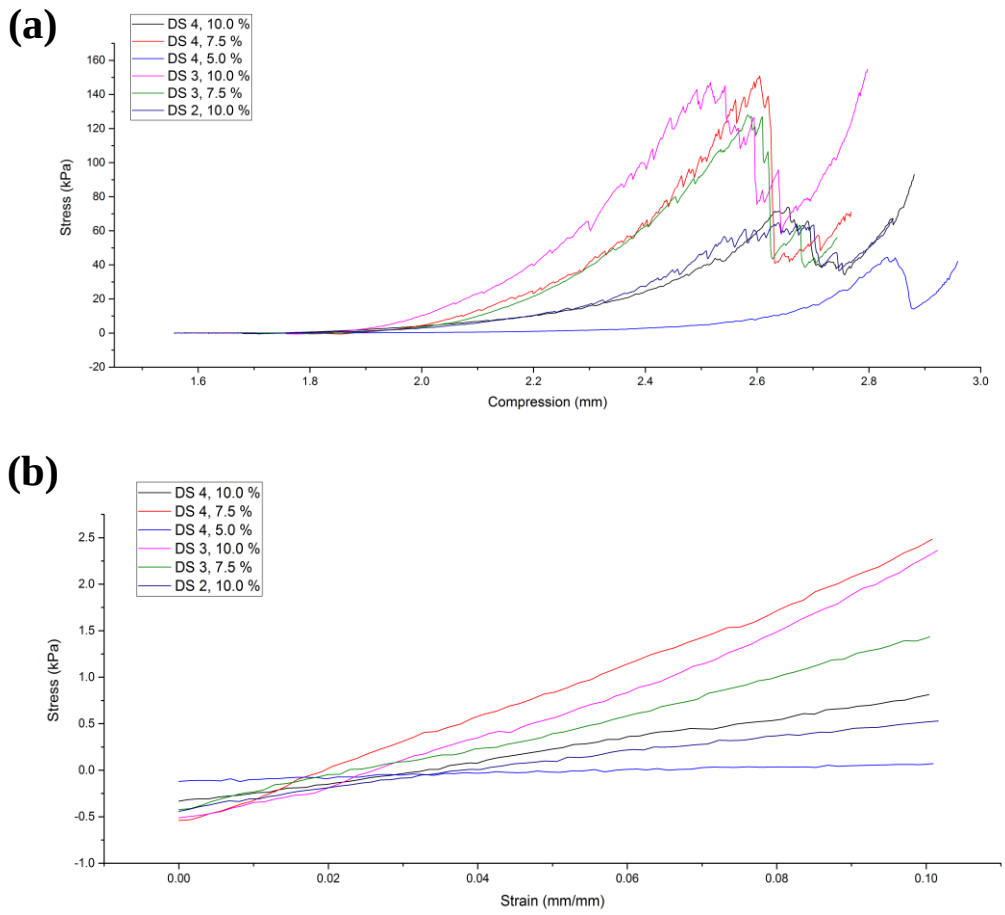

Figure 2.18. Stress-strain curves of PEGDA-PHEDA hydrogels obtained by uniaxial compression. The concentration and DS of PHEDA were controlled while keeping the PEGDA concentration at 10 %. The plots in (a) show the stress-strain curves in all strain range, and those at the first 10 % strain are magnified and presented in (b).

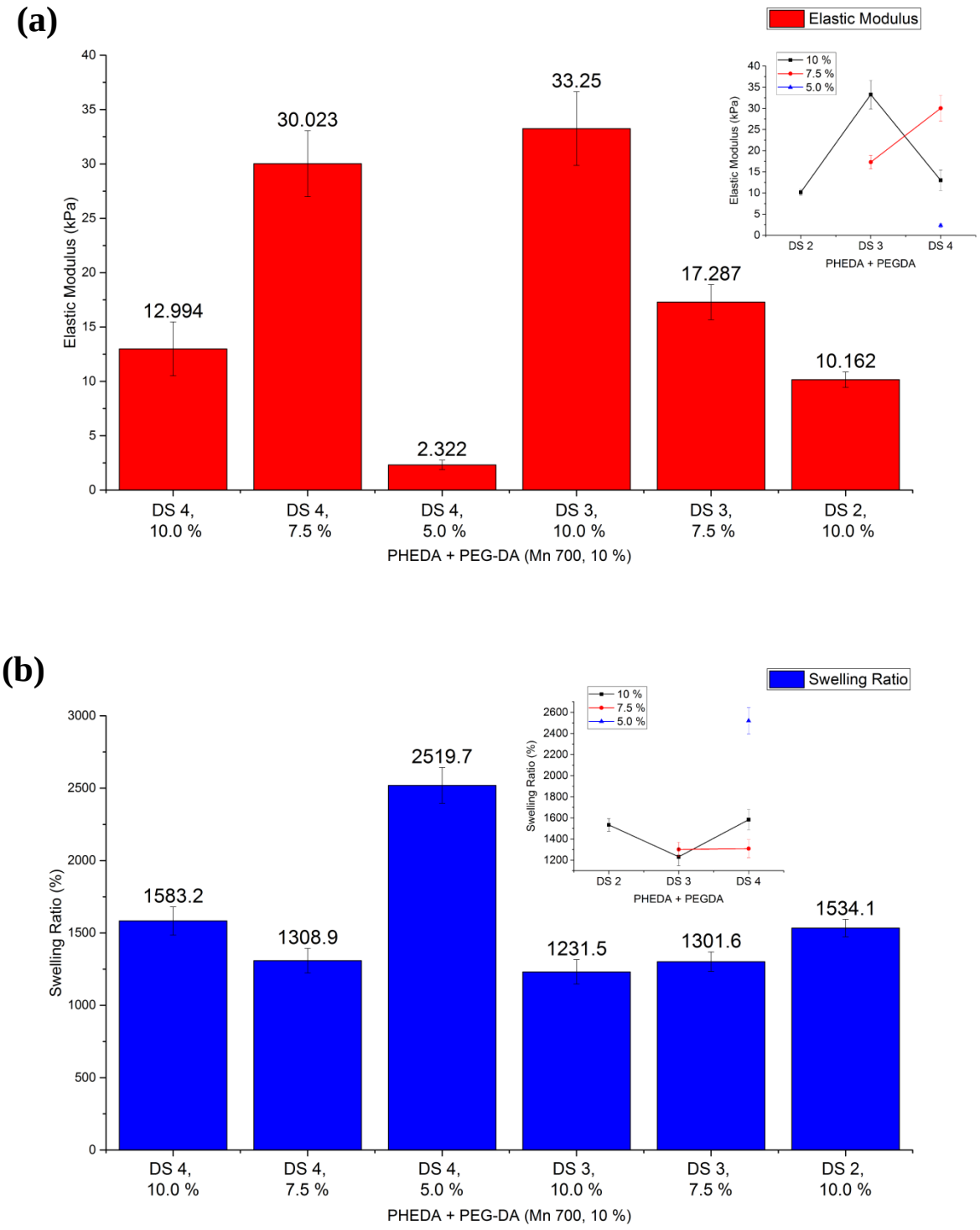

Figure 2.19. (a) Elastic moduli (kPa) and (b) degree of swelling (%) PEGDA-PHEDA hydrogels.

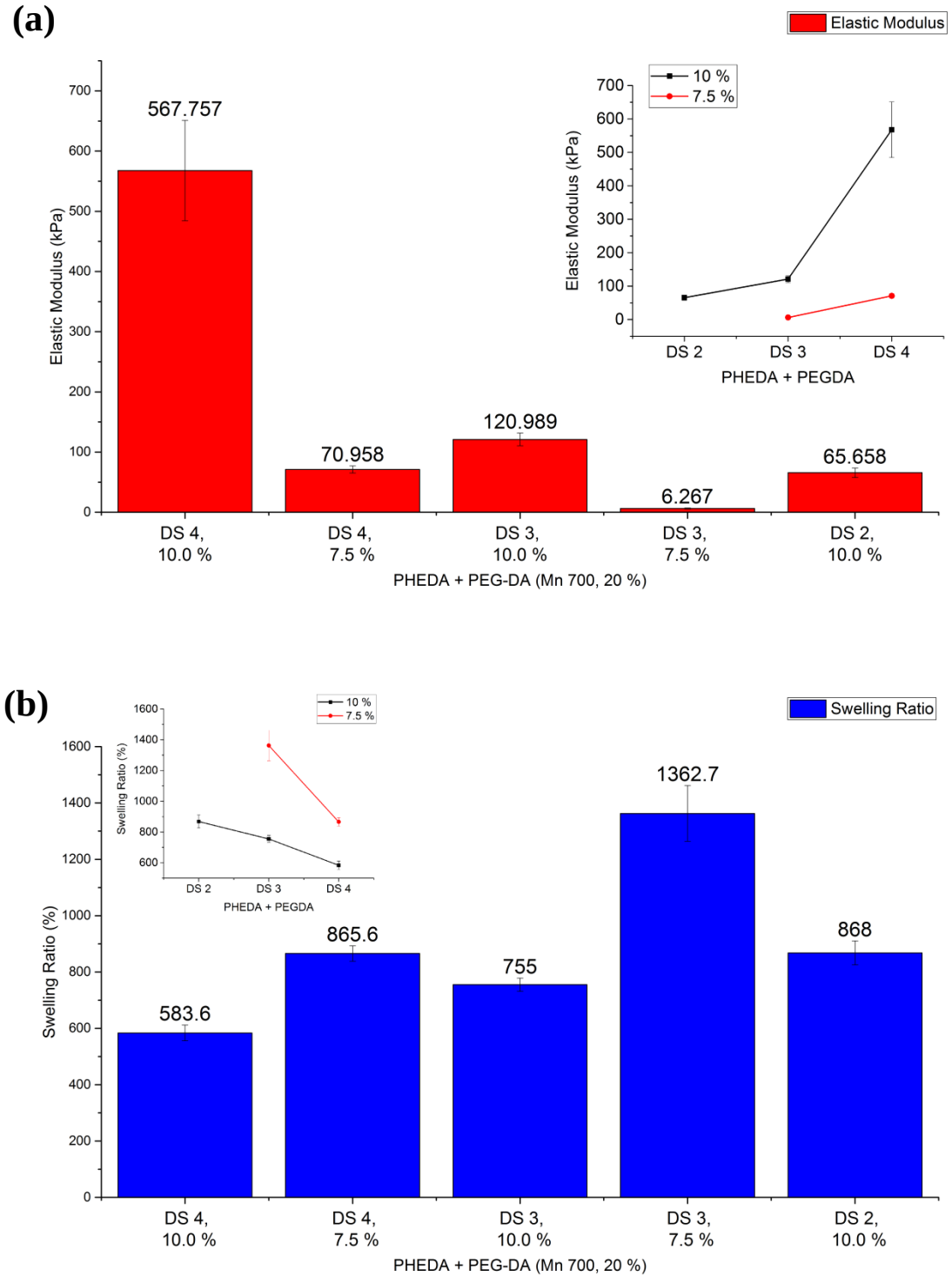

Figure 2.20. (a) Elastic modulus (kPa) and (b) Swelling ratio (%) data for hydrogels made by PHEDA (DS x, y %) and PEGDA (Mn 700, 20%). All data was acquired after 1-day swelling in PBS buffer at room temperature with four samples.

2.3.7. Comparison of crosslinking efficiency of PHHZA and PHEDA

In the previous section, the PEGDA-PHEDA hydrogels and OAlg-PHHZA hydrogels were fabricated and characterized. It is well known that both amine and hydrazide can undergo Michael addition and Schiff base formation since they are both nucleophiles (i.e. they are not mutually exclusive), though in different reactivities. Therefore, in this section, PHHZA was used to crosslink PEGDA and PHEDA was used to crosslink OAlg to compare the relative reactivities of amine and hydrazide towards Michael addition and Schiff base formation (Figure 2.21).

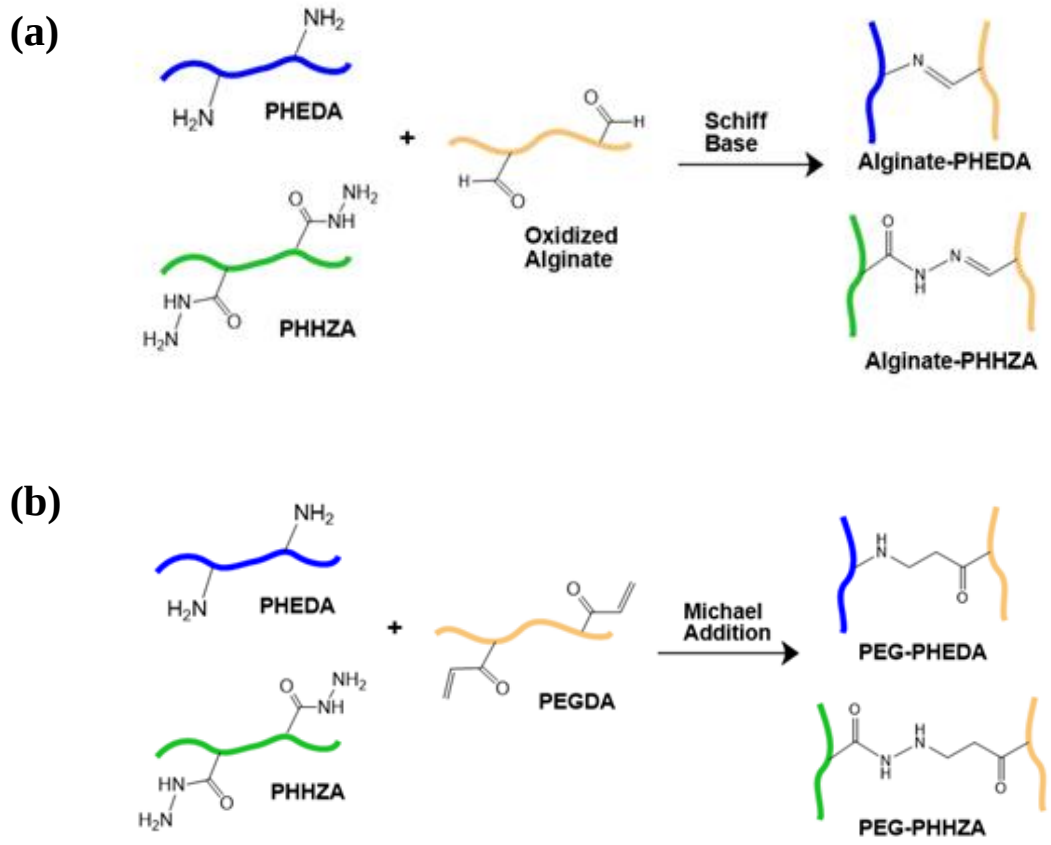

Figure 2.21. Hydrogel fabrication of PHHZA and PHEDA via (a) Schiff base formation, and (b) Michael addition.

PHEDA was able to crosslink OAlg (DS 40, 5 %) to form the hydrogels. There were several notable differences from the PHHZA-linked hydrogels. First, the rate of gelation for the alginate-PHEDA hydrogels was much higher (within 5 seconds at room temperature) than that of alginate-PHHZA hydrogels. Second, their moduli were also larger at the same range of concentration and DS. Third, the PHEDA with the lowest DS (DS1) was able to form hydrogels at the same range of concentration, whereas the lowest critical DS for gelation became higher with decreasing concentrations for PHHZA. These results suggested that the Schiff base reaction by primary amine groups of PHEDA were more facile than hydrazide groups of PHHZA, due to the higher nucleophilicity. As a result, more rigid hydrogels were formed at the same DS and concentration. Taken together, these results demonstrated that the mechanical properties of the hydrogels crosslinked by the polyaspartamide crosslinkers via Schiff base formation could be controlled in a wide range. It should be noted that due to the extremely fast gelation time, there may have been some of the conditions in which the homogenous mixing between the two polymers could not be achieved under the given condition, diminishing the reproducibility. Going forward, it is imperative that a method that guarantees more robust mixing be developed. This quick gelling property could find use as an injectable hydrogel system for drug delivery and wound healing applications.

Interestingly the OAlg-PHEDA hydrogels showed highly accelerated degradation rates compared to OAlg-PHHZA hydrogels. All hydrogels that were fabricated by 2 hours of reaction time were completely dissolved in PBS buffer within 1 hour of incubation. More detailed investigation of reaction time on the mechanical properties of OAlg-PHEDA was performed (Table 2.11). The data showed that the elastic moduli of all conditions regardless its DS and concentrations of PHEDA decreased with the reaction time.

This interesting result suggest that there may be a competing force that could prevent further crosslinking reaction, or induce hydrogel degradation. The first possibility may be the remaining amine group can attack the amide bond in polyaspartamide backbone. Since PHEDA has a high density of amine groups, they could induce the hydrolysis of the Schiff base linkages. [2] It is also possible that the increased hydroxide content within the hydrogel by the protonation of amine groups likely facilitated the hydrolysis process. The fast degradation behavior was not shown for the OAlg-PHHZA hydrogels, likely due to the lower nucleophilicity compared to free amine.

Incomplete reaction between PHEDA and OAlg due to the extremely fast hydrogel formation also may have contributed to this fast degradation, as there may be a significant portion of unreacted PHEDA remaining within the hydrogel network. Compared to the unreacted amines in PHEDA that are part of the hydrogel network, those in PHEDA that are can more easily diffuse within the hydrogel network and participate in the hydrogel degration. This fast gelation/degradation behavior warrants further investigation in future studies.

37 °C Incubation Time	1 h	3 h	5 h	10 h
DS 4, 10%	130.8728	59.6956	24.07482	17.43015
(Standard deviation)	7.15054	5.14155	5.38634	9.85448
DS 3, 10%	67.99088	37.11587	12.81956	5.90101
(Standard deviation)	3.38686	9.39513	4.40342	1.57489
DS 2, 10%	81.04557	29.28346	15.30729	4.02465
(Standard deviation)	3.55303	4.85393	1.96138	1.59955
DS 1, 10%	46.24357	28.05137	22.06341	10.36764
(Standard deviation)	5.67976	7.53632	8.85155	2.57923
DS 4, 7.5%	66.3909	28.53438	8.07463	2.72517
(Standard deviation)	6.76657	1.87694	2.7465	0.30292
DS 3, 7.5%	52.01776	17.79765	15.48971	3.53885
(Standard deviation)	5.17672	7.83394	2.63672	0.59171
DS 2, 7.5%	25.08652	13.55883	10.22681	3.97801
(Standard deviation)	3.96919	0.99557	2.0076	1.64043
DS 1, 7.5%	23.59405	11.33796	7.37377	2.82029
(Standard deviation)	2.82182	1.42116	1.55342	0.61824
DS 4, 5.0%	12.37212	7.30202	4.29263	1.93722
(Standard deviation)	2.86989	0.43936	0.41151	0.34471
DS 3, 5.0%	12.3998	5.68362	3.43137	1.23822
(Standard deviation)	2.08067	2.7325	0.51351	0.6533
DS 2, 5.0%	8.92908	3.74734	2.54087	0
(Standard deviation)	1.67479	0.18625	0.26427	0
DS 1, 5.0%	6.47509	3.56045	0.9456	0
(Standard deviation)	2.17614	0.78702	0.33911	0

Table 2.11. Gelation-time-dependence Elastic modulus (kPa) for hydrogels made by PHEDA (DS x, y %) and OAlg (DS 40, 5%). All data is acquired from four samples to each condition.

2.3.8. Degradation properties of PHHZA and PHEDA hydrogels

It has been demonstrated that the polyamine-based hydrogels containing hydrolysable groups could undergo accelerated degradation process possibly due to the increased local hydroxide ions with the protonation of amine groups and/or the nucleophilic attack of the unreacted amine groups on the ester groups. [25] Since PHEDA and PHHZA contain multiple nucleophilic amine and hydrazide groups that may stay unreacted after hydrogel formation, and the hydrogels containing hydrolysable groups, it was thus postulated that the hydrogels could undergo degradation via hydrolysis. First the hydrogels were incubated in PBS (pH 7.4) at 37 ℃ and their degradation was monitored by measuring the change in moduli over time (Figure 2.22, Table 2.12, Table 2.13). The degradation rate constants (k_d) were obtained by fitting the profile with Eq.(1).

For alginate-PHHZA hydrogels, those with higher DS and concentration of PHHZA showed lower degradation rate and delayed dissolution, indicating the hydrogels with greater mechanical strength showed greater resistance towards degradation (Figure 2.22.(a)-(b)). Between two conditions, 10 % (DS3) and 7.5 % (DS4) which had similar initial moduli, the degradation rate was higher for 10 % (DS3). Similarly, the degradation rate of 7.5 % (DS3) was higher than that of 5% (DS4). These results alluded to the greater presence of unreacted hydrazide groups at higher PHHZA concentrations likely facilitating the hydrogel degradation via increased hydrolysis.

The degradation of PEG-PHEDA hydrogels followed the similar trend as alginate-PHHZA hydrogels; lower degradation rates at higher PHEDA concentrations at a given DS (Figure 2.22.(c)-(d)). Unlike alginate-PHHZA hydrogels, the degradation rate was not as significantly affected by the difference in DS, despite the wide range of initial moduli. In addition, the degradation rates of the PEG-PHEDA hydrogels were generally higher than those of alginate-PHHZA hydrogels at their respective DS concentrations, even though their initial moduli were much larger. Combined with the extremely fast degradation of PEG-PHEDA hydrogels, it is concluded that the unreacted primary amine groups in PHEDA could more rapidly facilitate the hydrolysis of Schiff base or ester groups than the hydrazide groups in PHHZA.

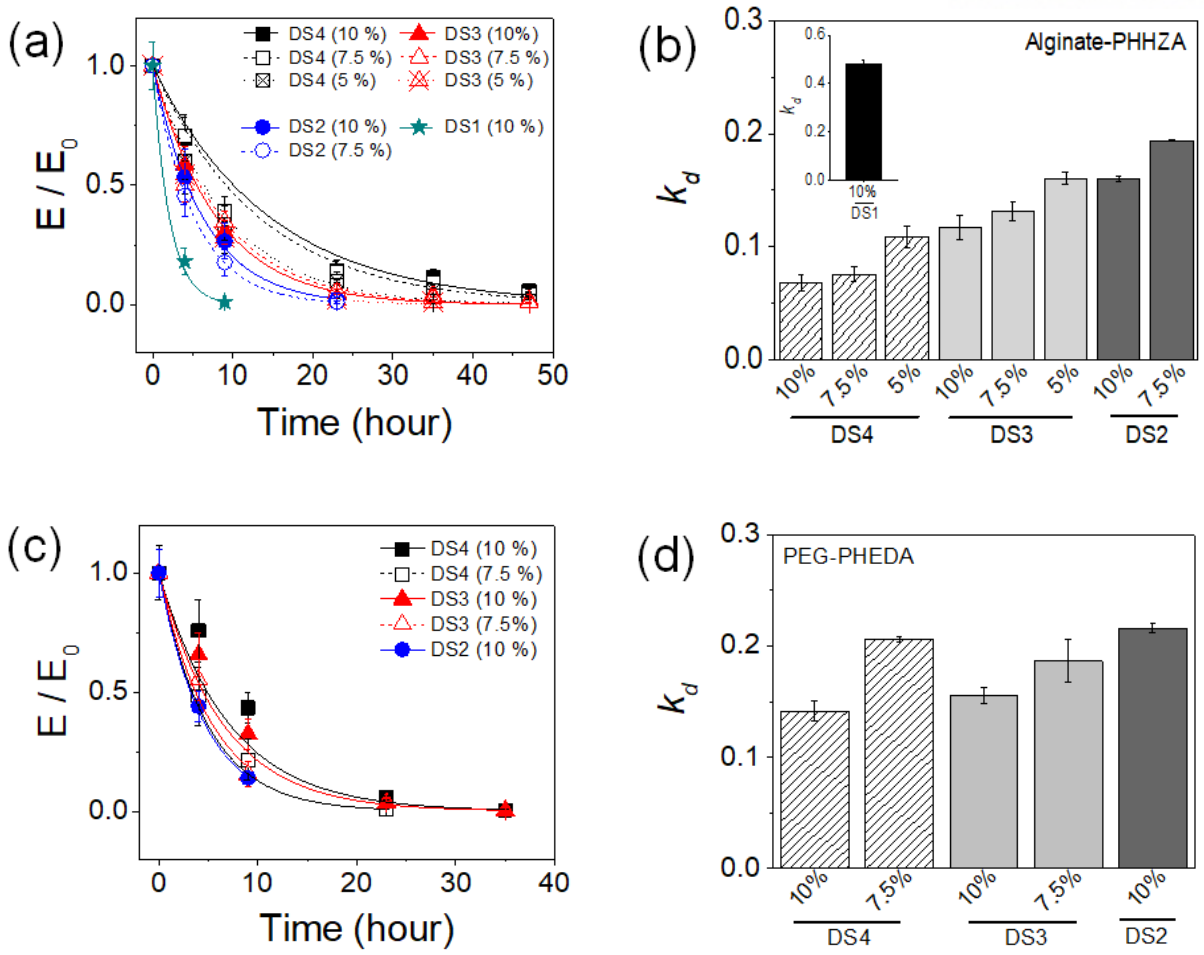

Figure 2.22. Degradation of (a,b) alginate-PHHZA and (c,d) PEG-PHEDA hydrogels were determined by measuring the change in moduli (E/E_0) over time and calculating degradation rate constants (k_d). The moduli (E) measured at various time points were normalized with the initial value (E_0). k_d were calculated by fitting with Eq.(1).

37 °C Swelling Time	1 h	5 h	10 h	24 h	36 h	48 h
DS 4, 10%	104.5864	72.62461	37.32087	15.10062	12.20317	6.01874
(Standard deviation)	5.0692	5.75821	1.48057	0.886	1.11675	0.58491
DS 4, 7.5%	65.3909	46.09901	25.68725	8.95492	6.2593	2.89192
(Standard deviation)	6.33348	9.23194	1.31449	1.10073	1.03143	0.35387
DS 4, 5.0%	35.02097	21.10644	11.09706	3.48879	2.1321	0.55859
(Standard deviation)	1.27318	1.39964	0.16691	0.16291	0.19192	0.02491
DS 3, 10%	97.17435	57.0373	29.48904	4.96939	3.88692	1.78993
(Standard deviation)	7.58847	3.04265	3.05244	0.43308	0.07985	0.30702
DS 3, 7.5%	57.21012	28.63967	19.8916	3.18436	1.63488	0.50408
(Standard deviation)	2.6939	3.63839	0.41672	0.20847	0.14956	0.12118
DS 3, 5.0%	24.19807	13.17922	6.79836	0.54873	0.24374	
(Standard deviation)	0.54796	1.61937	0.34618	0.01768	0.04861	
DS 2, 10%	31.3617	16.78426	8.34686	0.75762	0	
(Standard deviation)	5.17281	0.77678	0.56316	0.11371	0	
DS 2, 7.5%	22.23894	10.15547	3.95097	0.25789		
(Standard deviation)	0.95153	0.3133	0.03042	0.06326		
DS 1, 10%	5.9698	1.09068	0			
(Standard deviation)	0.30917	0.08402	0			

Table 2.12. Swelling-time-dependence Elastic modulus (kPa) for hydrogels made by PHHZA (DS x, y %) and OAlg (DS 40, 5%) at 37 °C. All data is acquired from four samples to each condition. Zero value means too weak hydrogel, so it couldn't be measured by UTM.

37 °C Swelling Time	1 h	5 h	10 h	24 h	36 h	48 h
DS 4, 10%	1323.436	1002.345	573.8207	76.90482	6.58513	0
(Standard deviation)	28.1007	29.66829	75.15962	10.44805	0.64716	0
DS 4, 7.5%	581.0077	279.9726	125.4554	5.01391	0	
(Standard deviation)	10.83392	6.72018	17.68928	0.76348	0	
DS 3, 10%	885.7716	581.2572	286.7335	32.09098	2.4658	0
(Standard deviation)	32.64945	40.62007	52.74131	2.21647	0.21562	0
DS 3, 7.5%	241.6042	133.0102	37.26435	0		
(Standard deviation)	16.05712	7.66051	3.36338	0		
DS 2, 10%	246.5199	108.6129	34.48287	0		
(Standard deviation)	36.53718	10.63486	2.07402	0		

Table 2.13. Swelling-time-dependence Elastic modulus for hydrogels made by PHEDA (DS x, y %) and PEGDA (Mn 700, 20%). All data is acquired from four samples to each condition. Zero value means too weak hydrogel, so it couldn't be measured by UTM.

2.3.9. Hydrogel synthesis using PHMCA

PHMCA was used to induce crosslinking with various gel-forming polymers (DS from 1 to 4, concentration from 2.5 to 10 %), but the hydrogel could not be obtained. Other PHMCA with higher DS (DS 5 to 7) couldn't be tested because of their low solubility to water and self-gelation properties during dissolution.

Scheme 2.12 (a) to (g) represents different reaction routes. First, Michael addition was employed to fabricate the hydrogels with PHMCA. Four-arm polyethylene glycol (Mn 8,000) having (a) vinyl sulfone and (b) methacrylate were used. [26] Both functional groups can theoretically react with thiol, but the hydrogel did not form using PHMCA. Similarly, hydrogels did not form with PHMCA reaction with (c) PEG-dimethacrylate (Mn 740) and (d) PEGDA (Mn 700). [27] Disulfide formation was also employed to fabricate hydrogel with PEG-dithiol (Mn 2,000) as the macromer with various catalysts; (e) NaI/H2O2 and (f) 3,3`-Dithiodipropionic acid (DTDP), and oxidant solvent; (g) DMSO. [28 - 31] But none these conditions resulted in hydrogel formation

There are two possibilities. First, the DS of thiol in PHMCA was not sufficient enough to reach the minimum requirement to make hydrogel structure. Hydrogel should be able to withstand the osmotic pressure in an aqueous environment to maintain its structure. If the crosslinking density in polymer solution is lower than a critical point, the chemical reaction between thiol in PHMCA and the gel-forming polymers was not significant enough for hydrogel formation. In this experiment, DS 4 has only 5 % (DTNB assay) or 4.2 % (^{13}C-NMR) of thiol DS.

The other possibility is the folded PHMCA structure. The polymer backbone of the derivatives is polypeptide, and thiol-contained peptide can easily make a folded structure as nanoparticles. [32] Even though we checked live thiol group using various methods in section 2.3.2, if enough polymer chains participated in the nanostructure formation, the effective concentration may have been much lower than the critical value for gelation. This aspect needs to be investigated in future studies.

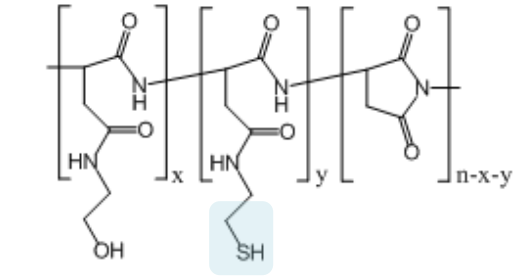

poly(2-hydroxyethyl-co-2-mercaptoethyl aspartamide)
(PHMCA)

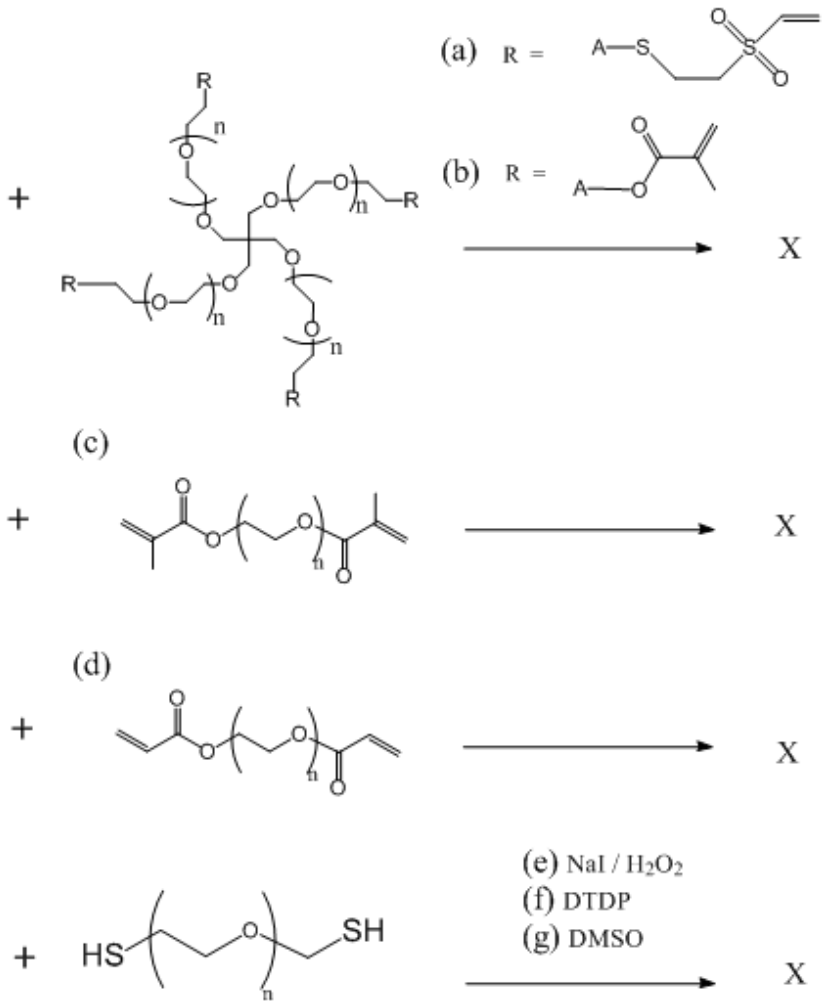

Scheme 2.12. Crosslinking schemes for PHMCA with various gel-forming macromers; (a) 4-arm PEG-vinyl sulfone (Mn 8,000), (b) 4-arm PEG-dimethacrylate (Mn 8,000), (c) 2-arm PEG-dimethacrlyate (Mn 740, Sigma Aldrich), (d) 2-arm PEG-diacrylaye (Mn 700), and 2-arm PEG-dithiol (Mn 2,000) with catalysts; (e) NaI / H_2O_2, (f) 3,3`-Dithiodipropionic acid (DTDP), and thiol oxidative solvent; (g) DMSO.

2.3.10. Drug release kinetics from polyaspartamide hydrogels

With the ability to control the mechanical and diffusional properties as well as induce degradation, the polyaspartamide-linked hydrogels were evaluated for controlled drug delivery applications. FITC-linked bovine serum albumin (FITC-BSA) as a model protein drug was encapsulated in PHHZA- or PHEDA-linked hydrogels with varying DS and concentration, and the time-dependent release profiles were obtained by fluorescence which is based on FITC-BSA standard curve in Figure 2.23 (Figure 2.24, Table 2.14, and Table 2.15). In this experiment, FITC-BSA was used instead of BSA, because the degraded polyaspartamide being a beta-polypeptide hindered a typically-used BCA protein assay method.

The release profiles from alginate-PHHZA hydrogels showed a typical diffusion-controlled release, with a power-law dependence on time (Figure 2.24.(a)). [10, 33] The kinetic rate constants (k_1), obtained by fitting the profiles with Ritger-Peppas model (Eq.(3)), closely followed the trend of swelling ratios shown in Figure S6 in Supplementary Information, where the values became smaller with DS and concentration of PHHZA as expected (Figure 2.24.(b)). This result demonstrated that the drug release was further expedited in a more swellable hydrogel. In addition, the exponent values (n) were in between 0.3 and 0.4 for all conditions, confirming that the release followed a Fickian diffusion mechanism (Figure 2.24.(c)).[33, 34]

In contrast to the alginate-PHHZA hydrogels, the drug release from PEG-PHEDA hydrogels displayed a sigmoidal release profile, suggesting there was a more gradual increase in drug release rate than a typical initial burst release commonly found in diffusion-controlled systems (Figure 2.24.(d)). Since PEG-PHEDA hydrogels demonstrated faster degradation rate than alginate-PHHZA hydrogels, it was suggested that the degradation was a more significant factor for the drug release in PEG-PHEDA hydrogels than alginate-PHHZA hydrogels. Therefore, a Weibull model (Eq.(4)) which is better suited for fitting sigmoidal profiles, was used to fit the release profiles of the PEG-PHEDA hydrogels, which produced release rate constant (k_2) and lag time constant (T). [14] k_2 values, similar to k_1 values for alginate-PHHZA hydrogels, became smaller with DS and concentration of PHEDA (Figure 2.24.(e)). The trend in T values, which represent the amount of time required for the 50 % release and thus signify the delay in release, was expectedly opposite to the k_2 values, becoming larger with DS and concentration of PHEDA (Figure 2.24.(f)). Taken together, the drug release rate and release pattern could be controlled using the polyaspartamide-linked hydrogels with varying crosslinking density.

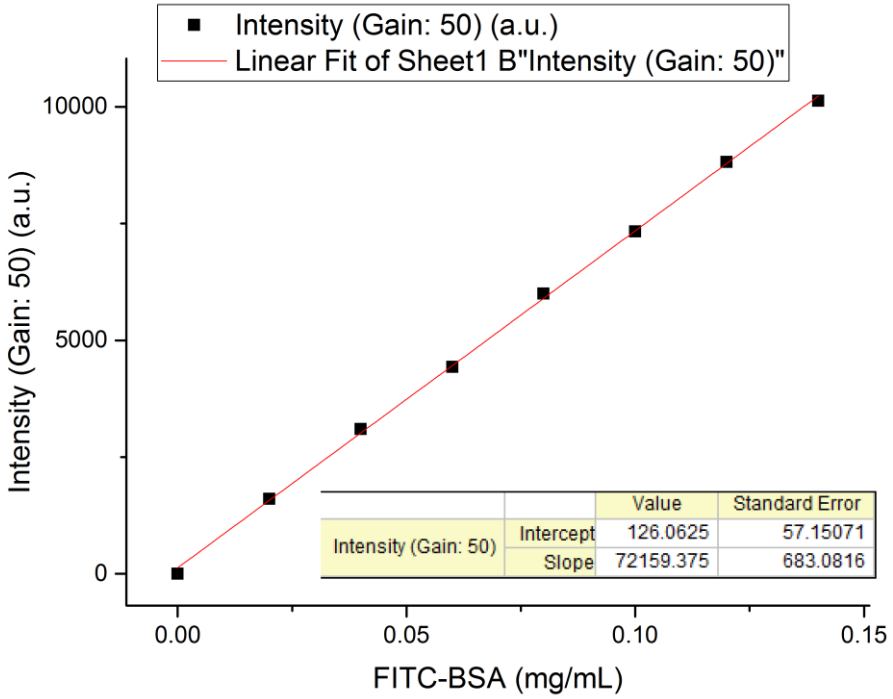

Figure 2.23. Standard curve for FITC-BSA (Gain: 50). [Intensity = 72159 * FITC-BSA + 126.06] is calculated by linear fitting to raw data.

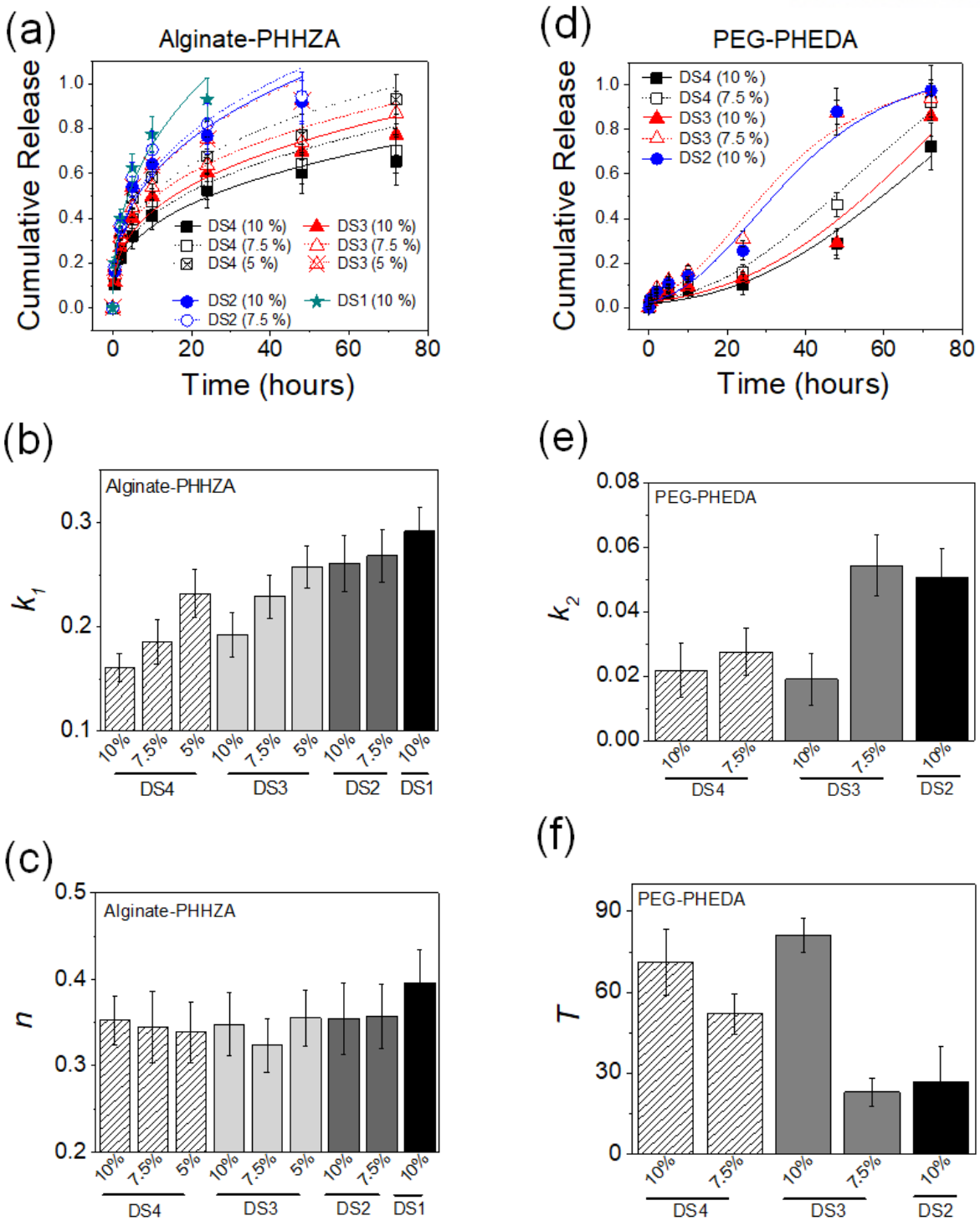

Figure 2.24. Drug release studies of (a-c) alginate-PHHZA and (d-f) PEG-PHEDA hydrogels. The release profiles (cumulative release over time) in (a) and (d) were fitted with Eq.(2) and Eq.(3), respectively. From the release profiles of alginate-PHHZA hydrogels in (a), (b) kinetic rate constants (k_1) and (c) exponents (n) were obtained. From the release profiles of PEG-PHEDA hydrogels in (d), (e) kinetic rate constants (k_2) and (f) lag time constants (T) were obtained.

37 °C Swelling Time	0.5 h	2 h	5 h	10 h	24 h	48 h	72 h
DS 4, 10%	0.0227	0.0491	0.0707	0.0906	0.1156	0.1322	0.1440
(Standard deviation)	0.0019	0.0014	0.0021	0.0029	0.0030	0.0033	0.0037
DS 4, 7.5%	0.0251	0.0602	0.0869	0.1043	0.1240	0.1411	0.1542
(Standard deviation)	0.0003	0.0031	0.0030	0.0031	0.0030	0.0029	0.0028
DS 4, 5.0%	0.0322	0.0673	0.1079	0.1279	0.1488	0.1697	0.2043
(Standard deviation)	0.0008	0.0036	0.0040	0.0042	0.0043	0.0044	0.0044
DS 3, 10%	0.0255	0.0596	0.0882	0.1092	0.1327	0.1532	0.1699
(Standard deviation)	0.0009	0.0039	0.0029	0.0032	0.0035	0.0039	0.0044
DS 3, 7.5%	0.0321	0.0684	0.0990	0.1182	0.1399	0.1626	0.1911
(Standard deviation)	0.0016	0.0041	0.0038	0.0046	0.0050	0.0055	0.0054
DS 3, 5.0%	0.0401	0.0731	0.1190	0.1400	0.1653	0.2031	
(Standard deviation)	0.0005	0.0004	0.0019	0.0024	0.0025	0.0018	
DS 2, 10%	0.0361	0.0785	0.1189	0.1409	0.1685	0.2020	
(Standard deviation)	0.0010	0.0049	0.0053	0.0056	0.0056	0.0055	
DS 2, 7.5%	0.0404	0.0814	0.1284	0.1551	0.1801	0.2077	
(Standard deviation)	0.0007	0.0018	0.0037	0.0055	0.0043	0.0043	
DS 1, 10%	0.0444	0.0874	0.1375	0.1702	0.2046		
(Standard deviation)	0.0007	0.0008	0.0015	0.0020	0.0027		

Table 2.14. The amount of FITC-BSA (mg/mL) released over time (h) for OAlg-PHHZA hydrogels measured at 37 °C. The average and standard deviation values were obtained from eight separate samples.

37 °C Swelling Time	0.5 h	2 h	5 h	10 h	24 h	36 h	48 h
DS 4, 10%	0.0048	0.0094	0.0136	0.0170	0.0223	0.0380	0.1764
(Standard deviation)	0.0006	0.0009	0.0009	0.0007	0.0007	0.0005	0.0025
DS 4, 7.5%	0.0073	0.0132	0.0187	0.0232	0.0343	0.1017	0.2033
(Standard deviation)	0.0004	0.0004	0.0005	0.0005	0.0007	0.0111	0.0107
DS 3, 10%	0.0061	0.0116	0.0166	0.0207	0.0291	0.0638	0.1891
(Standard deviation)	0.0003	0.0003	0.0002	0.0003	0.0005	0.0028	0.0023
DS 3, 7.5%	0.0109	0.0191	0.0270	0.0356	0.0680	0.1927	~~0.2063~~
(Standard deviation)	0.0005	0.0004	0.0007	0.0006	0.0009	0.0031	~~0.0032~~
DS 2, 10%	0.0084	0.0158	0.0236	0.0311	0.0562	0.1936	~~0.2143~~
(Standard deviation)	0.0002	0.0003	0.0003	0.0004	0.0009	0.0036	~~0.0033~~

Table 2.15. The amount of FITC-BSA (mg/mL) released over time (h) for PEGDA-PHEDA hydrogels measured at 37 °C. The average and standard deviation values were obtained from eight separate samples.

2.3.11. In vitro evaluation of polyaspartamide hydrogels

The ability to incorporate various amine-based molecules onto the polymer backbone via facile ring-opening nucleophilic addition is a hallmark of polyaspartamide. This aspect could open the door to accommodating moieties other than those involved with crosslinking reactions. This versatility of the polyaspartamide linker was further explored by conjugating cell adhesion peptide (i.e. RGD peptide) onto the PHHZA or PHEDA. Using this linker, the resulting peptide-conjugated hydrogels could be used as a cell culture platform.

GRGDS peptide, which is mostly used in 3T3 fibroblast as cell adhesion peptide, was selected and synthesized by the solid state synthesis method (Figure 2.25). Then, the peptide was reacted with polysuccinimide prior to the conjugation of the hydroxyl and reactive functional groups, and the polyaspartamide derivatives were confirmed by ^{13}C-NMR (Figure 2.26).

First, the cells were encapsulated in the RGD-containing polyaspartamide-linked hydrogels and their viability was assessed. [35-37] However, almost all cells were dead in 3D cell encapsulation method (section 2.2.18 and Figure 2.2.(a)). It may have been due to the excess of free amine groups within the hydrogels causing damage to the cell membrane. Second, pseudo-3D cell encapsulation method (Figure 2.2.(b)) was tried. But there were two problems with this method; first the cells didn't go into the mesh structure at the re-swelling step, and the degradation of polyaspartamide hydrogel in cell medium was extremely fast. All hydrogels tested were dissolved within 36 hours. For the same reason, 2D cell encapsulation method (Figure 2.2.(c)) also could not be used.

Therefore, surface coating method was demonstrated to assess both their biocompatibility and capability of allowing cell adhesion to the hydrogel (Figure 2.2.(d)). The alginate hydrogel was fabricated on top of a GRGDS peptide-linked PHHZA (RGD-PHHZA) coated surface in order to conjugate the RGD-PHHZA to the hydrogel surface (Figure 2.2.(e)). Then, 3T3 fibroblasts were placed on top of the hydrogels and allowed to adhere after hydrogel fabrication (Figure 2.27) Pure alginate hydrogel and PHHZA-linked alginate hydrogel (without peptide) were used as controls. In Day 1, only a few cells were adhered to the alginate hydrogel via non-specific interaction, judging from their round morphology, which was expected since the pure alginate does not contain cell-specific moieties (i). There was more cell adhesion and spreading on the PHHZA-alginate hydrogels (a, c, e, g) than the pure alginate hydrogels possibly due to some cells of unreacted amine groups on PHHZA by electrostatic interaction, a similar mechanism to poly(L-lysine) as a cell adhesion material. [38] The number of viable cells was much higher on RGD-PHHZA-alginate hydrogels in both DS 4 and DS 3 compared to PHHZA-alginate, indicating the RGD-specific cell adhesion further promoted the cell viability. However, DS 4 (a, e) had less cells than DS 3 (e, g), suggesting the cytotoxicity of hydrazide group in PHHZA. Furthermore, in Day 3, the RGD peptide effect was demonstrated as there was more proliferation. There result highlighted the versatility of the polyaspartamide

crosslinker by providing cell-responsive moieties in addition to controlling the mechanical properties of the hydrogels.

PHEDA was also coated on an alginate hydrogel and cell adhesion and viability was assessed (Figure 2.28). Surprisingly in Day 1, RGD-PHEDA (a, e) showed more death cells than PHEDA (c, g). Also, the cell morphology on PHEDA DS 4 (c) and 3 (g) was very similar to that shown in pure alginate gel (i). This result could be explained by degradation of PHEDA on alginate gel; the degraded PHEDA was released to the surrounding and there was less amine content on the hydrogel surface causing toxicity. RGD-DS 4 with the largest amount of amine group (e) has more death cells and less live cell than RGD-DS 3 (f). On the other hand, the presence of GRGDS peptide on PHEDA may have prevented the degradation, thereby presenting more amine groups on the hydrogels leading to decreased cell viability. But it should be noted that the cells that remained attached to the all hydrogel conditions survived and proliferated over time, demonstrating the overall biocompatibility and bioactivity of the PHEDA-coated hydrogels.

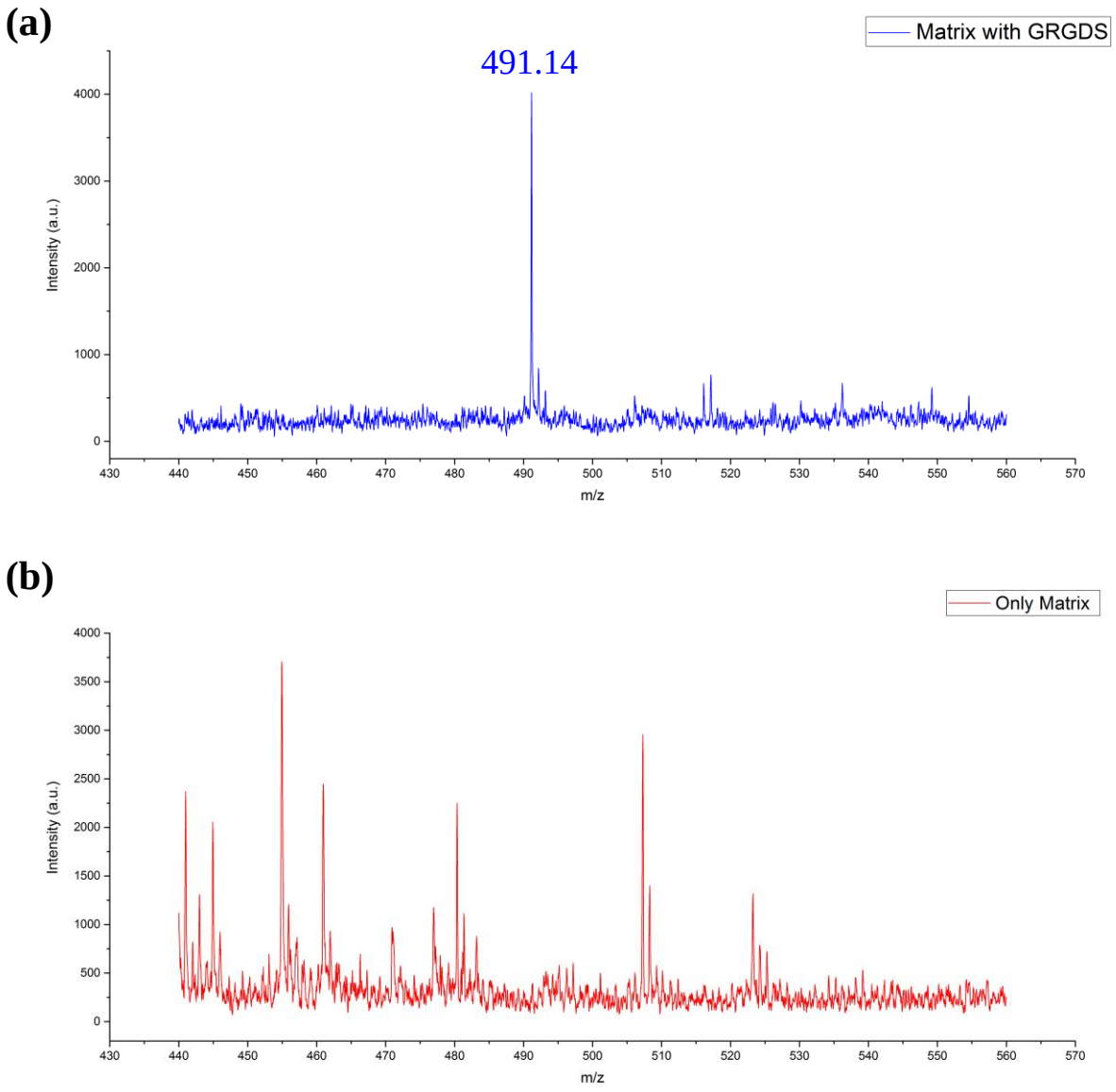

Figure 2.25. Mass analysis for GRGDS peptide using MALDI-TOF-MS. α-cyano-4-hydroxycinnamic acid (HCCA) and ethanol/acetonitrile (60 : 40) were used as matrix and solvent, respectively. Spectrum (a) is for the mixture with GRGDS peptide, which shows the expected peak at the m/z value of 449.14 (the theoretical value for $[GRGDS+H]^+$ is 491.221). Spectrum (b) is for the matrix only, which does not have the characteristic peak.

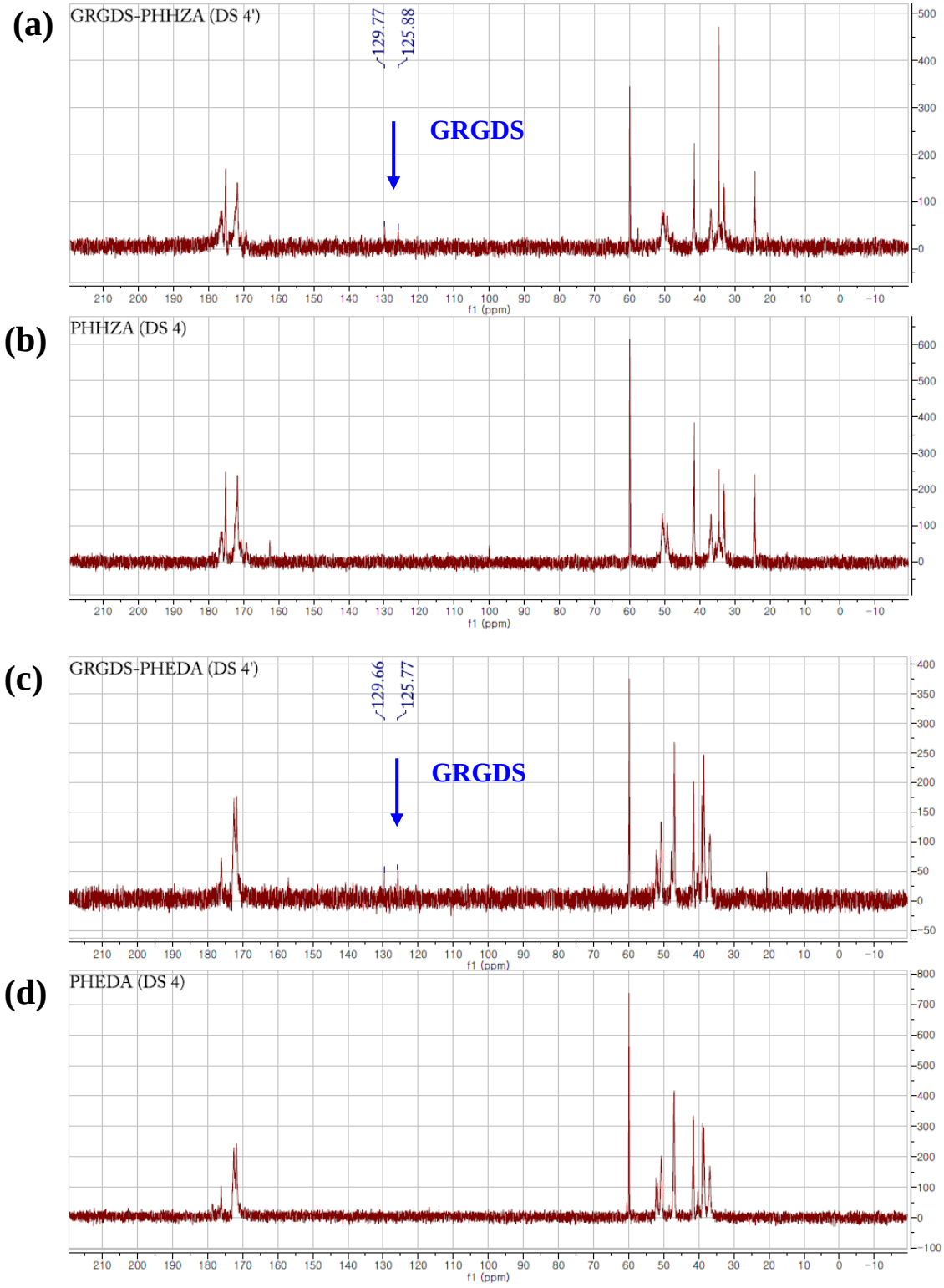

Figure 2.26. ^{13}C-NMR spectrum of (a) GRGDS-PHHZA (DS 4'), (b) PHHZA (DS 4), (c) GRGDS-PHEDA (DS 4'), and (d) PHEDA (DS 4). (a) and (c) show the conjugated-GRGDS peak at 129 ppm and 125 ppm.

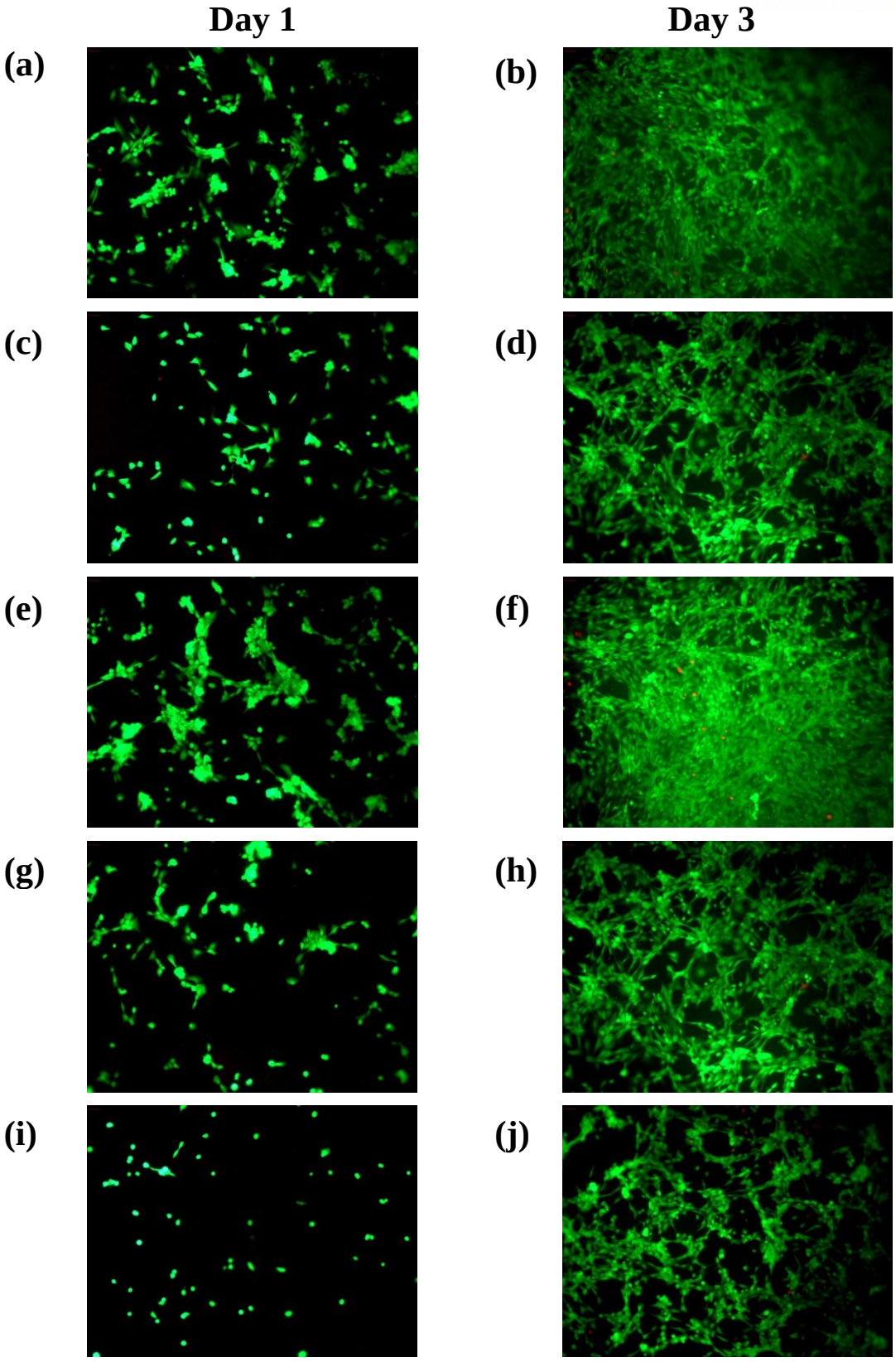

Figure 2.27. The 3T3 fibroblasts cultured on alginate hydrogels coated with PHHZA, visualized with a fluorescent labeling of live (green) and dead (red) cells at Day 1 and 3. (a, b) RGD-PHHZA (DS 4), (c, d) PHHZA (DS 4), (e, f) RGD-PHHZA (DS 3'), (g, h) PHHZA (DS 3), (i, j) no coating.

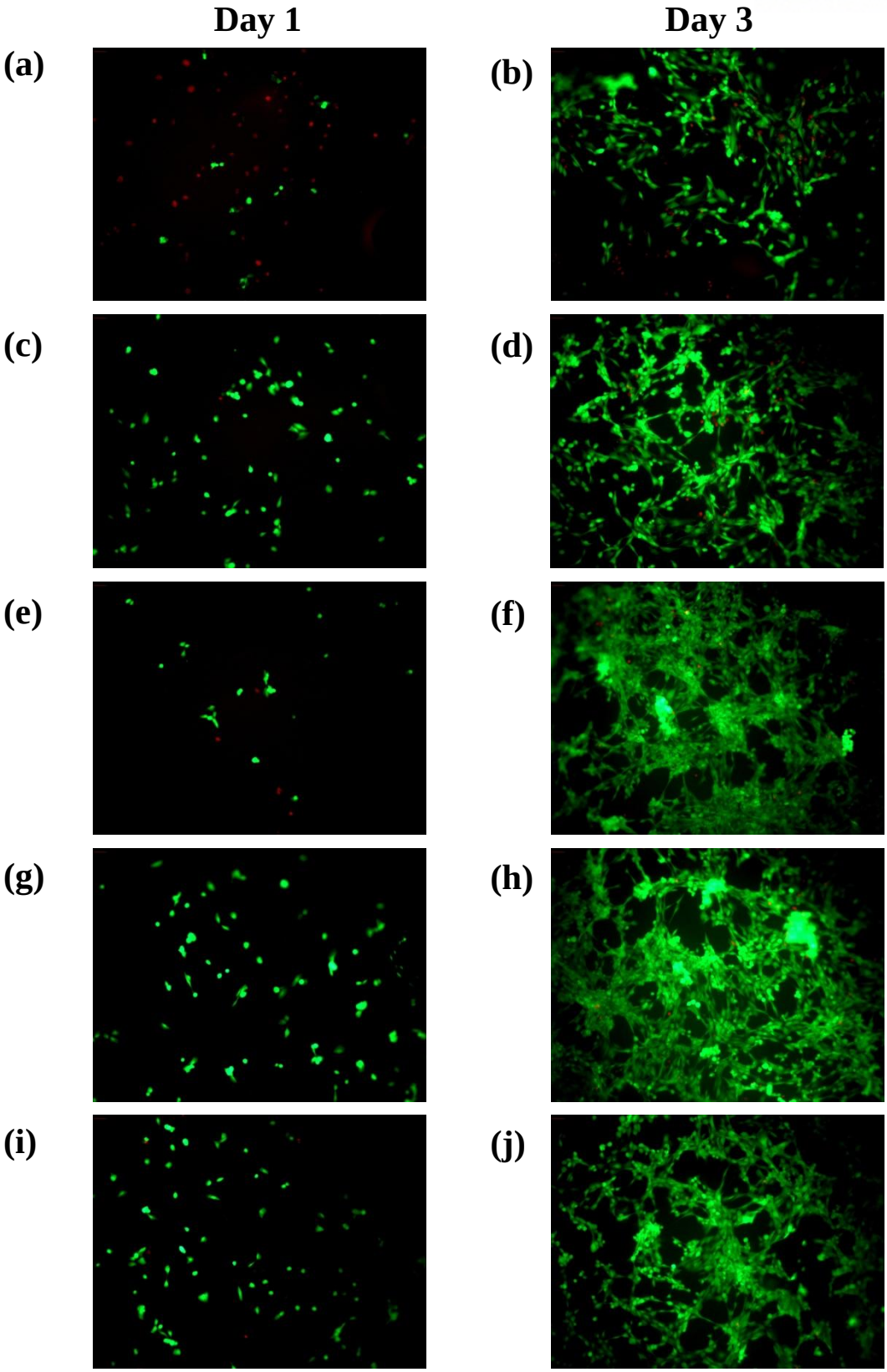

Figure 2.28. The 3T3 fibroblasts cultured on alginate hydrogels coated with PHEDA, visualized with a fluorescent labeling of live (green) and dead (red) cells at Day 1 and 3. (a, b) RGD-PHEDA (DS 4), (c, d) PHEDA (DS 4), (e, f) RGD-PHEDA (DS 3'), (g, h) PHEDZA (DS 3), (i, j) no coating.

2.4. Conclusion

This study introduced a highly versatile polymeric crosslinker which allows for developing hydrogels with controllable degradation and mechanical properties as well as presenting bioactive molecules for cell adhesion. Polyaspartamide, derivatized from polysuccinimide, could accommodate various functional moieties via ring-opening nucleophilic addition. The degree of substitution (DS) of reactive functional groups on the polyaspartamide also could be controlled efficiently by varying the amount of nucleophilic reactant. Here, two different polyaspartamide crosslinkers having amine and hydrazide as nucleophilic functional groups were prepared, namely PHEDA and PHHZA which were capable of in situ crosslinking reaction under physiological conditions and showed different reactivities towards gel-forming polymers. The mechanical properties of the resulting hydrogels could be controlled in a wide range simply by changing the DS, while maintaining the overall polymer concentration. In addition, the hydrogels crosslinked by PHEDA and PHHZA were all shown to undergo degradation under physiological conditions, likely due to unreacted functional groups involved in hydrolysis. Adjusting the mechanical properties, combined with the degradation behavior, of the hydrogels allowed the controlled release of encapsulated drug molecules. Furthermore, by using a polyaspartamide crosslinker conjugated with cell-responsive peptides, cell-adhesive hydrogels as cell-culture scaffolds could also be prepared. With these collection of tunable physical and biological properties, it is expected that the strategy of utilizing polyaspartamide-based crosslinkers to create hydrogels with diverse functionalities could be successfully applied to biomedical engineering, including but not limited to drug delivery and tissue engineering.

2.5. Reference

[1] Tomida, M.; Nakato, T.; Matsunami, S.; Kakuchi, T. Convenient synthesis of high molecular weight poly(succinimide) by acid-catalysed polycondensation of l-aspartic acid. *Polymer.* **1997**, 38, 4733-4736.

[2] Nakato, T.; Kusuno, A.; Kakuchi, T. Synthesis of poly(succinimide) by bulk polycondensation of L-aspartic acid with an acid catalyst. *J Polym Sci A Polym Chem.* **2000**, 38, 117-122.

[3] Cha, C.; Jeong, JH; Tang, X; Zill, AT; Prakash, YS; Zimmerman, SC. Top-down synthesis of versatile polyaspartamide linkers for single-step protein conjugation to materials. *Bioconjugate Chem.* **2011**, 22, 2377-2382.

[4] Jeong, J. H.; Cha, C.; Kaczmarowski, A.; Haan, J.; Oh, S.; Kong, H. Polyaspartamide vesicle induced by metallic nanoparticles. *Soft Matter.* **2012**, 8, 2237-2242.

[5] Ellman, G. L. Tissue sulfhydryl groups. *Arch. Biochem. Biophys.* **1959**, 82 (1), 70–77.

[6] Stocks, S. J.; Jones, A. J. M.; Ramey, C. W.; Brooks, D. E. A fluorometric assay of the degree of modification of protein primary amines with polyethylene glycol. *Anal Biochem.* **1986**, 154, 232-234.

[7] Bouhadir, K. H.; Hausman, D.S.; Mooney, D. J. Synthesis of cross-linked poly(aldehyde guluronate) hydrogels. *Polymer.* **1999**, 40, 3575-3584.

[8] Boontheekul, T; Kong, H-J; Mooney, D. J. Controlling alginate gel degradation utilizing partial oxidation and bimodal molecular weight distribution. *Biomaterials.* **2005**, 26, 2455-2465.

[9] Bouhadir, K. H.; Lee, K. Y.; Alsberg, E.; Damm, K. L.; Anderson, K. W.; Mooney, D. J. Degradation of partially oxidized alginate and its potential application for tissue engineering. *Biotechnol Prog.* **2001**, 17, 945-50.

[10] Kim, S; Sim, S. B.; Lee, K.; Cha, C. Comprehensive examination of mechanical and diffusional effects on cell behavior using a decoupled 3d hydrogel system. *Macromol Biosci.* **2017**, 17, 1700162.

[11] Jang, J; Hong, J.; Cha, C. Effects of precursor composition and mode of crosslinking on mechanical properties of graphene oxide reinforced composite hydrogels. *J Mech Behav Biomed Mater.* **2017**, 69, 282-293.

[12] Cha, C.; Kohman, R. H.; Kong, H. Biodegradable polymer crosslinker: independent control of stiffness, toughness, and hydrogel degradation rate. *Adv Funct Mater.* **2009**, 19, 3056-3062.

[13] Escobar, F.; Anseth, K. S.; Schultz, K. M. Dynamic changes in material properties and degradation of poly(ethylene glycol)–hydrazone gels as a function of pH. *Macromolecules.* **2017**, 50, 7351-7360.

[14] Dash, S; Murthy, P. N.; Nath, L.; Chowdhury, P. Kinetic modeling on drug release from controlled drug delivery systems. *Acta Pol Pharm.* **2010**, 67, 217-223.

[15] Ritger, P. L.; Peppas, N. A. A simple equation for description of solute release II. Fickian and anomalous release from swellable devices. *J Control Release.* **1987**, 5, 37-42.

[16] Liu, H.; Wang, C; Gao, Q; Chen, J; Ren, B; Liu, X; Tong, Z. Facile fabrication of well-defined hydrogel beads with magnetic nanocomposite shells. *Int J Pharm.* **2009**, 376, 92-88.

[17] Plow, E. F.; Haas, T. A.; Zhang, L.; Loftus, J.; Smith, J. W. Ligand Binding to Integrins. *J. Biol. Chem.* **2000**, 275 (29), 21785–21788.

[18] Kharkar, P. M.; Rehmann, M. S.; Skeens, K. M.; Maverakis, E.; Kloxin, A. M. Thiol-ene click hydrogels for therapeutic delivery. *ACS Biomater Sci Eng.* **2016**, 2(2), 165-179.

[19] Choh, S.Y.; Cross, D.; Wang, C. Facile synthesis and characterization of disulfide-cross-linked hyaluronic acid hydrogels for protein delivery and cell encapsulation. *Biomacromolecules.* **2011**, 12(4), 1126-1136.

[20] Dahlmann, J.; Krause, A.; Möller, L.; Kensah, G.; Möwes, M.; Diekmann, A.; Martin, U.; Kirschning, A.; Gruh, I.; Dräger, G. Fully defined in situ cross-linkable alginate and hyaluronic acid hydrogels for myocardial tissue engineering. *Biomaterials.* **2013**, 34(4), 940-951.

[21] Nam, K.; Kimura, T.; Kishida, A. Controlling coupling reaction of EDC and NHS for preparation of collagen gels using ethanol/water co-solvents. *Macromol Biosci.* **2008**, 8(1), 32-37.

[22] Zhang, L.; Zheng, S.; Kang, D. E.; Shin, J. Y.; Suh, H.; Kim, I. Synthesis of multi-amine functionalized hydrogel for preparation of noble metal nanoparticles: utilization as highly active and recyclable catalysts in reduction of nitroaromatics. *RSC Adv.*, **2013**, 3, 4692-4703.

[23] Martinsen, A.; Skjåk-Braek, G.; Smidsrød, O. Alginate as immobilization material: I. Correlation between chemical and physical properties of alginate gel beads. *Biotechnol Bioeng.* **1989**, 33(1), 79-89.

[24] Schüll, C.; Frey, H. Grafting of hyperbranched polymers: From unusual complex polymer topologies to multivalent surface functionalization. *Polymer.* **2013**, 54 (21), 5443-5455.

[25] Liang, Y.; Jensen, T. W.; Roy, E. J.; Cha, C.; DeVolder, R. J.; Kohman, R. E.; Zhang, B. Z.; Textor, K. B.; Rund, L. A.; Schook, L. B.; Tong, Y. W.; Kong, H. Tuning the non-equilibrium state of a drug-encapsulated poly(ethylene glycol) hydrogel for stem and progenitor cell mobilization. *Biomaterials.* **2011**, 32, 2004-2012.

[26] Lutolf, M. P.; Hubbell, J. A. Synthesis and Physicochemical Characterization of End-Linked Poly(ethylene glycol)-co-peptide Hydrogels Formed by Michael-Type Addition. *Biomacromolecules*, **2003**, 4 (3), 713–722.

[27] Phelps, E. A.; Enemchukwu, N. O.; Fiore, V. F.; Sy, J. C.; Murthy, N.; Sulchek, T. A.; Barker, T. H.; García, A. J. Maleimide cross-linked bioactive PEG hydrogel exhibits improved reaction kinetics and cross-linking for cell encapsulation and in situ delivery. *Adv. Mater,* **2012**, 24 (1), 64-70.

[28] Fairbanks, B. D.; Singh, S. P.; Bowman, C. N.; Anseth, K. S. Photodegradable, Photoadaptable Hydrogels via Radical-Mediated Disulfide Fragmentation Reaction. *Macromolecules.* **2011**, 44 (8), 2444–2450.

[29] Niu, G.; Yang, Y.; Zhang, H.; Yang, J.; Song, L.; Kashima, M.; Yang, Z.; Cao, H.; Zheng, Y.; Zhu, S.; Yang, H. Synthesis and characterization of acrylamide/N-vinylpyrrolidone copolymer with pendent thiol groups for ophthalmic applications. *Acta Biomater.* **2009**, 5 (4), 1056-1063.

[30] Yu, H.; Feng, Z.; Zhang, A.; Suna, L.; Qiana, L. Synthesis and characterization of three-dimensional crosslinked networks based on self-assemly of α-cyclodextrins with thiolated 4-arm PEG using a three-step oxidation. *Soft Matter,* **2006**, 2, 343-349.

[31] Tam, J. P.; Wu, C. R.; Liu, W.; Zhang, J. W. Disulfide bond formation in peptides by dimethyl sulfoxide. Scope and applications. *J. Am. Chem. Soc.*, **1991**, 113 (17), 6657–6662.

[32] Vlies, A. J.; Neil, C. P.; Hasegawa, U.; Hammond, N.; Hubbell, J. A. Synthesis of Pyridyl Disulfide-Functionalized Nanoparticles for Conjugating Thiol-Containing Small Molecules, Peptides, and Proteins. *Bioconjugate Chem.*, **2010**, 21 (4), 653–662.

[33] Ritger PL, Peppas NA. A simple equation for description of solute release II. Fickian and anomalous release from swellable devices. J Control Release. 1987;5:37-42.

[34] Serra L, Doménech J, Peppas NA. Drug transport mechanisms and release kinetics from molecularly designed poly(acrylic acid-g-ethylene glycol) hydrogels. Biomaterials. 2006;27:5440-51.

[35] Hoffman A. S. Hydrogels for biomedical applications. *Adv. Drug Deliv. Rev.* **2012**, 64, 18-23.

[36] Tibbitt, M. W.; Anseth K. S. Hydrogels as Extracellular Matrix Mimics for 3D Cell Culture. *Biotechnol Bioeng.* **2009**, 103 (4), 655–663.

[37] Hern, D. L.; Hubbell, J. A. Incorporation of adhesion peptides into nonadhesive hydrogels useful for tissue resurfacing. *J Biomed Mater Res.* **1998**, 39, 266-276.

[38] Crompton, K. E.; Goud, J. D.; Bellamkonda, R. V.; Gengenbach, T. R.; Finkelstein, D. I., Horne, M. K.; Forsythe, J. S. Polylysine-functionalised thermoresponsive chitosan hydrogel for neural tissue engineering. *Biomaterials.* **2007**, 28, 441-449.

Chapter 3. Thermoresponsive Polyaspartamide Chain

3.1. Introduction

Thermoresponsive hydrogels, based on sol-gel transition derived from polymer chains hydrophobic interaction, have been long explored for drug delivery applications, because the body temperature could be used as a trigger to induce drug release. [1, 2] Hydrogel properties could be varied to control the lower critical solution temperature (LCST) as well as the degree of swelling. [3] Several biocompatible polymers displaying thermoresponsiveness have been reported. For example, poly(ethylene glycol) (PEG), poly(methacrylic acid) (PMAA), and poly(vinyl alcohol) (PVA) have LCST at ~120 ^{o}C, ~75 ^{o}C, and ~125 ^{o}C, respectively, but the high temperatures are not suitable for biological applications. However, poly(N-isopropylacrylamide) (PNIPAM) has LCST at ~32 ^{o}C, near the body temperature, and therefore extensively investigated. [1] The thermoresponsiveness of PNIPAM has been attributed to the hydrophobic interaction between isopropyl groups leading to polymer chain collapse.

Polyaspartamide having thermoresponsiveness by introducing isopropyl groups has been previously explored. For example, Kim et al. demonstrated N,N-diisopropylaminoethyl, N-isopropylaminoethyl and N-isopropylamine pendent groups conjugated polyaspartamide hydrogels with thermoresponsive property, respectively. [4-7] Wu et al. also demonstrated isopropyl pendent group conjugated polyaspartamide nanoparticles with drug delivery system. [8] However, the ability to control both mechanical properties and thermoresponsiveness has not been explored to date.

In this chapter, thermoresponsive polyaspartamide chain with isopropyl group is introduced. Poly(2-hydroxyethyl-co-isopropyl) (PHIPA) was synthesized with varying DS and performed turbidity test with change in temperature.

3.2. Experimental section

3.2.1. Synthesis of PHIPA; isopropyl-linked polyaspartamide

Isopropyl group attached polyaspartamide, termed poly(2-hydroxyethyl-co-isopropyl) (PHIPA), was synthesized by a similar method to synthesize other polyaspartamide derivatives in Chapter 2. In this experiment, isopropylamine (Sigma Aldrich) was used to make thermoresponsible polyaspartamide chain. Considering the low boiling point of this reagent at 34 ^{o}C, The entire reaction was processed at room temperature with a closed environment. First, PSI (0.8 g) was completely dissolved in DMF (10 mL). The desired amount of isopropylamine (1 eq. to the target succinimide ring) was added to the solution and stirred for 2-days. Then, the desired amount of ethanolamine (1.5eq. to unopened succinimide ring) were added to the solution and stirred for 1-day at same environment. Finally, the mixture was dialyzed and lyophilized to obtain the final product.

Polysuccinimide (PSI)	0.8 g			
Desired Propyl DS	20 %	40 %	60%	80 %
Desired Hydroxyl DS	80 %	60 %	40 %	20 %
Isopropylamine (1 eq.)	0.0975 g	0.1950 g	0.2925 g	0.3900 g
Ethanolamine (1.5 eq.)	597.6 uL	448.2 uL	298.8 uL	149.4 uL

Table 3.1. Amount of the chemicals used to synthesize poly(2-hydroxyethyl-co-isopropyl) (PHIPA).

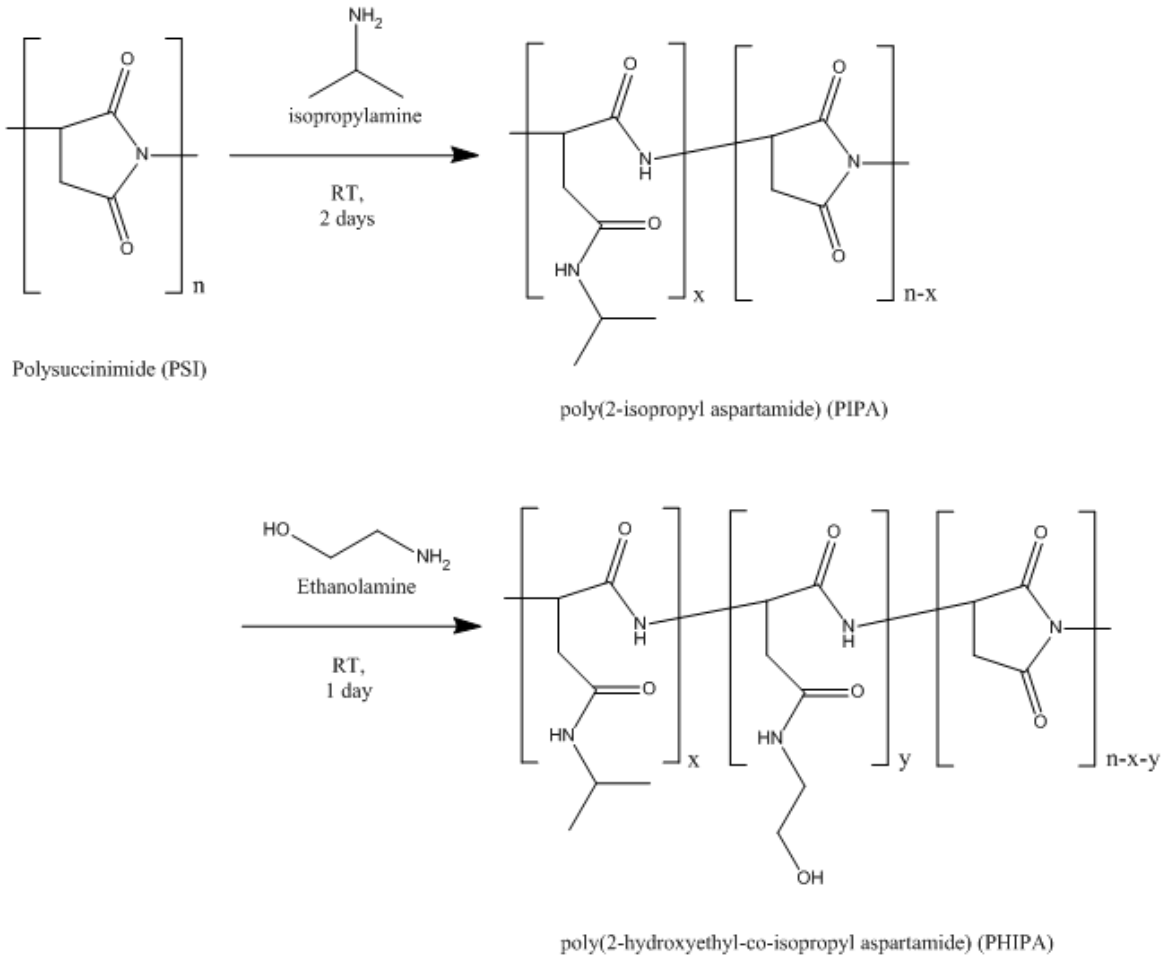

Scheme 3.1. Synthesis of poly(2-hydroxyethyl-co-isopropyl) (PHIPA).

3.2.2. Thermoresponsive turbidity test

UV/Vis spectrophotometer (Multiskan GO, Thermo Fisher) was used to measure the absorption spectrum from 340 nm to 800 nm for PHIPA solutions (DS 0, 20, 40, 60, 80). The temperature was increased from 24 ^{o}C to 44 ^{o}C by 2 ^{o}C increment, and the absorbance was measured. For each temperature, it was allowed to sit for 10 min to reach the equilibrium. All absorbance values were averaged with four samples.

3.3. Result and discussion

3.3.1. Characterization of PHIPA

The PHIPA (DS 20 to 80) samples were characterized by both FT-IR and ^{13}C-NMR. First, FT-IR spectra are shown in Figure 3.1. The peaks for isopropyl group (1386 cm^{-1}) and C-H stretching (2940 cm^{-1}) in methyl group increased with isopropyl DS. Also, N-H stretching (1535 cm^{-1}) showed the similar trend. Even though the amount of N-H bond is same for all DS, it is expected that the N-H neighbored isopropyl group demonstrated a chain collapse effect and it enhanced the N-H stretching intensity. On the other hand, both C-O stretching (1060 cm^{-1}) and O-H stretching (3300 cm^{-1}) decreased with isopropyl DS, since the sum of isopropyl and hydroxyl group should be constant in all DS conditions.

^{13}C-NMR spectra, which were measured without NOE to make an accurate integration value, are presented in Figure 3.2 and Table 3.2. Two $–CH_3$ peaks of isopropyl group were at 21.4 ppm and 19.8 ppm. In this study the average of these tow integration values was used as DS of isopropyl group. Also, one carbon in $–CH_2$-OH of hydroxyl group had 59.8 ppm and represented DS of hydroxyl group. As Table 3.2 represented, DS of hydroxyl and isopropyl group were very close to the theoretical value.

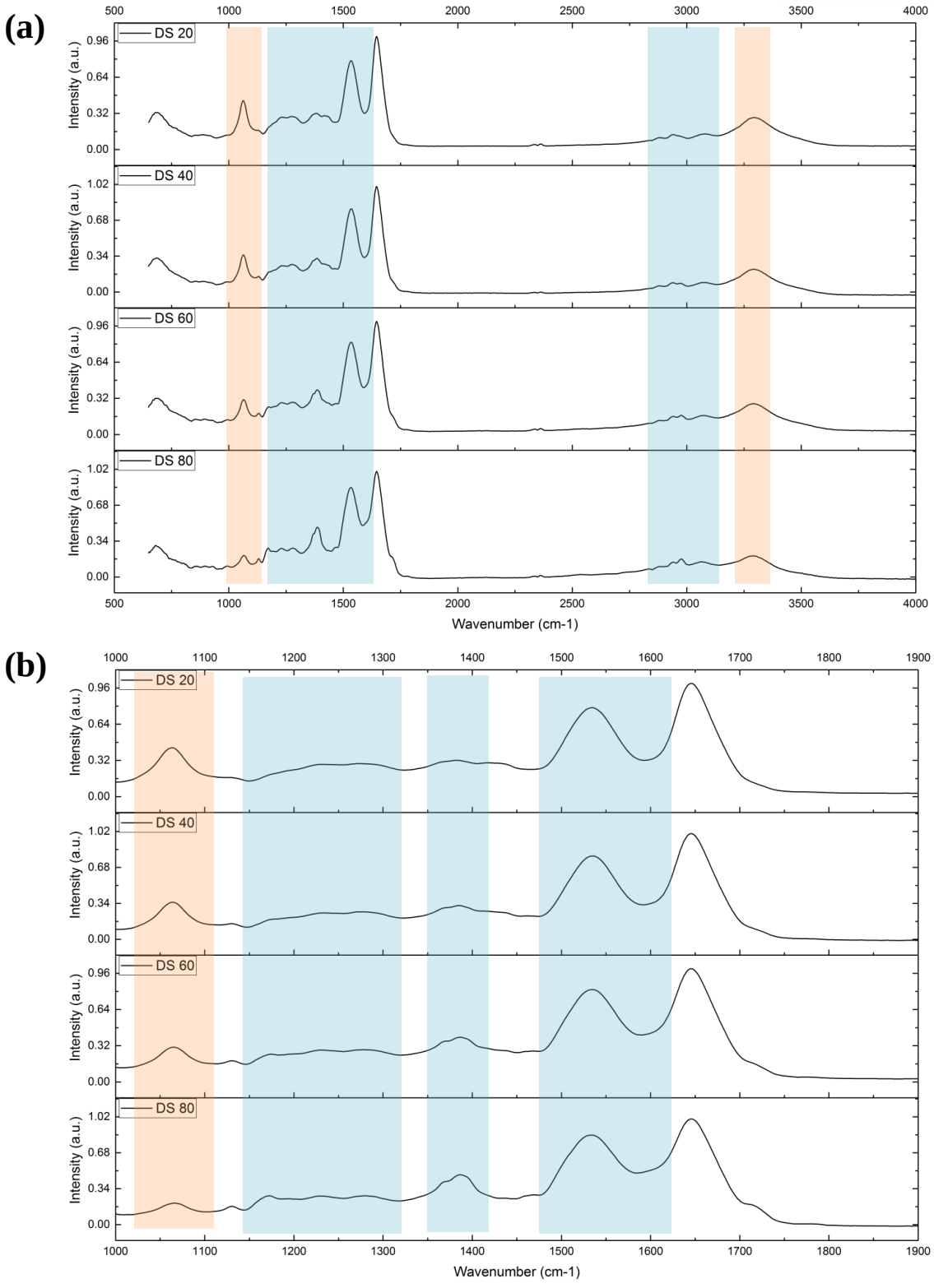

Figure 3.1. FT-IR spectra of PHIPA (DS = 20, 40, 60, 80) measured by ATR method. The peaks in blue region are increasing with DS. The peaks in red region are decreasing with DS. The spectra in (a) are the full measured spectra, while those from 1000 cm^{-1} to 1900 cm^{-1} are magnified and presented in (b).

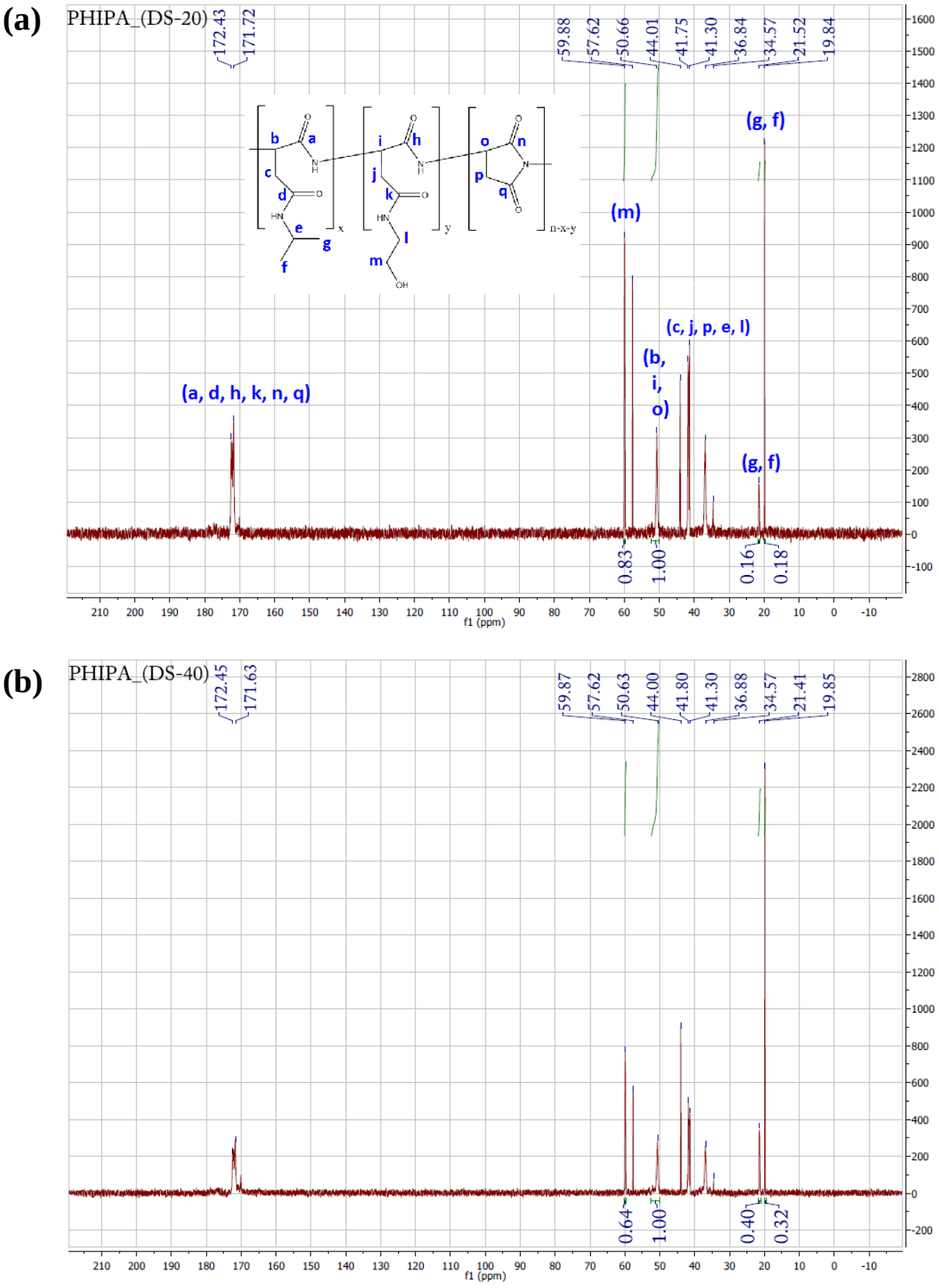

Figure 3.2. ^{13}C-NMR spectra of PHIPA. (a) DS 20, (b) DS 40, (c) DS 60, and (d) DS 80.

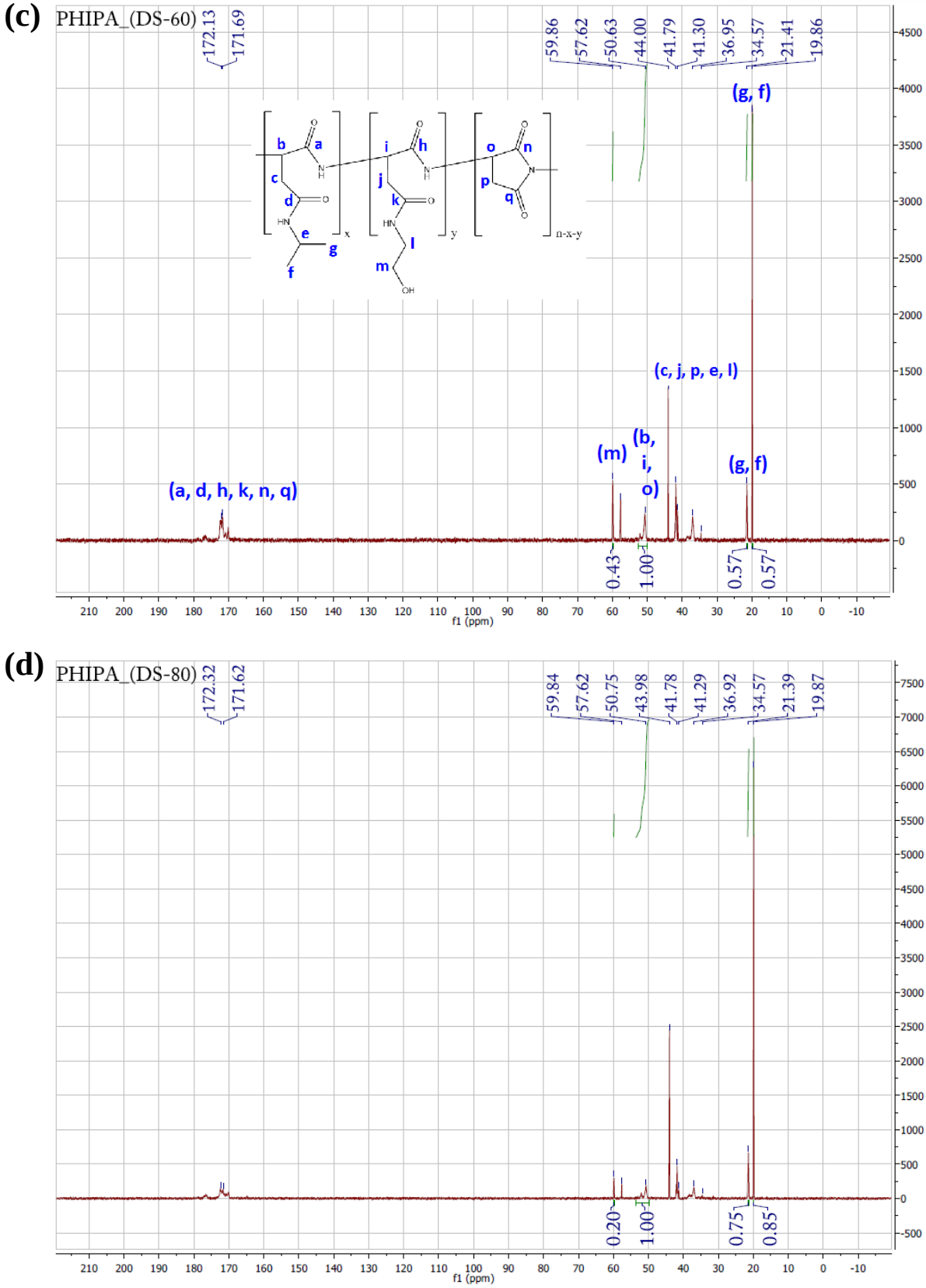

Figure 3.2. ^{13}C-NMR spectra of PHIPA. (a) DS 20, (b) DS 40, (c) DS 60, and (d) DS 80.

	DS 20	DS 40	DS 60	DS 80
Designed isopropyl DS	20 %	40 %	60 %	80 %
Designed hydroxyl DS	80 %	60 %	40 %	20 %
^{13}C-NMR 1st isopropyl group integration value	0.16	0.40	0.57	0.75
^{13}C-NMR 2nd isopropyl group integration value	0.18	0.32	0.57	0.85
^{13}C-NMR hydroxyl group integration value	0.83	0.64	0.43	0.20
Measured isopropyl DS	17 %	36 %	57 %	80 %
Measured hydroxyl DS	83 %	64 %	43 %	20 %

Table 3.2. DS of isopropyl group for PHIPA measured by ^{13}C-NMR.

3.3.2. Thermoresponsive polyaspartamide chain

Hydrophobic interaction by isopropyl groups in PHIPA could lead to the chain collapse as the environmental temperature increase. This interaction was expected to trigger increasing turbidity as well as change in absorbance in UV-Vis range, so temperature-dependence absorption spectrum was obtained to evaluate the thermoresponsiveness of PHIPA.

Figure 3.3 represents the decrease in absorption of polyaspartamide with increasing temperature. DS 0, which has 100 % hydroxyl group and no isopropyl group in polyaspartamide chain, has a significantly decreasing peak at 382 nm. On the other hand, DS 20 to 80 have decreasing peaks at both 382 nm and 500 nm. The change in absorbance at 500 nm is matched with the previous study for LCST of isopropyl group. [8] Average and normalized absorbance values with temperature at 382 nm and 500 nm are shown in Figure 3.4. If there exist LCST between 24 ^{o}C to 45 ^{o}C, a rapid change in absorbance at 500 nm should be observed, but decrease in absorbance was more gradual and smaller with isopropyl DS. It is possible that the number of isopropyl groups in PHIPA under the given concentration was not significant enough to show LCST behavior.

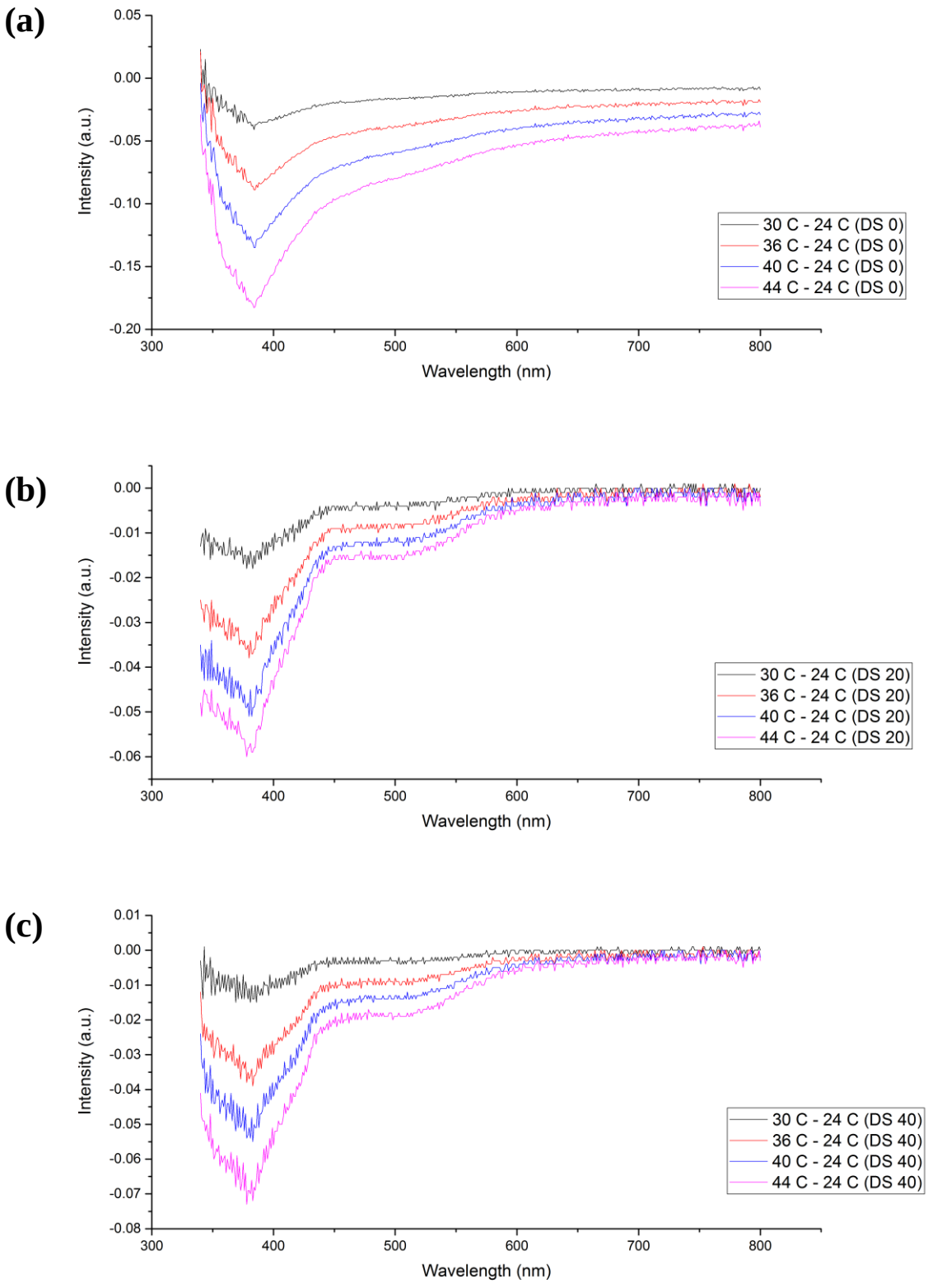

Figure 3.3. UV-Vis absorption spectra of PHIPA (10 % in DI water). (a) DS 0, (b) DS 20, (c) DS 40, (d) DS 60, (e) DS 80. Black, red, blue, and pink spectra represent the absorbance intensity difference between 30 ^{o}C and 24 ^{o}C, 36 ^{o}C and 24 ^{o}C, 40 ^{o}C and 24 ^{o}C, and 44 ^{o}C and 24 ^{o}C, respectively.

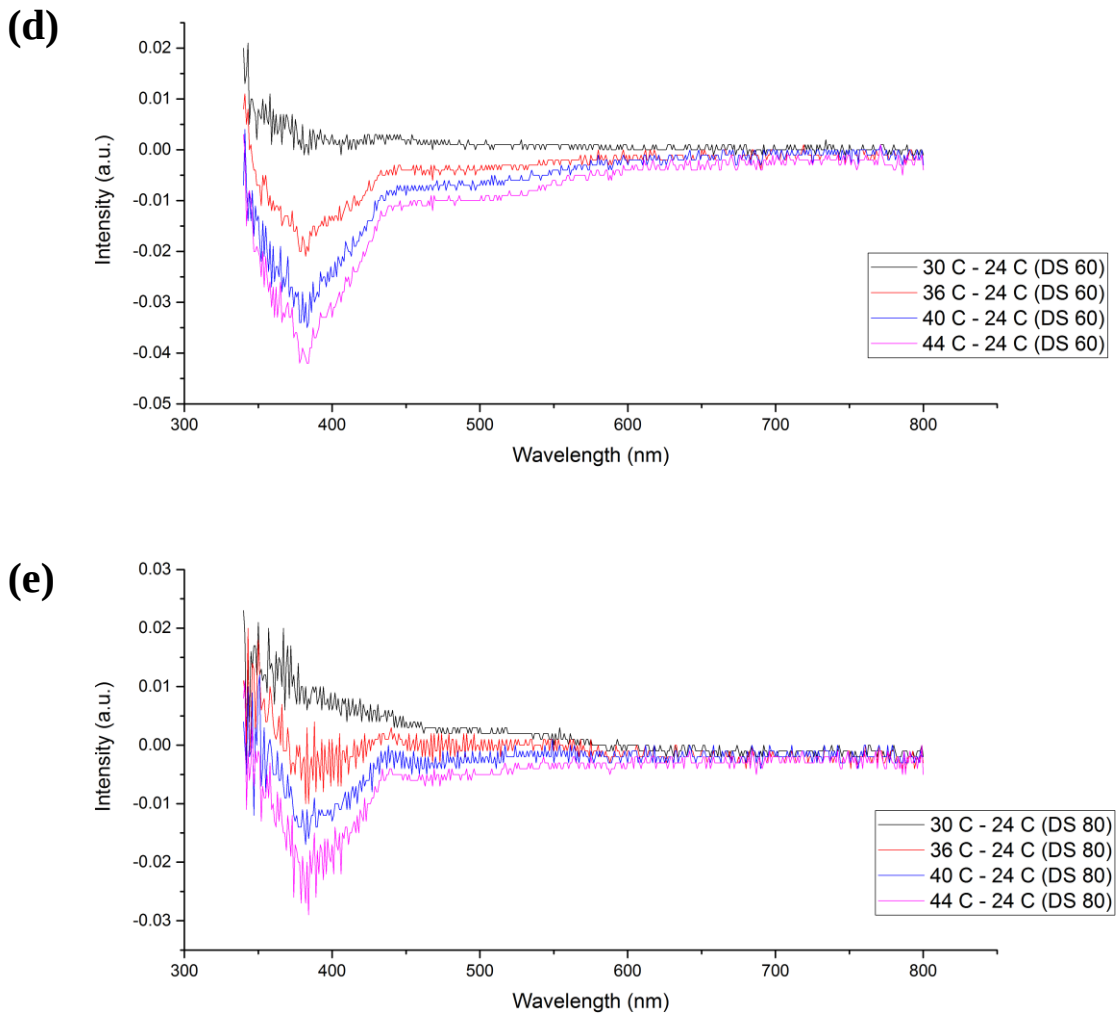

Figure 3.3. Absorption spectrum difference of PHIPA (10 % in DI water). (a) DS 0, (b) DS 20, (c) DS 40, (d) DS 60, (e) DS 80. Black, red, blue, and pink represent the absorbance intensity difference between 30 ^{o}C and 24 ^{o}C, 36 ^{o}C and 24 ^{o}C, 40 ^{o}C and 24 ^{o}C, and 44 ^{o}C and 24 ^{o}C, respectively.

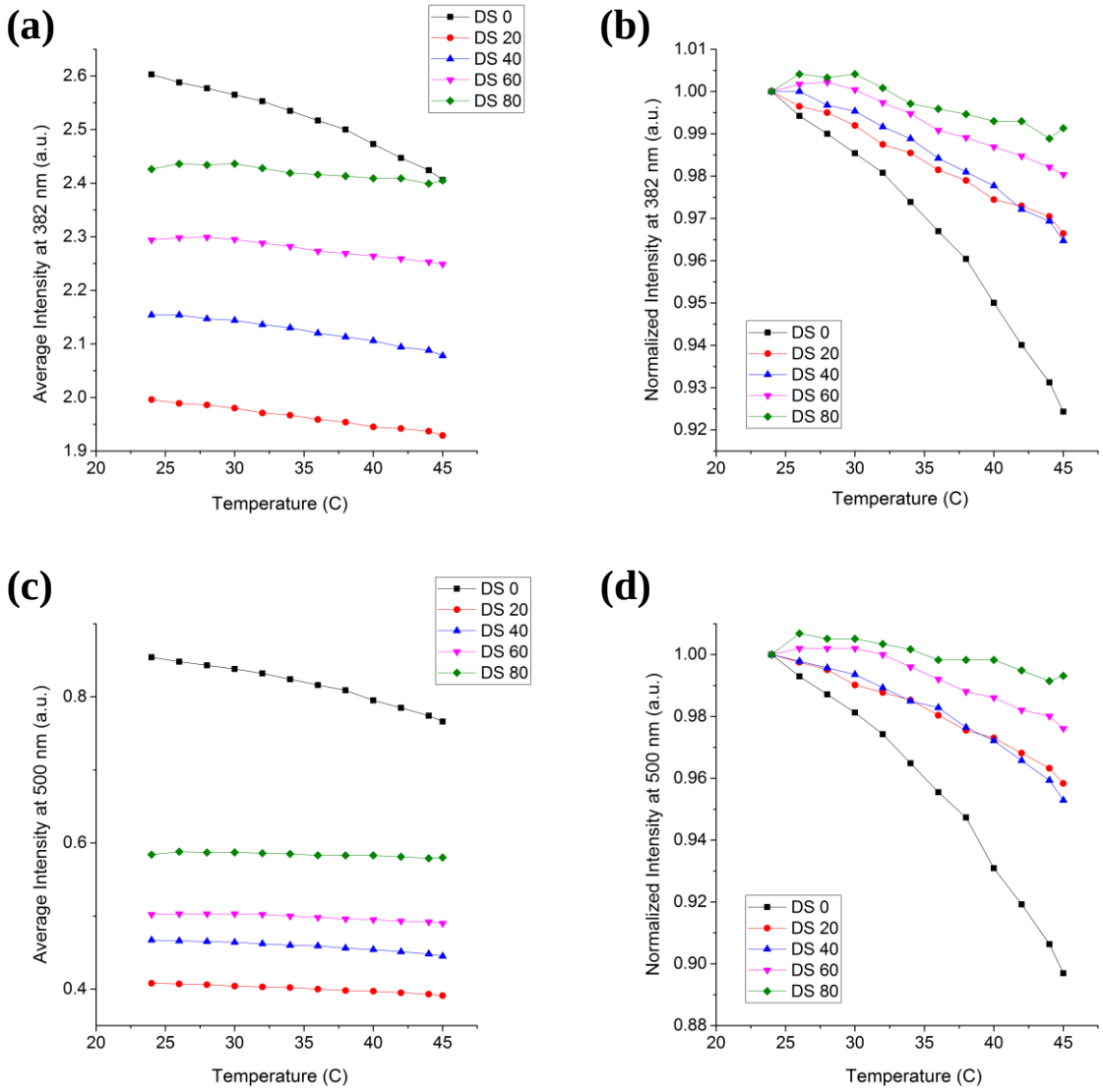

Figure 3.4. Absorbance at (a, b) 382 nm and (c, d) 500 nm of PHIPA (10 %, DS 0, 20, 40, 60, 80) with temperature from 24 ^{o}C to 45 ^{o}C. (a) and (c) represent the average intensity, and (b) and (d) represent the normalized intensity.

3.4. Conclusion

The polyaspartamide with isopropyl groups, PHIPA, was successfully synthesized and characterized by both FT-IR and ^{13}C-NMR. The turbidity test to PHIPA solution with increasing temperature from 22 ^{o}C to 45 ^{o}C had been expected to demonstrate LCST property of the polyaspartamide by the linked-isopropyl group. With only small change in absorbance, significant absorbance change was not observed. For future studies, the effects of the concentration of PHIPA and the range of temperature on the thermoresponsiveness of PHIPA should be explored. Furthermore, the effect of PHIPA incorporated into a hydrogel system on the drug release kinetics should also be explored. It is expected that the results presented in this chapter will provide a blueprint for continuing efforts to utilize this polymer for biomedical applications.

3.5. Reference

[1] Jeong B.; Kim, S. W.; Bae Y. H. Thermosensitive sol–gel reversible hydrogels. *Adv. Drug Deliv. Rev.* **2002**, 54, 37-51.

[2] Klouda, L. Thermoresponsive hydrogels in biomedical applications: A seven-year update. *Eur. J. Pharm. Biopharm.* **2015**, 97, 338-349.

[3] Schild, H.G. ; Tirrell, D.A. Microcalorimetric detection of lower critical solution temperatures in aqueous polymer solutions. *J. Phys. Chem.* **1990**, 94, 4352-4356.

[4] Moon, J. R.; Kim, J. Biodegradable thermo- and ph-responsive hydrogels based on amphiphilic polyaspartamide derivatives containing N,N-Diisopropylamine pendants. *Macromol. Res.*, **2008**, 16, 489-491.

[5] Bach, Q. V.; Moon, J. R.; Lee, D. S.; Kim, J. Lower critical solution temperature behavior of amphiphilic copolymers based on polyaspartamide derivatives. *J. Appl. Polym. Sci.* **2008**, 107, 509-513.

[6] Moon, J. R.; Park, Y. H.; Kim, J.; Synthesis and characterization of novel thermo- and pH-responsive copolymers based on amphiphilic polyaspartamides. *J. Appl. Polym. Sci.* **2009**, 111, 998-1004.

[7] Moon, J. R.; Kim, M. W.; Kim, D.; Jeong, J. H.; Kim, J. Synthesis and self-assembly behavior of novel polyaspartamide derivatives for anti-tumor drug delivery. *Colloid Polym. Sci.*, **2011**, 289, 63–71.

[8] Gu, X.; Wang, J.; Liu, X.; Zhao, D.; Wang, Y.; Gao, H.; Wu, G. Temperature-responsive drug delivery systems based on polyaspartamides with isopropylamine pendant groups. *Soft Matter.* **2013**, 9, 7267-7273.

Acknowledgement

As a first graduate member in Laboratory for Integrative Biomaterials Engineering, I really appreciate my research advisor, Prof. Chaenyung Cha. I joined this laboratory at the beginning of 2016, and started my own research project for the first time in my life. There were many trials and errors along the way, but his guidance helped me reach my ultimate goal of master's degree. I would also like to express my sincere gratitude to my lab members for their help and support.

I would also like to thank my friends who are always there for me. I will always cherish the great memories we made throughout my college life. They have given me heartwarming support and advice when I needed the most, which help me navigate through the difficult times. Thanks, guys!

For my research, I had to lean on several sophisticated, large-scale research instruments that were not available in my lab. So I am grateful to UCRF (UNIST Central Research Facility) staff who were kind enough to spend time with me to help learn these instruments; Sun-hye Son (FT-IR and Confocal Raman), Sun-pil Han (NMR), Yeong-bi Kang (SEM), and Kyung-sun Lee (MALDI-TOF-MS).

In 2014, I had a chance to conduct research as an undergraduate intern at Dr. Gert von Helden's research group in Fritz Haber Institute of Max Planck Society, Berlin, Germany. That experience as an inexperienced youngster really shaped my life's goal as a researcher. Especially, I would like to thank Dr. Jongcheol Seo who was not only my research supervisor at that time but also a mentor. His guidance and advice truly made me have a newfound perspective on my life.

Finally, I would not be here without the unconditional love and support from my family. I love you all!